E 23-610

FINAL SCIENTIFIC REPORT

FINITE ELEMENT STRESS ANALYSIS OF AUTOMOBILE TIRES

By

S. Chandrashekara
Graduate Student

Submitted to

GENERAL TIRE & RUBBER COMPANY
AKRON, OHIO

GEORGIA INSTITUTE OF TECHNOLOGY
SCHOOL OF ENGINEERING SCIENCE AND MECHANICS
ATLANTA, GEORGIA 30332

1978

Finite Element Stress Analysis of Automobile Tires

Final Scientific Report

Submitted to

General Tire & Rubber Company

Akron, Ohio

by

S. Chandrashekara
Graduate Student
School of Engineering Science and Mechanics
Georgia Institute of Technology
Atlanta, Georgia 30332

(Approved by: S. N. Atluri, Professor & Project Director)

Introduction

The work reported herein was performed at the School of Engineering Science and Mechanics, Georgia Institute of Technology, by Mr. S. Chandrashekara, graduate student. This research was supported by the General Tire and Rubber Company, Akron, Ohio in the form of a Graduate Research Assistantship to Mr. S. Chandrashekara. Dr. S. N. Atluri, Professor of Engineering Science and Mechanics at Georgia Tech served as the project director and thesis advisor to Mr. Chandrashekara.

The first part of this report, pages (i) to (102), were submitted by Mr. Chandrashekara, as a thesis titled "Laminated Plate Analysis by Hybrid Stress Finite Element Method", in partial fulfillment of the requirement for the degree Master of Science in Engineering Science and Mechanics at Georgia Tech with Professor S. N. Atluri as the thesis advisor.

The Appendices I and II were written by Professor S. N. Atluri.

The writers gratefully acknowledge the research support from The General Tire and Rubber Company.

TABLE OF CONTENTS

LIST OF ILLUSTRATIONS

LIST OF NOTATIONS

a	length of the side of plate
$B(\sigma_{ij})$	stress energy density
h	half thickness of the layer
t	total thickness of the plate
u,v,w	displacements in the Cartesian coordinates
μ	Poisson's ratio
π	complementary energy functional
ρ_m	interelement boundary
$\partial\Omega_m$	boundary comprising of interelement boundary and the physical boundaries where tractions and displacements are prescribed
S_j	interlayer boundary
S_{u_m}	physical boundary where displacements are specified
S_{σ_m}	physical boundary where tractions are specified

Other notations are explained wherever they first appear.

SUMMARY

Unidirectionally reinforced multilayer plates with various loading conditions are studied using the finite element method. The method is based on a hybrid stress model in which self-equilibrated stresses are assumed within the element and the continuity requirements along the interlayer and interelement boundaries are then enforced. The analysis also takes into account transverse shear deformation which is of particular importance in the case of composite materials such as those for automobile tires. Triangular elements are chosen for analysis and the results obtained in this dissertation are compared with earlier results using finite element techniques and also using classical laminated plate theory.

CHAPTER I

INTRODUCTION

Perhaps the most interesting and useful development in the field of structural analysis since the early 60's has been the finite element method of analysis. The fields of application of methods based on finite element concepts have expanded steadily to virtually all forms of engineering involving structural design. Also, the capability of finite element methods to deal with complex geometrical shapes hitherto regarded as insoluble combined with the availability of high speed digital computers have made finite element concepts the most widely applied in aerospace, civil, mechanical and shipbuilding industries.

Although the concept of finite elements can be developed intuitively based on the physical approximation of substituting the actual continuum with a set of discrete (finite) elements, it is important to realize that it can also be based on the minimization principles. The continuous functions for the mechanical or physical quantities pertaining to the continuum are replaced by approximate functions which are smooth in each element but are continuous in the whole body. These approximate functions are constructed using the unknown parameters such as the values of the quantities at

the nodal points of elements combined with a set of interpolation functions. The strain energy functions are sought which are expressed in terms of the nodal values and when the energy is minimized with respect to nodal parameters, a number of algebraic equations governing the unknown parameters are obtained. In effect, what we have done is to replace the original differential equations governing the behavior of the continuum with a set of newly derived algebraic equations.

It has been established that variational methods involving energy principles are applicable to the structural analysis of various assemblies of finite elements. In the same way as variational methods being extensively used in the mathematical formulation of finite element methods, the development of finite elements has aided the advancement of new variational principles. One such most important development is with regard to variational principles with relaxed continuity requirements.[1,2,3,4,5,6] The finite element models developed by using these principles are called "Hybrid finite element models." Usually, these models employ stationary principles wherein two or more fields are varied simultaneously. In brief, the concept consists of assuming displacement and/or stress fields to be continuous within each element, but the continuity or equilibrium conditions along the interelement boundaries are relaxed in such a way that they are satisfied in an integral average

sense and hence will be completely satisfied when the element size becomes infinitesimally small. Thus the continuity or the equilibrium conditions along the inter-element boundaries become conditions of constraint and appropriate boundary variables are used as the corresponding Lagrangian multipliers. In the present thesis, Hybrid stress model has been used for solving multilayer plate problems.

1.1. Literature Survey

Several literatures cite the various finite element models based on modified variational principles.[1,2,3,4,5,6] Fraeijs de Vuebeke has proposed the so-called Equilibrium Model[7] and Fraeijs de Vuebeke and Sander[8] have used this model for analyzing plate bending using oblique coordinates. The hybrid stress model used in this thesis and the equilibrium model proposed as above both follow from the same principle. In both cases, equilibrium equations are satisfied a priori within the element. In the equilibrium model, the equilibrium conditions are maintained for the boundary tractions of two neighboring elements. These latter equilibrium conditions are conditions of constraint along boundaries and the traction continuity along the boundaries is exactly satisfied but the displacements along the inter-element boundary are satisfied in an integral average sense. No multilayered plate problem is solved and results are shown for several rectangular and square single layer plates. The

same concept has been utilized by Mau, Pian, Tong[9] and Pian, Mau[10] for the analysis of multilayered plates and shells. Here also, as in the previous case the equilibrium conditions of constraint are applied along the boundaries between two elements (interelement boundary) and the traction continuity along these boundaries is satisfied exactly. On the boundary between two layers (interlayer boundary), they still match a compatible displacement field. In other words, displacement continuity on the interelement boundary is effected in an average sense while the traction continuity on the interlayer boundary is effected in an average sense. Solutions have been given for several numerical plate problems and are compared with elasticity solution and solution given by Barker, Lin and Data[11] who have used a three-dimensional element with a cubic displacement variation along the plane and a linear variation of displacement along the thickness. An iterative technique called conjugate gradient routine has been used to minimize the total potential energy of the system and results have been compared with elasticity solution and the classical plate theory solution.

1.2. Tire Stress Analysis

A complete stress analysis of a tire should establish the nature of stresses and deformations at all points in the tire under loading conditions which are of importance. This encompasses both theoretical and experimental approaches.

In fact, the studies in the past have relied heavily on trial and error designs and full scale experimental testing. The existing literature[15,16,17,18,19] on tire stress analysis is confined mainly to elastic treatments with some approximations in force-deformation relations and material characteristics. Some of these studies[15,16,17] attempt to predict the tire equilibrium shape instead of a detailed stress distribution analysis. However, all these analyses have not been able to completely overcome the inherent complexity of the problem arising out of the following:

(i) Effects of transverse shear deformation which is particularly important in case of composite materials.

(ii) Complexity due to materials characterization: The tire carcass being a composite of rubber matrix with textile, steel or glass cords, offers great difficulty in writing the stress-strain relations for the structure as a whole.

(iii) Prescribing external loads on tire: Consideration of the simplest cases of inflation pressure and centrifugal force limits the existing solutions to special cases. In general, the loading also involves an asymmetric system of forces acting at the tire-ground interface. Very recently, this aspect has been particularly treated by matrix analysis.

(iv) Effects of geometric and material nonlinearities created by large deformations.

The present study attempts to overcome some of these difficulties. Since the warping of the cross-section (as a result of transverse shear deformation and discontinuous material properties) is quite severe in case of multilayer laminates, it is appropriately taken care of by assigning rotational degrees of freedom for each layer.

Also, since the present finite element study discretizes the structure into layered elements, different material properties can be assigned to different layers to represent a truly anisotropic material behavior. However, the study is limited to case of orthotropic material properties.

The present analysis is limited to plates with the above refinements. From here, the extension of analysis to shells (toroidal shell which the tire is composed of), consideration of geometric non-linearities and proper consideration of forces at tire-ground surface can be made.

In addition to overcoming some of the complexities mentioned above, the present study also takes advantage of a refined finite element model to predict the behavior of the structure.

CHAPTER II

THEORETICAL DEVELOPMENTS

2.1. Functional for the Finite Element Model

The method outlined here is based on hybrid stress model derived from the modified complementary energy principle. In this case, the conditions assumed a priori are: (i) Satisfaction of equilibrium equations within the domain of the element, and (ii) Existence of a strain-energy density function. Instead of consideration of equilibrium of boundary traction as in the equilibrium model, the boundary displacements are interpolated in terms of a finite number of boundary displacements at the nodes. The interpolation functions giving the boundary displacements are so constructed that when the nodal displacements of two neighboring elements coincide, the displacements along the entire boundary are compatible. Also since the assumed stresses must satisfy the prescribed boundary tractions along the portion of the boundary where tractions are prescribed, we could simply enforce a condition $\bar{T}_i - T_i = 0$ on such boundary where $\bar{T}_i$ are prescribed traction. This would be a condition of constraint on that particular boundary and corresponding Lagrange multipliers are the boundary displacements.

Thus we can write the functional in general as:

$$\Pi = \sum_m \Big[\int_{\Omega_m} -B(\sigma_{ij})\, d\Omega - \int_{S_{\sigma_m}} (\bar{T}_i - T_i)\, u_{is}\, ds + \int_{S_{u_m}} T_i \bar{u}_i\, ds + \int_{\rho_m} T_i u_{i\rho}\, ds \Big]$$

For the numerical formulation, we choose u_{is} on S_{σ_m} in the same way as $u_{i\rho}$ on ρ_m. These $u_{i\rho}$ are interpolated in terms of the nodal displacements q on ρ_m. Similarly one can assume $\bar{u}_i$ on S_{u_m} which is of the same type as $u_{i\rho}$ on ρ_m, but we assign values to q on S_{u_m} so as to correspond to the prescribed $\bar{u}_i$.

Thus, the functional reduces to:

$$\Pi = \sum_m \Big[\int_{\Omega_m} -B(\sigma_{ij})\, d\Omega + \int_{\partial\Omega_m} T_i u_{i\rho}\, ds - \int_{S_{\sigma_m}} \bar{T}_i u_{i\rho}\, ds \Big]$$

where

$$\partial\Omega_m = \rho_m + S_{u_m} + S_{\sigma_m}$$

For the case of a laminated system, the functional can be written down as:

$$\Pi = \sum_m \Big[\sum_j \Big\{ \int_{\Omega_j} B(\sigma_{ij})\, d\Omega + \int_{S_j} T_i u^j_{i\rho}\, ds \Big\} + \int_{\partial\Omega_m} T_i u^m_{i\rho}\, ds - \int_{S_{\sigma_m}} \bar{T}_i u_{i\rho}\, ds \Big] \qquad (1)$$

where $u^j_{i\rho}$ is the displacement specified on the interlayer boundary S_j and $u^m_{i\rho}$ is the displacement specified on the interelement boundary $\partial\Omega m$.

2.2. Finite Element Discretization

This process consists in assuming a stress field which is in equilibrium within the element and boundary displacement field in terms of the nodal values of the displacements. The two fields are independently assumed and the interpolation functions applied to interlayer or interelement boundaries are so constructed as to give the required type of variation of the displacements along those boundaries.

For the sake of convenience, the two boundary displacements are separately written. In what follows, the finite element discretization is done for multilayered plates with transverse loading. The self-equilibrated stress field $\underset{\sim}{\sigma}$ is chosen in the form

$$\underset{\sim}{\sigma} = \underset{\approx}{A}\,\underset{\sim}{\beta} \qquad (2)$$

where $\underset{\approx}{A}$ is a matrix of cartesian coordinates giving the stress distribution and $\underset{\sim}{\beta}$ is a vector of stress parameters. From this, the boundary traction field is derivable as:

$$\underset{\sim}{T} = \underset{\approx}{B}\,\underset{\sim}{\beta} \qquad (3)$$

where $\underset{\approx}{B}$ is a matrix of boundary coordinates.

This traction field can be split up into two fields, one giving the boundary traction along interlayer boundary, i.e.,

$$\underset{\sim}{T}_j = \underset{\approx}{B}_j \underset{\sim}{\beta} \quad \text{on} \quad S_j \tag{4a}$$

and the other on the interelement boundary as:

$$\underset{\sim}{T}_m = \underset{\approx}{B}_m \underset{\sim}{\beta} \quad \text{on} \quad \partial\Omega_m \tag{4b}$$

The displacement field is assumed in general as:

$$\underset{\sim}{u} = \underset{\approx}{L}\, \underset{\sim}{q} \tag{5}$$

where $\underset{\approx}{L}$ is again a matrix of boundary coordinates and $\underset{\sim}{q}$ is a vector of nodal displacements for the element.

The displacement field along the interlayer boundary is written as:

$$\underset{\sim}{u}^{j}_{i\rho} = \underset{\approx}{L}_j \underset{\sim}{1} \tag{5a}$$

and that on the interelement boundary is:

$$\underset{\sim}{u}^{m}_{i\rho} = \underset{\approx}{L}_1 \underset{\sim}{1} \tag{5b}$$

then,

$$\int_{\Omega_j} E(\sigma_{ij})\, d\Omega = \frac{1}{2}\, \underset{\sim}{\beta}^T \underset{\approx}{H}\, \underset{\sim}{\beta}$$

where

$$\underset{\approx}{H} = \int_{\Omega_j} \underset{\approx}{A}^T \underset{\approx}{S}\, \underset{\approx}{A}\, d\Omega$$

$$\int_{S_j} T_j\, u_{ip}^j\, ds = \int_{S_j} (\underset{\approx}{B}_j\, \underset{\sim}{\beta})^T\, \underset{\approx}{L}_j\, \underset{\sim}{q}\, ds = \underset{\sim}{\beta}^T \underset{\approx}{G}_j\, \underset{\sim}{q}$$

where

$$\underset{\approx}{G}_j = \int_{S_j} \underset{\approx}{B}_j^T\, \underset{\approx}{L}_j\, ds \qquad (6a)$$

The summation for interlayer boundaries (i.e. summation over j) includes only the above two integrals. The integral pertaining to the interelement boundary is:

$$\int_{\partial\Omega_m} T_m\, u_{ip}^m\, ds = \int_{\partial\Omega_m} (\underset{\approx}{B}_m\, \underset{\sim}{\beta})^T\, \underset{\approx}{L}_m\, \underset{\sim}{q}\, ds$$

$$= \underset{\sim}{\beta}^T \underset{\approx}{G}_m\, \underset{\sim}{q}$$

where

$$\underset{\approx}{G}_m = \int_{\partial\Omega_m} \underset{\approx}{B}_m^T\, \underset{\approx}{L}_m\, ds \qquad (6b)$$

The integral due to external loading is given by:

$$\int_{S_{\sigma_m}} \bar{T}_i\, u_{ip}\, ds = \int_{S_{\sigma_m}} \bar{T}_i\, \underset{\approx}{L}_j\, \underset{\sim}{q}\, ds \qquad (6c)$$

The prescribed tractions are on the interlayer boundary (transverse loading case).

$$\int_{S_{\sigma_m}} \bar{T}_i u_{if} \, ds = \underset{\sim}{\bar{Q}}^T \underset{\sim}{q} \qquad (6d)$$

where

$$\underset{\sim}{Q}^T = \int_{S_{\sigma_m}} \bar{T}_i \underset{\approx}{L}_j \, ds$$

Proper substitution in the functional gives:

$$\pi = \sum_m \left[\sum_j \left\{ -\frac{1}{2} \underset{\sim}{\beta}^T \underset{\approx}{H} \underset{\sim}{\beta} + \underset{\sim}{\beta}^T \underset{\approx}{G}_j \underset{\sim}{q} \right\} + \underset{\sim}{\beta}^T \underset{\approx}{G}_m \underset{\sim}{q} - \underset{\sim}{\bar{Q}}^T \underset{\sim}{q} \right]$$

When β is used to represent the stress parameters of all layers, we write the functional as one summation over the number of elements as:

$$\pi = \sum_m \left[-\frac{1}{2} \underset{\sim}{\beta}^T \underset{\approx}{H}^1 \underset{\sim}{\beta} + \underset{\sim}{\beta}^T \underset{\approx}{G}_j^1 \underset{\sim}{1} + \underset{\sim}{\beta}^T \underset{\approx}{G}_m \underset{\sim}{q} - \underset{\sim}{\bar{Q}}^T \underset{\sim}{q} \right]$$

Where $\underset{\approx}{H}^1$ and $\underset{\approx}{G}_j^1$ are supermatrices with $\underset{\approx}{H}$ and $\underset{\approx}{G}_j$ as diagonal elements. Since $\underset{\sim}{\beta}$'s are independently assumed, $\frac{\partial \pi}{\partial \underset{\sim}{\beta}} = 0$ gives:

$$0 = -\underset{\approx}{H}^1 \underset{\sim}{\beta} + \underset{\approx}{G}_j^1 \underset{\sim}{1} + \underset{\approx}{G}_m \underset{\sim}{q}$$

from which

$$\underset{\sim}{\beta} = \underset{\approx}{H}^{-1} \underset{\approx}{G}_j \underset{\sim}{q} + \underset{\approx}{H}^{-1} \underset{\approx}{G}_m \underset{\sim}{q} \qquad (6e)$$

and

$$\underset{\sim}{\beta}^T \underset{\approx}{H} \underset{\sim}{\beta} = \underset{\sim}{\beta}^T \underset{\approx}{G}_j \underset{\sim}{q} + \underset{\sim}{\beta}^T \underset{\approx}{G}_m \underset{\sim}{q}$$

then

$$\Pi = \sum_m \left[-\tfrac{1}{2} \underset{\sim}{\beta}^T \underset{\approx}{G}_j \underset{\sim}{q} - \tfrac{1}{2} \underset{\sim}{\beta}^T \underset{\approx}{G}_m \underset{\sim}{q} + \underset{\sim}{\beta}^T \underset{\approx}{G}_j \underset{\sim}{q} + \underset{\sim}{\beta}^T \underset{\approx}{G}_m \underset{\sim}{q} - \underset{\approx}{Q}^T \underset{\sim}{q} \right]$$

or

$$\Pi = \sum_m \left[\tfrac{1}{2} \underset{\sim}{\beta}^T \underset{\approx}{G}_j \underset{\sim}{q} - \tfrac{1}{2} \underset{\sim}{\beta}^T \underset{\approx}{G}_m \underset{\sim}{q} - \underset{\approx}{Q}^T \underset{\sim}{q} \right]$$

From the expression for $\underset{\sim}{\beta}$, substituting for $\underset{\sim}{\beta}^T$:

$$\Pi = \sum_m \left[\tfrac{1}{2} \left(\underset{\sim}{q}^T \underset{\approx}{G}_j^T \underset{\approx}{H}^{-1T} + \underset{\sim}{q}^T \underset{\approx}{G}_m^T \underset{\approx}{H}^{-1T} \right) \underset{\approx}{G}_j \underset{\sim}{q} \right.$$

$$\left. + \tfrac{1}{2} \left(\underset{\sim}{q}^T \underset{\approx}{G}_j^T \underset{\approx}{H}^{-1T} + \underset{\sim}{q}^T \underset{\approx}{G}_m^T \underset{\approx}{H}^{-1T} \right) \underset{\approx}{G}_m \underset{\sim}{q} - \underset{\approx}{Q}^T \underset{\sim}{q} \right]$$

Thus

$$\Pi = \sum_m \left[\tfrac{1}{2} \underset{\sim}{q}^T \left(\underset{\approx}{G}_j^T \underset{\approx}{H}^{-1T} \underset{\approx}{G}_j + \underset{\approx}{G}_m^T \underset{\approx}{H}^{-1T} \underset{\approx}{G}_j + \right. \right.$$

$$\left. \left. \underset{\approx}{G}_j^T \underset{\approx}{H}^{-1T} \underset{\approx}{G}_m + \underset{\approx}{G}_m^T \underset{\approx}{H}^{-1T} \underset{\approx}{G}_m \right) \underset{\sim}{q} - \underset{\approx}{Q}^T \underset{\sim}{q} \right]$$

Thus, element stiffness matrix is given by:

$$\underset{\approx}{k}_m = \underset{\approx}{G}_j^{1T} \underset{\approx}{H}^{-1} \underset{\approx}{G}_j^{1} + \underset{\approx}{G}_m^{T} \underset{\approx}{H}^{-1} \underset{\approx}{G}_j + \underset{\approx}{G}_j^{1T} \underset{\approx}{H}^{-1} \underset{\approx}{G}_m + \underset{\approx}{G}_m^{T} \underset{\approx}{H}^{-1} \underset{\approx}{G}_m \qquad (7)$$

and the element load vector

$$\underset{\sim}{Q} = \underset{\approx}{\bar{Q}}^{T} \underset{\sim}{q} \qquad (8)$$

When a transformation is introduced to relate the element nodal displacements $\underset{\sim}{q}$ to a column of independent global displacement $\underset{\sim}{q}^*$, the functional becomes:

$$\Pi = \frac{1}{2} \underset{\sim}{q}^{*T} \underset{\approx}{K}^{*} \underset{\sim}{q}^{*} - \underset{\sim}{q}^{*T} \underset{\sim}{Q}^{*}$$

The application of minimum principle yields the matrix equation

$$\underset{\approx}{K}^{*} \underset{\sim}{q}^{*} = \underset{\sim}{Q}^{*} \qquad (9)$$

which when solved gives the global displacements.

To obtain stresses, the expression for β as given by Eq. (6e) is substituted in Eq. (2) giving

$$\underset{\sim}{\sigma} = \underset{\approx}{A} \left(\underset{\approx}{H}^{-1} \underset{\approx}{G}_j^{1} + \underset{\approx}{H}^{-1} \underset{\approx}{G}_m^{1} \right) \underset{\sim}{q} \qquad (10)$$

With the values of $\underset{\sim}{q}$ known, stresses are evaluated at any desired point.

2.3. Stress Field Generation

It is now necessary to write a series of self-equilibrating stress distributions covering all possibilities giving a complete stress system. As suggested by Ahmad and Irons[12], any self-equilibrating stress field can be expressed as the sum of three stress fields in different sets of parallel planes. In other words, one can write stress systems in xy-planes, varying arbitrarily with z and similar systems in yz- and xz-planes. Thus stresses have to be derived from three interpretations avoiding all redundant terms to keep the variables independent. The stress functions are chosen from Table 1 of Ref. 12.

The basic criteria in the derivation of stress field are:

(i) The normal stress in the z-direction is zero.

$$\text{i.e. } \sigma_{zz} = 0$$

(ii) The normal stresses in the x and y directions and the inplane shear stress (i.e. σ_{xx}, σ_{yy}, τ_{xy}) vary linearly in x, y and z.

(iii) The transverse shear stresses vary quadratically in z.

(iv) Since, later in the theoretical development, a cubic variation for the normal displacement w

is used, the shear strains, being the first order derivatives of displacements will be quadratic. Thus, the transverse shear stresses vary quadratically in x and y in addition to z.

With this as background, we write the following three stress functions arrived at by various relevent interpretations. The parameters β's are numbered according to the order in which the various interpretations are chosen.

$$\varphi_1 = \beta_3 xy^2 + \beta_{14} x^2y^2 + \beta_{20} x^3y^2 + \beta_{21} x^2y^3 +$$
$$z (\beta_2 y + \beta_6 y^2 + \beta_7 xy + \beta_8 x^2y +$$
$$\beta_9 xy^2 + \beta_{11} y^3 + \beta_{17} x^3y + \beta_{18} xy^3 +$$
$$\beta_{28} x^2y^2) + z^2 (\beta_1 + \beta_4 x + \beta_5 y +$$
$$\beta_{10} xy + \beta_{15} y^2 + \beta_{16} x^2 + \beta_{23} y^3 +$$
$$\beta_{25} x^3 + \beta_{26} xy^2 + \beta_{27} x^2y) +$$
$$z^3 (\beta_{12} y + \beta_{13} x + \beta_{19} xy + \beta_{22} y^2 +$$
$$\beta_{24} x^2)$$

$$\varphi_2 = \beta_{29}x^2 + \beta_{32}x^2y + \beta_{41}x^3y + \beta_{42}x^2y^2 + \beta_{48}x^3y^2 + \beta_{49}x^2y^3 + z(\beta_{30}x + \beta_{33}x^2 + \beta_{35}xy + \beta_{36}x^2y + \beta_{37}xy^2 + \beta_{40}x^3 + \beta_{45}x^3y + \beta_{46}xy^3 + \beta_{56}x^2y^2) + z^2(\beta_{31}y + \beta_{34}x + \beta_{38}xy + \beta_{43}y^2 + \beta_{44}x^2 + \beta_{51}y^3 + \beta_{53}x^3 + \beta_{54}xy^2 + \beta_{55}x^2y + z^3(\beta_{39}x + \beta_{47}xy + \beta_{50}y^2 + \beta_{52}x^2)$$

$$\varphi_3 = \beta_{57}y^2 + \beta_{58}xy + \beta_{61}xy^2 + \beta_{62}x^2y + \beta_{68}xy^3 + \beta_{70}x^2y^2 + \beta_{76}x^3y^2 + \beta_{77}x^2y^3 + z(\beta_{59}x^2 + \beta_{60}y^2 + \beta_{63}xy + \beta_{64}x^2y + \beta_{65}xy^2 + \beta_{69}y^3 + \beta_{73}x^3y + \beta_{74}xy^3 + \beta_{84}x^2y^2) + z^2(\beta_{66}xy + \beta_{71}y^2 + \beta_{72}x^2 + \beta_{79}y^3 + \beta_{81}x^3 + \beta_{82}xy^2 + \beta_{83}x^2y) + z^3(\beta_{75}xy + \beta_{78}y^2 + \beta_{80}x^2)$$

The stresses are derived from the stress-functions as follows:

$$\sigma_{xx} = \frac{\partial^2 \varphi_3}{\partial y^2} + \frac{\partial^2 \varphi_2}{\partial z^2}$$

$$\sigma_{yy} = \frac{\partial^2 \varphi_1}{\partial z^2} + \frac{\partial^2 \varphi_3}{\partial x^2}$$

$$\sigma_{zz} = \frac{\partial^2 \varphi_2}{\partial x^2} + \frac{\partial^2 \varphi_1}{\partial y^2}$$

$$\sigma_{xy} = -\frac{\partial^2 \varphi_3}{\partial x \, \partial y}$$

$$\sigma_{yz} = -\frac{\partial^2 \varphi_1}{\partial y \, \partial z}$$

$$\sigma_{zx} = -\frac{\partial^2 \varphi_2}{\partial x \, \partial z}$$

Substituting for ϕ_1, ϕ_2, and ϕ_3, we get

$$\begin{aligned}\sigma_{xx} = {} & 2\beta_{57} + (2\beta_{34} + 2\beta_{61})x + 2\beta_{31}y + \\ & (2\beta_{38} + 2\beta_{68})xy + (2\beta_{44} + 2\beta_{70})x^2 + \\ & 2\beta_{43}y^2 + (2\beta_{53} + 2\beta_{76})x^3 + 2\beta_{51}y^3 + \\ & 2\beta_{54}xy^2 + (2\beta_{55} + 6\beta_{77})x^2y + \\ & z\{2\beta_{60} + (2\beta_{65} + 6\beta_{39})x + 6\beta_{69}y + \\ & (6\beta_{47} + 6\beta_{74})xy + (6\beta_{52} + 2\beta_{84})x^2 + \end{aligned}$$

contd.

$$6\beta_{50}y^2\} + z^2\{2\beta_{71} + 6\beta_{79}y + 2\beta_{82}x\} + z^3(2\beta_{78})$$

$$\sigma_{yy} = 2\beta_1 + 2\beta_4 x + (2\beta_5 + 2\beta_{62})y + (2\beta_{10} + 6\beta_{67})xy + 2\beta_{16}x^2 + (2\beta_{15} + 2\beta_{70})y^2 + 2\beta_{25}x^3 + (2\beta_{73} + 2\beta_{77})y^3 + (2\beta_{26} + 6\beta_{76})xy^2 + 2\beta_{27}x^2y + z\{2\beta_{59} + 6\beta_{13}x + (6\beta_{12} + 2\beta_{64})y + (6\beta_{19} + 6\beta_{73})xy + 6\beta_{24}x^2 + (6\beta_{22} + 2\beta_{84})y^2\} + z^2\{2\beta_{72} + 6\beta_{81}x + 2\beta_{83}y\} + z^3(2\beta_{80})$$

$$\sigma_{zz} = 2\beta_{19} + 2\beta_3 x + 2\beta_{32}y + 6\beta_{41}xy + 2\beta_{14}x^2 + 2\beta_{42}y^2 + 2\beta_{20}x^3 + 2\beta_{49}y^3 + 6\beta_{48}xy^2 + 6\beta_{21}x^2y + z\{(2\beta_6 + 2\beta_{33}) + (2\beta_9 + 6\beta_{40})x + (6\beta_{11} + 2\beta_{36})y + (6\beta_{18} + 6\beta_{45})xy + 2\beta_{28}x^2 + 2\beta_{56}y^2\} + z^2\{(2\beta_{15} + 2\beta_{44}) + (2\beta_{26} + 6\beta_{53})x +$$

contd.

$$+ (6\beta_{23} + 2\beta_{55})y\} + z^3(2\beta_{22} + 2\beta_{52})$$

$$\sigma_{xy} = -\beta_{58} - 2\beta_{61}y - 2\beta_{62}x - 3\beta_{67}x^2 - 3\beta_{68}y^2 - 4\beta_{70}xy - 6\beta_{76}x^2y - 6\beta_{77}xy^2 + z(-\beta_{63} - 2\beta_{64}x - 2\beta_{65}y - 3\beta_{73}x^2 - 3\beta_{74}y^2 - 4\beta_{84}xy) + z^2(-\beta_{66} - 2\beta_{82}y - 2\beta_{83}x) + z^3(-\beta_{75})$$

$$\sigma_{yz} = -\beta_2 - 2\beta_6y - \beta_7x - \beta_8x^2 - 2\beta_9xy - 3\beta_{11}y^2 - \beta_{17}x^3 - 3\beta_{18}x^2y - 2\beta_{28}x^2y + z(-2\beta_5 - 2\beta_{10}x - 4\beta_{15}y - 6\beta_{23}y^2 - 4\beta_{26}xy - 2\beta_{27}x^2) + z^2(-3\beta_{12} - 3\beta_{19}x - 6\beta_{22}y)$$

$$\sigma_{zx} = -\beta_{30} - 2\beta_{33}x - \beta_{35}y - 2\beta_{36}xy - \beta_{37}y^2 - 3\beta_{40}x^2 - 3\beta_{45}x^2y - \beta_{46}y^3 - 2\beta_{56}xy^2 + z(-2\beta_{34} - 2\beta_{38}y - 4\beta_{44}x - 3\beta_{53}x^2 - 2\beta_{54}y^2 - 4\beta_{55}xy) + z^2(-3\beta_{39} - 3\beta_{47}y - 6\beta_{52}x)$$

Applying the conditions on the stress field as enunciated in the beginning of this section, we set the following parameters to zero in the stress functions.

In ϕ_1, these parameters are:

β_3 , β_{14} , β_{15} , β_{16} , β_{17} , β_{18} , β_{21} , β_{22} , β_{23} ,

β_{24} , β_{25} , β_{26} , β_{27} , β_{28}

In ϕ_2, they are:

β_{29} , β_{32} , β_{41} , β_{42} , β_{43} , β_{45} , β_{46} , β_{48} ,

β_{49} , β_{50} , β_{51} , β_{52} , β_{53} , β_{54} , β_{55} , β_{56}

In ϕ_3, they are:

β_{66} , β_{67} , β_{68} , β_{70} , β_{71} , β_{72} , β_{73} , β_{74} , β_{75} ,

β_{76} , β_{77} , β_{78} , β_{79} , β_{80} , β_{81} , β_{82} , β_{83} , β_{84}

Considering all the remaining parameters as β^1 (in order to rewrite the final expressions for stresses in terms of β), the following expressions for stresses are finally obtained.

$$\sigma_{xx} = 2\beta^1_{57} + (2\beta^1_{34} + 2\beta^1_{61})x + 2\beta^1_{31}y + 2\beta^1_{38}xy + z\{2\beta^1_{60} + (2\beta^1_{65} + 6\beta^1_{39})x + 6\beta^1_{39}y + 6\beta^1_{47}xy\}$$

$$\sigma_{yy} = 2\beta^1_{1} + 2\beta^1_{4}x + (2\beta^1_{5} + 2\beta^1_{62})y + 2\beta^1_{10}xy + z\{2\beta^1_{59} + 6\beta^1_{13}x + (2\beta^1_{64} + 6\beta^1_{12})y + 6\beta^1_{19}xy\}$$

$$\sigma_{zz} = 0$$

$$\sigma_{xy} = -\beta^1_{58} - 2\beta^1_{62}x - 2\beta^1_{61}y + z(-\beta^1_{63} - 2\beta^1_{64}x - 2\beta^1_{65}y)$$

$$\sigma_{yz} = -\beta^1_{2} - \beta^1_{7}x - 2\beta^1_{6}y - 2\beta^1_{9}xy - \beta^1_{8}x^2 + \beta^1_{36}y^2 + z(-2\beta^1_{5} - 2\beta^1_{10}x) + z^2(-3\beta^1_{12} - 3\beta^1_{19}x)$$

$$\sigma_{zx} = -\beta^1_{30} + 2\beta^1_{6}x - \beta^1_{35}y - 2\beta^1_{36}xy + \beta^1_{9}x^2 - \beta^1_{37}y^2 + z(-2\beta^1_{34} - 2\beta^1_{38}y) + z^2(-3\beta^1_{39} - 3\beta^1_{47}y)$$

To regulate and thereby simplify the parameters in these expressions, we introduce the new parameters β such that in σ_{xx}

$$2\beta^1_{57} = \beta_1 \quad ; \quad 2\beta^1_{34} + 2\beta^1_{61} = \beta_4 \quad ; \quad 2\beta^1_{31} = \beta_7$$

$$2\beta^1_{38} = \beta_{10} \quad ; \quad 2\beta^1_{60} = \beta_{12} \quad ; \quad 2\beta^1_{65} + 6\beta^1_{39} = \beta_{15}$$

$$6\beta^1_{69} = \beta_{18} \quad ; \quad 6\beta^1_{47} = \beta_{21}$$

In σ_{yy}

$$2\beta^1_1 = \beta_2 \quad ; \quad 2\beta^1_4 = \beta_5 \quad ; \quad 2\beta^1_5 + 2\beta^1_{62} = \beta_8$$

$$2\beta^1_{10} = \beta_{11} \quad ; \quad 2\beta^1_{59} = \beta_{13} \quad ; \quad 6\beta^1_{13} = \beta_{16}$$

$$2\beta^1_{64} + 6\beta^1_{12} = \beta_{19} \quad ; \quad 6\beta^1_{69} = \beta_{22}$$

In σ_{xy}

$$-\beta^1_{58} = \beta_3 \quad ; \quad -2\beta^1_{62} = \beta_6 \quad ; \quad -2\beta^1_{61} = \beta_9$$

$$-\beta^1_{63} = \beta_{14} \quad ; \quad -2\beta^1_{64} = \beta_{17} \quad ; \quad -2\beta^1_{65} = \beta_{20}$$

In σ_{yz}

$$-\beta^1_2 = \beta_{23} \quad ; \quad -\beta^1_7 = \beta_{25} \quad ; \quad -2\beta^1_6 = -\beta_{26}$$

$$-2\beta^1_9 = \beta_{28} \quad ; \quad -\beta^1_8 = \beta_{30} \quad ; \quad -2\beta^1_{36} = \beta_{29}$$

and from

$$2\,\beta^{1}_{34} + 2\,\beta^{1}_{61} = \beta_4$$

we have

$$2\,\beta^{1}_{34} = \beta_4 + \beta_9$$

From

$$6\,\beta^{1}_{39} + 2\,\beta^{1}_{65} = \beta_{15}$$

we get

$$6\,\beta^{1}_{39} = \beta_{15} + \beta_{20}$$

Thus, the final expressions for the stresses are written as:

$$\sigma_{xx} = \beta_1 + \beta_4 x + \beta_7 y + \beta_{10} xy + z\,(\beta_{12} + \beta_{15} x + \beta_{18} y + \beta_{21} xy)$$

$$\sigma_{yy} = \beta_2 + \beta_5 x + \beta_8 y + \beta_{11} xy + z(\beta_{13} + \beta_{16} x + \beta_{19} y + \beta_{22} xy)$$

$$\sigma_{zz} = 0$$

$$\sigma_{xy} = \beta_3 + \beta_6 x + \beta_9 y + z(\beta_{14} + \beta_{17} x + \beta_{20} y)$$

$$\sigma_{yz} = \beta_{23} + \beta_{25} x - \beta_{26} y + \beta_{28} xy + \beta_{30} x^2 - \frac{\beta_{29}}{2} y^2 + z\{(\beta_6 + \beta_8) + \beta_{11} x\} - \frac{z^2}{2}\{(\beta_{17} + \beta_{19}) + \beta_{22} x\}$$

$$\sigma_{zx} = \beta_{24} + \beta_{26} x + \beta_{27} y + \beta_{29} xy - \frac{\beta_{28}}{2} x^2 + \beta_{31} y^2 - z\{(\beta_4 + \beta_9) + \beta_{10} y\} - \frac{z^2}{2}\{(\beta_{15} + \beta_{20}) + \beta_{21} y\}$$

(11)

2.4. Element Shape and Area Coordinates

In the following development, triangular elements have been used for analysis. Being perhaps the most attractive shape, they are well suited to the analysis of structures with irregular boundaries and it is easy to vary the element size in the vicinity of stress concentrations etc. They also can best describe the topology for shell structures.

Instead of writing the stiffness matrices for triangular elements in rectangular cartesian coordinates, we use natural or area coordinates for the same purpose. Natural coordinates rely on the element geometry for their definition. They have the property that one particular coordinate has unit value at one node of the element and zero value at other nodes, its variation between nodes being linear. The use of natural coordinates, which are invariant with respect to the orientation of the triangle, for the three node triangular element (known as area coordinates in particular) in deriving interpolation functions is particularly advantageous because of special closed form integration formulas that can be used to evaluate the integrals in the element equations.

The area coordinates are denoted as ζ_i (i = 1,2,3) as in Fig. 1. These describe the location of any point p within or on the boundary of the element 1-2-3. The cartesian coordinates of a point are linearly related to the area coordinates by the following equations.

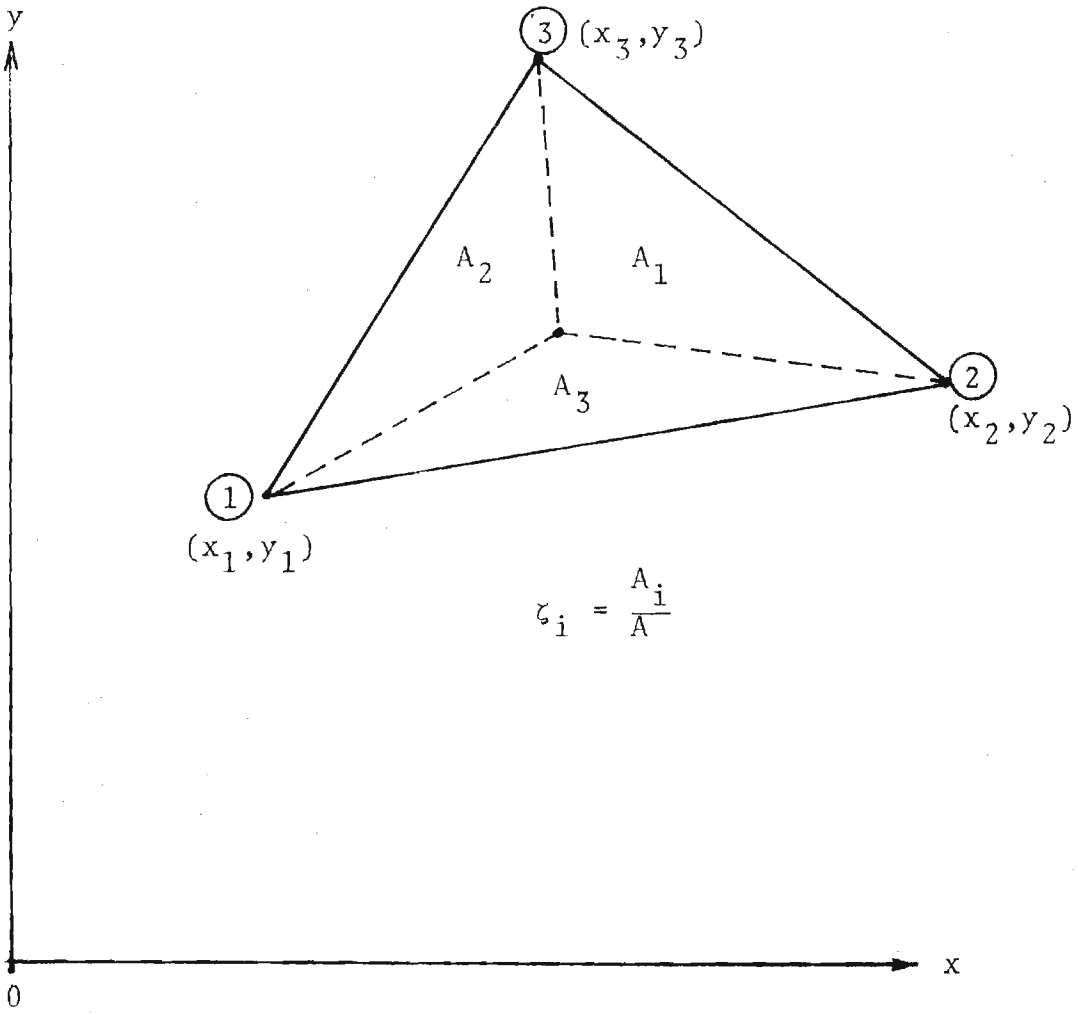

Fig. 1. Area Coordinates for the Element

$$x = x_1\zeta_1 + x_2\zeta_2 + x_3\zeta_3$$

$$y = y_1\zeta_1 + y_2\zeta_2 + y_3\zeta_3$$

In other words, the position of the point may be specified relative to the triangle by the three areas A_1, A_2 and A_3 or, more conveniently by the non-dimensionalized areas:

$$\zeta_1 = \frac{A_1}{A} \quad , \quad \zeta_2 = \frac{A_2}{A} \quad , \quad \zeta_3 = \frac{A_3}{A}$$

where $A = A_1 + A_2 + A_3$ = area of the triangle.

Since any two area coordinates are sufficient to specify the point uniquely, we have another interdependence relation

$$\zeta_1 + \zeta_2 + \zeta_3 = 1$$

The relation between area coordinates and the rectangular cartesian coordinates is written down in the matrix form as follows.

$$\begin{Bmatrix} x \\ y \\ 1 \end{Bmatrix} = \begin{bmatrix} x_1 & x_2 & x_3 \\ y_1 & y_2 & y_3 \\ 1 & 1 & 1 \end{bmatrix} \begin{Bmatrix} \zeta_1 \\ \zeta_2 \\ \zeta_3 \end{Bmatrix} \qquad (12a)$$

By inversion

$$\begin{Bmatrix} \zeta_1 \\ \zeta_2 \\ \zeta_3 \end{Bmatrix} = \frac{1}{2A} \begin{bmatrix} y_{23} & x_{32} & x_2y_3 - x_3y_2 \\ y_{31} & x_{13} & x_3y_1 - x_1y_3 \\ y_{12} & x_{21} & x_1y_2 - x_2y_1 \end{bmatrix} \begin{Bmatrix} x \\ y \\ 1 \end{Bmatrix} \qquad (12b)$$

where

$$y_{23} = y_2 - y_3$$

$$x_{32} = x_3 - x_2 \quad \text{etc.,}$$

and

$$2A = (x_1 - x_3)(y_2 - y_3) - (x_2 - x_3)(y_1 - y_3)$$

For the purpose of establishing rules for differentiation and integration only ζ_1 and ζ_2 are considered as independent variables. Thus $\frac{\partial}{\partial \zeta_1}$ implies that ζ_2 is held constant and $\frac{\partial}{\partial \zeta_2}$ implies that ζ_1 is held constant, whereas

ζ_3 varies in both cases. The differentiation rule follows as:

$$\begin{Bmatrix} \frac{\partial}{\partial \zeta_1} \\ \\ \frac{\partial}{\partial \zeta_2} \end{Bmatrix} = [J] \begin{Bmatrix} \frac{\partial}{\partial x} \\ \\ \frac{\partial}{\partial y} \end{Bmatrix}$$

where J is the Jacobian Matrix and is given by:

$$[J] = \begin{bmatrix} x_{13} & y_{13} \\ x_{23} & y_{23} \end{bmatrix} \qquad (13)$$

and det [J] = 2A.

2.5. Element Nodal Degrees of Freedom

In our formulation, the in-plane displacements u and v are assumed to have linear variation while the normal displacement is assumed to have a cubic variation. Physically, this would mean that the triangular surface bends like a classical plate while it stretches linearly. Also, the fact that the transverse shear stresses are derived directly from the transverse shear strains which contain first order derivatives of w with respect to x and y, combined with the assumption that transverse shear stresses vary quadratically, necessitates a cubic variation for w. This variation is also

justified by the fact that transverse shear stresses σ_{xz} and σ_{yz} do work only on the rectangular boundary surfaces where such a variation is assumed.

In the case of multilayer plates, transverse shear deformation plays an important role because of discontinuous material properties. To account for these effects, the rotational degrees of freedom θ_x and θ_y are assumed different for each layer. With the assumption that θ_x and θ_y are constant across the thickness of any one layer, they are derived from the in-plane displacements u and v at the top and the bottom surface of each layer. Thus for each layer there will be 21 degrees of freedom with five degrees of freedom at corner nodes and one degree of freedom for the midside node.

Correspondingly, for a three layer element, there are nine degrees of freedom for a corner node and again one degree of freedom for the mid-side node, thus totaling to 33 degrees of freedom for the element. The degree of freedom disposition is shown in Fig. 2.

2.6. Boundary Displacement Fields

The two displacement fields, one each on the inter-layer and the interelement boundary are separately written to aid numerical computation. Thus the elements of the matrix $\underset{\approx}{G}$ in Eq. (5) are split up into two groups under $\underset{\approx}{G}_j$ in Eq. (5a) and $\underset{\approx}{G}_m$ in Eq. (5b).

Node	Layer	Position	Displacements
1 (Corner)	1	Top	u^1, v^1, w
		Bottom	u^2, v^2, w
	2	Top	u^2, v^2, w
		Bottom	u^3, v^3, w
	3	Top	u^3, v^3, w
		Bottom	u^4, v^4, w
2	All	Any	w
3	All	Any	w
4 (Corner)	1	Top	u^1, v^1, w
		Bottom	u^2, v^2, w
	2	Top	u^2, v^2, w
		Bottom	u^3, v^3, w
	3	Top	u^3, v^3, w
		Bottom	u^4, v^4, w
5	All	Any	w
6	All	Any	w
7 (Corner)	1	Top	u^1, v^1, w
		Bottom	u^2, v^2, w
	2	Top	u^2, v^2, w
		Bottom	u^3, v^3, w
	3	Top	u^3, v^3, w
		Bottom	u^4, v^4, w
8	All	Top	w
9	All	Bottom	w

Fig. 2. Degree of Freedom Disposition for the Triangular Element

On the interlayer boundary, the displacement distributions are functions of area coordinates only. Denoting by i and j the top and the bottom surfaces of any layer (Fig. 3) of thickness 2h and writing 1-4-7 as a subscript to denote the triangular shape, we have the in-plane displacements

$$
\begin{aligned}
u^i_{147} &= u^i_1 \zeta_1 + u^i_4 \zeta_2 + u^i_7 \zeta_3 \\
v^i_{147} &= v^i_1 \zeta_1 + v^i_4 \zeta_2 + v^i_7 \zeta_3 \\
u^j_{147} &= u^j_1 \zeta_1 + u^j_4 \zeta_2 + u^j_7 \zeta_3 \\
v^j_{147} &= v^j_1 \zeta_1 + v^j_4 \zeta_2 + v^j_7 \zeta_3
\end{aligned}
\qquad (14)
$$

The cubic variation of w over the triangular surface is obtained by using the procedure suggested by Silvester[13] for writing down the interpolation functions for higher order elements. Using these functions, the element equations can be made to contain derivatives and integrals of the area coordinates. Then:

$$
w = \sum_{i=1}^{9} \phi_i w_i \qquad (15)
$$

where

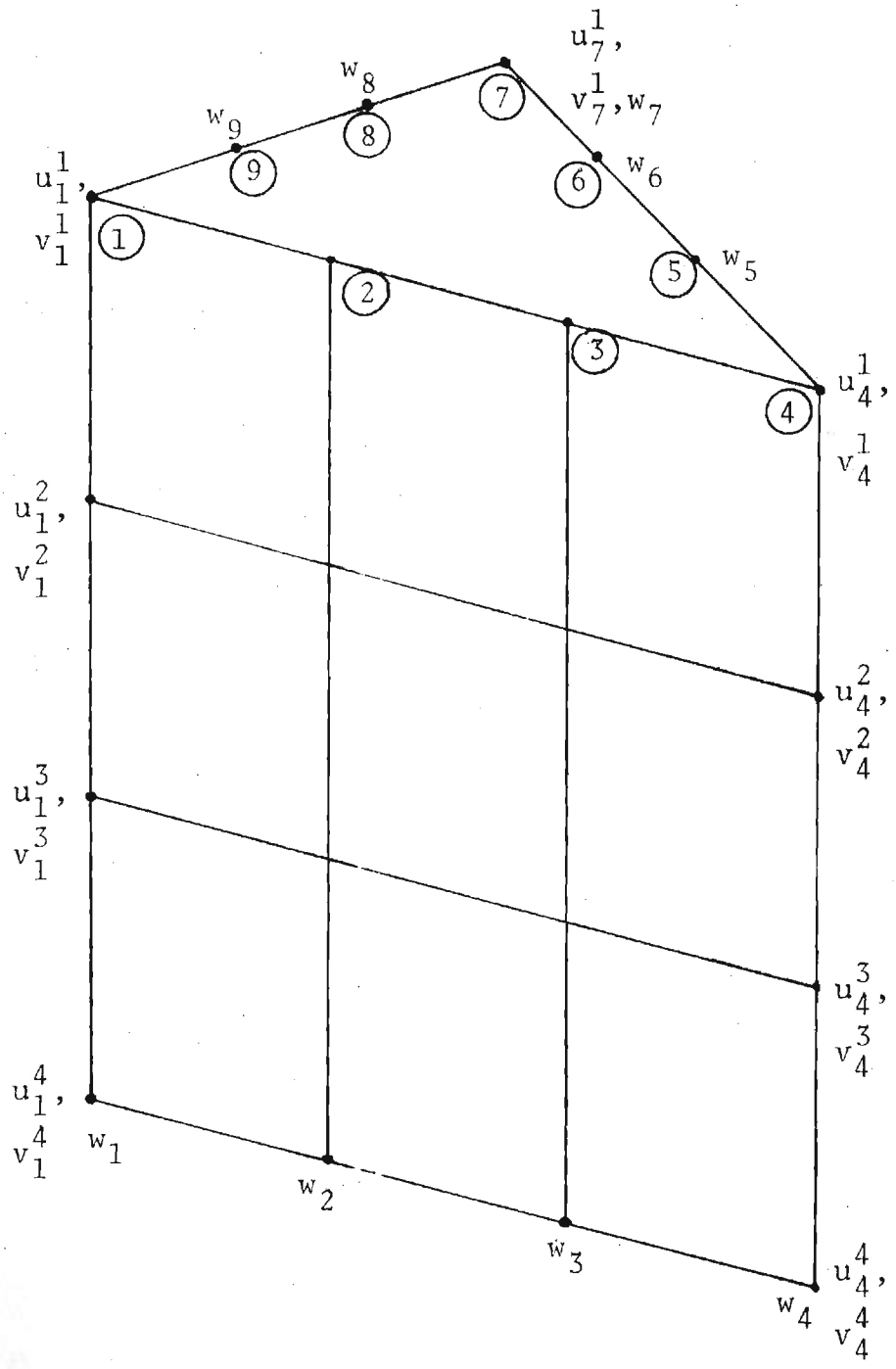

Fig. 3. Element Nodal Degrees of Freedom

$$\varphi_1 = \frac{1}{2}\zeta_1(3\zeta_1-1)(3\zeta_1-2)$$

$$\varphi_2 = \frac{9}{2}\zeta_1\zeta_2(3\zeta_1-1)$$

$$\varphi_3 = \frac{9}{2}\zeta_1\zeta_2(3\zeta_2-1)$$

$$\varphi_4 = \frac{1}{2}\zeta_2(3\zeta_2-1)(3\zeta_2-2)$$

$$\varphi_5 = \frac{9}{2}\zeta_2\zeta_3(3\zeta_2-1)$$

$$\varphi_6 = \frac{9}{2}\zeta_2\zeta_3(3\zeta_3-1)$$

$$\varphi_7 = \frac{1}{2}\zeta_3(3\zeta_3-1)(3\zeta_3-2)$$

$$\varphi_8 = \frac{9}{2}\zeta_1\zeta_3(3\zeta_3-1)$$

$$\varphi_9 = \frac{9}{2}\zeta_1\zeta_3(3\zeta_1-1)$$

There are no i,j superscripts on w since w remains the same for the entire thickness of the element. Thus, in Eq. (5a), elements of vector u^j_{ip} are (6x1), those of L_j and q are respectively (6x21) and (21x1).

The in-plane displacements on the rectangular boundary (interelement boundary) are linear interpolations of the corresponding nodal displacements. These consist of a

linearly interpolated displacements due to stretching and due to rotation of the two end nodes. For example, for any boundary, say 1-4, as in Fig. 4, (where S is the distance measured from node 1):

$$u_{14} = U_1 + U_2$$

where

$$U_1 = u_1 + \bar{u}$$

$$= u_1 + (u_4 - u_1)\frac{s}{\ell}$$

$$= u_1\left(1 - \frac{s}{\ell}\right) + u_4\left(\frac{s}{\ell}\right)$$

Again

$$u_1 = \frac{u_1^i + u_1^j}{2} \quad ; \quad u_2 = \frac{u_4^i + u_4^j}{2}$$

Similarly

$$U_2 = z(\theta_1 + \bar{\theta})$$

where

$$\bar{\theta} = (\theta_4 - \theta_1)\frac{s}{\ell}$$

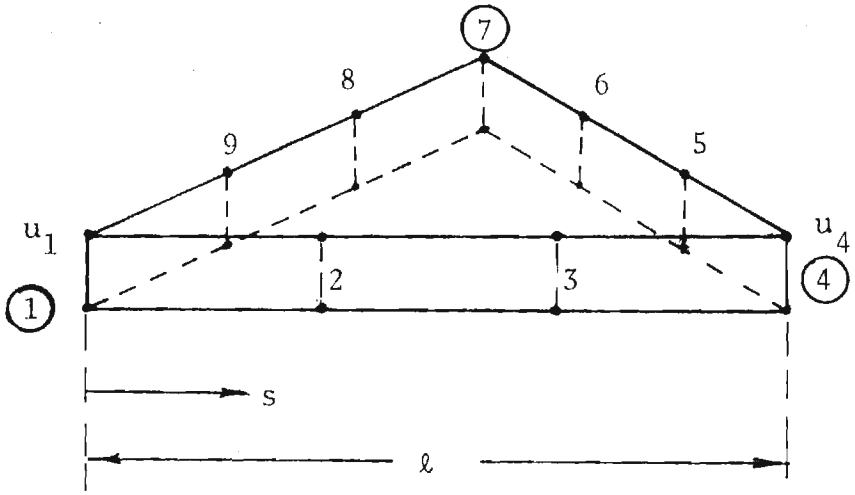

(a)

Rectangular Boundary 1-4

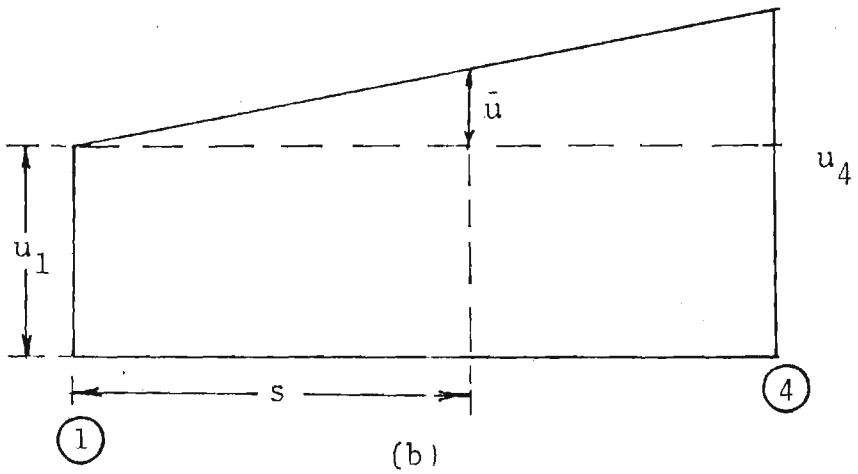

(b)

Variation of in-plane displacement 'u' along 1-4

Fig. 4. Variation of Interelement Boundary Displacements

and

$$\theta_1 = \frac{u_1^i - u_1^j}{2h}$$

$$\theta_4 = \frac{u_4^i - u_4^j}{2h}$$

Hence

$$u_{14} = \left[\frac{u_1^i + u_1^j}{2} \left(1 - \frac{s}{\ell} \right) + \frac{u_4^i + u_4^j}{2} \left(\frac{s}{\ell} \right) + z \left\{ \frac{u_1^i - u_1^j}{2h} \left(1 - \frac{s}{\ell} \right) + \frac{u_4^i - u_4^j}{2h} \left(\frac{s}{\ell} \right) \right\} \right]$$

Rearranging terms with proper subscripts to denote the boundary or the node,

$$u_{14} = \left(1 - \frac{s_{14}}{\ell_{14}} \right) \left(\frac{1}{2} + \frac{z}{2h} \right) u_1^i + \left(1 - \frac{s_{14}}{\ell_{14}} \right) \left(\frac{1}{2} - \frac{z}{2h} \right) u_1^j + \left(\frac{s_{14}}{\ell_{14}} \right) \left(\frac{1}{2} + \frac{z}{2h} \right) u_4^i + \left(\frac{s_{14}}{\ell_{14}} \right) \left(\frac{1}{2} - \frac{z}{2h} \right) u_4^j$$

$$v_{14} = \left(1 - \frac{s_{14}}{\ell_{14}} \right) \left(\frac{1}{2} + \frac{z}{2h} \right) v_1^i + \left(1 - \frac{s_{14}}{\ell_{14}} \right) \left(\frac{1}{2} - \frac{z}{2h} \right) v_1^j + \left(\frac{s_{14}}{\ell_{14}} \right) \left(\frac{1}{2} + \frac{z}{2h} \right) v_4^i + \left(\frac{s_{14}}{\ell_{14}} \right) \left(\frac{1}{2} - \frac{z}{2h} \right) v_4^j$$

Eq. (16) cont.

$$u_{47} = \left(1 - \frac{s_{47}}{\ell_{47}}\right)\left(\frac{1}{2} + \frac{z}{2h}\right) u_4^i + \left(1 - \frac{s_{47}}{\ell_{47}}\right)\left(\frac{1}{2} - \frac{z}{2h}\right) u_4^j$$

$$+ \left(\frac{s_{47}}{\ell_{47}}\right)\left(\frac{1}{2} + \frac{z}{2h}\right) u_7^i + \left(\frac{s_{47}}{\ell_{47}}\right)\left(\frac{1}{2} - \frac{z}{2h}\right) u_7^j$$

$$v_{47} = \left(1 - \frac{s_{47}}{\ell_{47}}\right)\left(\frac{1}{2} + \frac{z}{2h}\right) v_4^i + \left(1 - \frac{s_{47}}{\ell_{47}}\right)\left(\frac{1}{2} - \frac{z}{2h}\right) v_4^j$$

$$+ \left(\frac{s_{47}}{\ell_{47}}\right)\left(\frac{1}{2} + \frac{z}{2h}\right) v_7^i + \left(\frac{s_{47}}{\ell_{47}}\right)\left(\frac{1}{2} - \frac{z}{2h}\right) v_7^j$$

$$u_{71} = \left(1 - \frac{s_{71}}{\ell_{71}}\right)\left(\frac{1}{2} + \frac{z}{2h}\right) u_7^i + \left(1 - \frac{s_{71}}{\ell_{71}}\right)\left(\frac{1}{2} - \frac{z}{2h}\right) u_7^j$$

$$+ \left(\frac{s_{71}}{\ell_{71}}\right)\left(\frac{1}{2} + \frac{z}{2h}\right) u_1^i + \left(\frac{s_{71}}{\ell_{71}}\right)\left(\frac{1}{2} - \frac{z}{2h}\right) u_1^j$$

$$v_{71} = \left(1 - \frac{s_{71}}{\ell_{71}}\right)\left(\frac{1}{2} + \frac{z}{2h}\right) v_7^i + \left(1 - \frac{s_{71}}{\ell_{71}}\right)\left(\frac{1}{2} - \frac{z}{2h}\right) v_7^j$$

$$+ \left(\frac{s_{71}}{\ell_{71}}\right)\left(\frac{1}{2} + \frac{z}{2h}\right) v_1^i + \left(\frac{s_{71}}{\ell_{71}}\right)\left(\frac{1}{2} - \frac{z}{2h}\right) v_1^j$$

(16)

The normal displacement variation is written again by using Silvester's procedure.

$$w_{14} = \frac{1}{2}\left[\left(1-\frac{s_{14}}{\ell_{14}}\right)\left(2-\frac{3s_{14}}{\ell_{14}}\right)\left(1-\frac{3s_{14}}{\ell_{14}}\right)w_1 + 9\left(\frac{s_{14}}{\ell_{14}}\right)\left(1-\frac{s_{14}}{\ell_{14}}\right)\left(2-\frac{3s_{14}}{\ell_{14}}\right)w_2 - 9\left(\frac{s_{14}}{\ell_{14}}\right)\left(1-\frac{s_{14}}{\ell_{14}}\right)\left(1-\frac{3s_{14}}{\ell_{14}}\right)w_3 + \left(\frac{s_{14}}{\ell_{14}}\right)\left(1-\frac{3s_{14}}{\ell_{14}}\right)\left(2-\frac{3s_{14}}{\ell_{14}}\right)w_4\right]$$

$$w_{47} = \frac{1}{2}\left[\left(1-\frac{s_{47}}{\ell_{47}}\right)\left(2-\frac{3s_{47}}{\ell_{47}}\right)\left(1-\frac{3s_{47}}{\ell_{47}}\right)w_4 + 9\left(\frac{s_{47}}{\ell_{47}}\right)\left(1-\frac{s_{47}}{\ell_{47}}\right)\left(2-\frac{3s_{47}}{\ell_{47}}\right)w_5 - 9\left(\frac{s_{47}}{\ell_{47}}\right)\left(1-\frac{s_{47}}{\ell_{47}}\right)\left(1-\frac{3s_{47}}{\ell_{47}}\right)w_6 + \left(\frac{s_{47}}{\ell_{47}}\right)\left(1-\frac{3s_{47}}{\ell_{47}}\right)\left(2-\frac{3s_{47}}{\ell_{47}}\right)w_7\right]$$

$$w_{71} = \frac{1}{2}\left[\left(1-\frac{s_{71}}{\ell_{71}}\right)\left(2-\frac{3s_{71}}{\ell_{71}}\right)\left(1-\frac{3s_{71}}{\ell_{71}}\right)w_7 + 9\left(\frac{s_{71}}{\ell_{71}}\right)\left(1-\frac{s_{71}}{\ell_{71}}\right)\left(2-\frac{3s_{71}}{\ell_{71}}\right)w_8 - 9\left(\frac{s_{71}}{\ell_{71}}\right)\left(1-\frac{s_{71}}{\ell_{71}}\right)\left(1-\frac{3s_{71}}{\ell_{71}}\right)w_9 + \left(\frac{s_{71}}{\ell_{71}}\right)\left(1-\frac{3s_{71}}{\ell_{71}}\right)\left(2-\frac{3s_{71}}{\ell_{71}}\right)w_1\right]$$

(17)

These give the elements of matrix $\underset{\sim}{L}_m$ in Eq. (5b) and it has (9 x 21) elements. While writing the area integrals, we encounter integrations with respect to ζ_1, ζ_2, and ζ_3 on triangular boundaries (Eq. (6a) and with respect to s and z on the rectangular boundaries (Eq. (6b). These integrals are separately evaluated numerically by using relevant numerical integration techniques. In such a case, we shall use a one-dimensional formula for integrations on rectangular boundaries. For this purpose, it is necessary to write integration variables in the non-dimensionalized form with integration limits varying from -1 to +1. The non-dimensionalization of z is effected simply by writing:

$$\bar{z} = \frac{z}{h} \qquad (18a)$$

where z is measured from the mid-surface of the layer and 2h is the thickness of the element. In the s-direction on any rectangular boundary, we write the modification as:

$$\bar{s} = \frac{2s}{\ell} - 1$$

As s varies from 0 to ℓ (length of the side of the element), it can be seen that $\bar{s}$ varies from -1 to +1. Then

$$\frac{s}{\ell} = \frac{1}{2}(1 + \bar{s})$$

$$\left(1 - \frac{s}{\ell}\right) = \frac{1}{2}\left(1 - \bar{s}\right)$$

$$\left(1 - \frac{3s}{\ell}\right) = -\frac{1}{2}\left(1 + 3\bar{s}\right)$$

$$\left(2 - \frac{3s}{\ell}\right) = \frac{1}{2}\left(1 - 3\bar{s}\right)$$

$$\left(\frac{1}{2} + \frac{z}{2h}\right) = \frac{1}{2}\left(1 + \bar{z}\right) \qquad (18\,b)$$

and any integral of any function $f(s,z)$ is transformed as:

$$\int_{-h}^{h}\int_{o}^{\ell} f(s,z)\, ds\, dz = \frac{\ell h}{2}\int_{-1}^{1}\int_{-1}^{1} \bar{f}(\bar{s},\bar{z})\, d\bar{s}\, d\bar{z} \qquad (19)$$

2.7. Boundary Tractions

From the stress field chosen, it is possible to derive the boundary traction field as:

$$\underset{\sim}{T} = \underset{\approx}{\beta}\,\underset{\sim}{\beta}$$

To do this, we use the basic relation given in the index notation as:

$$T_i = \sigma_{ij}\, n_j$$

or

$$\begin{Bmatrix} T_x \\ T_y \\ T_z \end{Bmatrix} = \begin{bmatrix} \sigma_{xx} & \sigma_{xy} & \sigma_{xz} \\ \sigma_{yx} & \sigma_{yy} & \sigma_{yz} \\ \sigma_{zx} & \sigma_{zy} & \sigma_{zz} \end{bmatrix} \begin{Bmatrix} n_x \\ n_y \\ n_z \end{Bmatrix} \qquad (20)$$

where n_j are the direction cosines of the normal to the boundary.

The direction cosines of the normal to any boundary, say, for example 1-4, are derived as follows: The coordinates s and z for this boundary are shown in Fig. 5. Writing down the derivations in the cartesian coordinate system as shown in Fig. 5 we have the position vector $\vec{R}$ given by:

$$\vec{R} = x\vec{i} + y\vec{j} + z\vec{k}$$

where $\vec{i}$, $\vec{j}$, $\vec{k}$ are unit vectors in the cartesian coordinate system. But on this boundary, x and y are given by Eq. 12, i.e.,

$$x = x_1(1-\zeta_2) + x_2\zeta_2$$

$$y = y_1(1-\zeta_2) + y_2\zeta_2$$

ζ_3 being zero on this boundary.

Thus

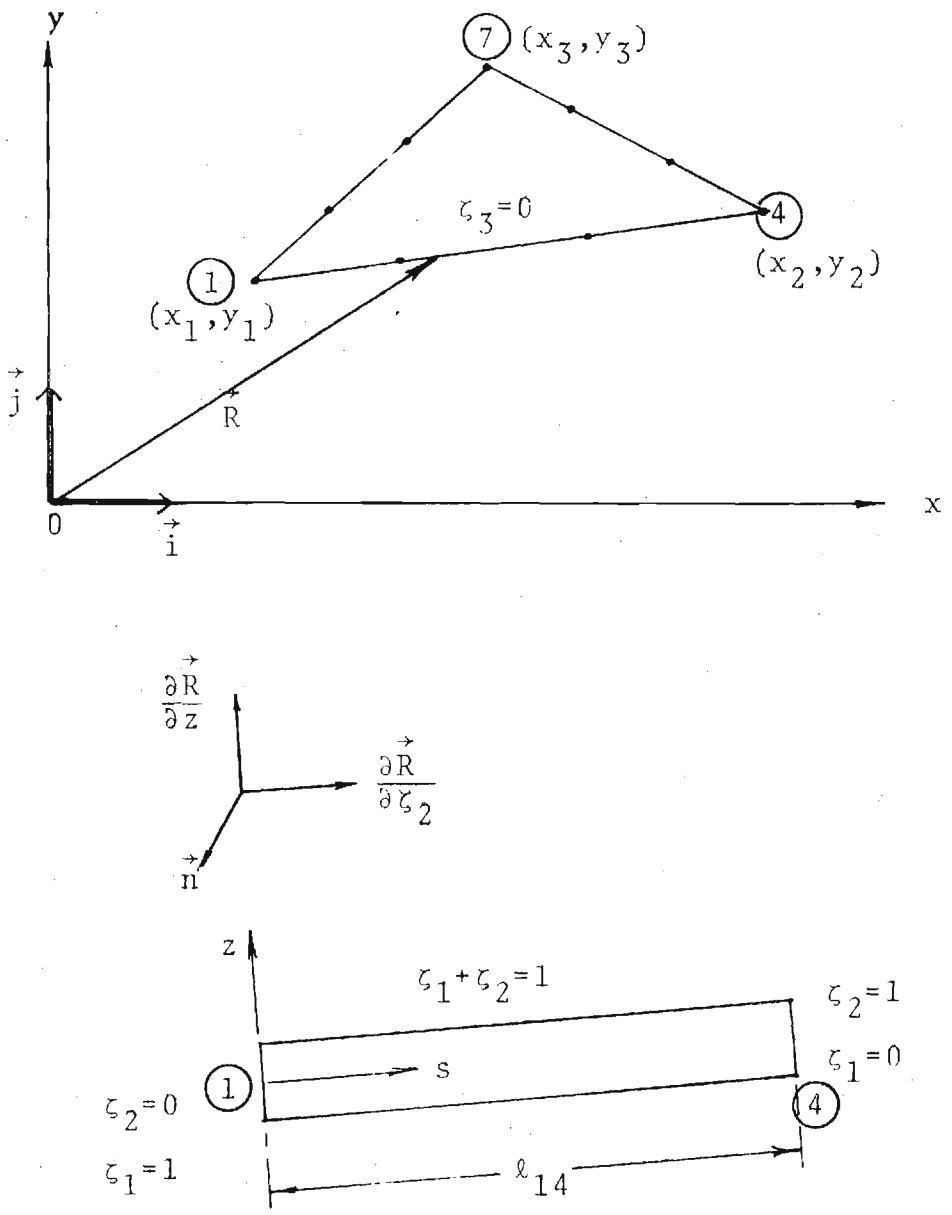

Fig. 5. Derivation of Direction Cosines on the Boundary

$$\vec{R} = \{ x_1(1-\zeta_2) + x_2\zeta_2 \}\,\vec{i} + \{ y_1(1-\zeta_2) + y_2\zeta_2 \}\,\vec{j} + z\vec{k}$$

By the basic vector mechanics and the right hand rule the magnitude and direction of the vector normal to this boundary is given by

$$n = \frac{\partial \vec{R}}{\partial \zeta_2} \times \frac{\partial \vec{R}}{\partial z}$$

$$= (y_2 - y_1)\,\vec{i} + (x_1 - x_2)\,\vec{j}$$

From this

$$n_x^{14} = \cos\alpha = \frac{y_2 - y_1}{|\vec{n}|} \qquad (21\,a)$$

$$n_y^{14} = \sin\alpha = \frac{x_1 - x_2}{|\vec{n}|}$$

where

$$|\vec{n}| = \sqrt{\{ (y_2 - y_1)^2 + (x_1 - x_2)^2 \}}$$

Similarly for boundaries 4-7 and 7-1

$$n_x^{47} = \frac{y_3 - y_2}{\sqrt{\{(y_3 - y_2)^2 + (x_2 - x_3)^2\}}} \qquad (21\,b)$$

$$n_y^{47} = \frac{x_2 - x_3}{\sqrt{\{(y_3 - y_2)^2 + (x_2 - x_3)^2\}}}$$

$$n_x^{71} = \frac{y_1 - y_3}{\sqrt{\{(y_1 - y_3)^2 + (x_3 - x_1)^2\}}}$$

$$n_y^{71} = \frac{x_3 - x_1}{\sqrt{\{(y_1 - y_3)^2 + (x_3 - x_1)^2\}}} \qquad (21c)$$

On all these boundaries

$$n_z = 0$$

On the upper triangular surface

$$n_x^{147} = n_y^{147} = 0$$

$$n_z^{147} = 1$$

On the lower triangular surface

$$n_x^{147} = n_y^{147} = 0$$

$$n_z^{147} = -1$$

Using these values of direction cosines and Eq. (20), the expressions for the boundary stresses are written. Denoting by superscripts, the boundaries of the element, they are:

$$T_x^{14} = (\sigma_{xx})_{\zeta_3 = 0}\, n_x^{14} + (\sigma_{xy})_{\zeta_3 = 0}\, n_y^{14}$$

$$T_y^{14} = (\sigma_{xy})_{\zeta_3 = 0}\, n_x^{14} + (\sigma_{yy})_{\zeta_3 = 0}\, n_y^{14}$$

$$T_z^{14} = (\sigma_{xz})_{\zeta_3 = 0}\, n_x^{14} + (\sigma_{yz})_{\zeta_3 = 0}\, n_y^{14}$$

$$T_x^{47} = (\sigma_{xx})_{\zeta_1=0}\, n_x^{47} + (\sigma_{xy})_{\zeta_1=0}\, n_y^{47}$$

$$T_y^{47} = (\sigma_{xy})_{\zeta_1=0}\, n_x^{47} + (\sigma_{yy})_{\zeta_1=0}\, n_y^{47}$$

$$T_z^{47} = (\sigma_{xz})_{\zeta_1=0}\, n_x^{47} + (\sigma_{yz})_{\zeta_1=0}\, n_y^{47}$$

$$T_x^{71} = (\sigma_{xx})_{\zeta_2=0}\, n_x^{71} + (\sigma_{xy})_{\zeta_2=0}\, n_y^{71}$$

$$T_y^{71} = (\sigma_{xy})_{\zeta_2=0}\, n_x^{71} + (\sigma_{yy})_{\zeta_2=0}\, n_y^{71}$$

$$T_z^{71} = (\sigma_{xz})_{\zeta_2=0}\, n_x^{71} + (\sigma_{yz})_{\zeta_2=0}\, n_y^{71}$$

$$T_x^{147}(\text{upper}) = (\sigma_{xz})_{z=h}\, n_z^{147} \;;\; T_y^{147}(\text{upper}) = (\sigma_{yz})_{z=h}\, n_z^{147}$$

$$T_x^{147}(\text{lower}) = -(\sigma_{xz})_{z=-h}\, n_z^{147} \;;\; T_y^{147}(\text{lower}) = -(\sigma_{yz})_{z=-h}\, n_z^{147}$$

$$T_z^{147}(\text{upper}) = T_z^{147}(\text{lower}) = 0 \qquad (22)$$

The expressions for the stresses are substituted from Eq. (11). In what follows, only two typical boundary tractions are written in detail.

$$T_x^{14} = \Big[\, \beta_1 + \beta_4(x_1\zeta_1 + x_2\zeta_2) + \beta_7(y_1\zeta_1 + y_2\zeta_2) +$$

$$\beta_{10}(x_1\zeta_1 + x_2\zeta_2)(y_1\zeta_1 + y_2\zeta_2) + z\,\{\, \beta_{12} +$$

Contd.

$$+ \beta_{15}(x_1\zeta_1 + x_2\zeta_2) + \beta_{18}(y_1\zeta_1 + y_2\zeta_2) +$$
$$+ \beta_{21}(x_1\zeta_1 + x_2\zeta_2)(y_1\zeta_1 + y_2\zeta_2)\}] n_x^{14} + [\beta_3 +$$
$$\beta_6(x_1\zeta_1 + x_2\zeta_2) + \beta_9(y_1\zeta_1 + y_2\zeta_2) + z\{\beta_{14} +$$
$$\beta_{17}(x_1\zeta_1 + x_2\zeta_2) + \beta_{20}(y_1\zeta_1 + y_2\zeta_2)\}] n_y^{14} \qquad (22a)$$

$$T_z^{14} = [\beta_{24} + \beta_{26}(x_1\zeta_1 + x_2\zeta_2) + \beta_{27}(y_1\zeta_1 + y_2\zeta_2) +$$
$$\beta_{29}(x_1\zeta_1 + x_2\zeta_2)(y_1\zeta_1 + y_2\zeta_2) - \frac{\beta_{28}}{2}(x_1\zeta_1 + x_2\zeta_2)^2 +$$
$$\beta_{31}(y_1\zeta_1 + y_2\zeta_2)^2 - z\{(\beta_4 + \beta_9) + \beta_{10}(y_1\zeta_1 + y_2\zeta_2)\}$$
$$- \frac{z^2}{2}\{(\beta_{15} + \beta_{20}) + \beta_{21}(y_1\zeta_1 + y_2\zeta_2)\}] n_x^{14} +$$
$$[\beta_{23} + \beta_{25}(x_1\zeta_1 + x_2\zeta_2) + \beta_{26}(y_1\zeta_1 + y_2\zeta_2) +$$
$$\beta_{28}(x_1\zeta_1 + x_2\zeta_2)(y_1\zeta_1 + y_2\zeta_2) + \beta_{30}(x_1\zeta_1 + x_2\zeta_2)^2$$
$$- \frac{\beta_{29}}{2}(y_1\zeta_1 + y_2\zeta_2)^2 - z\{(\beta_6 + \beta_8) + \beta_{11}(x_1\zeta_1 + x_2\zeta_2)\}$$
$$- \frac{z^2}{2}\{(\beta_{17} + \beta_{19}) + \beta_{22}(x_1\zeta_1 + x_2\zeta_2)\}] n_y^{14} \qquad (22b)$$

Since these expressions are used in conjunction with the displacements, it is necessary to convert the ζ coordinates to the coordinates $\bar{s}$ and $\bar{z}$, so that we have integrals modified as in Eq. (19).

Referring to Fig. 4, any distance on the boundary 1-4 is given by

$$s_{14}^2 = (x - x_1)^2 + (y - y_1)^2$$

where (x_1, y_1) are the coordinates of node 1 and (x,y) refer to the arbitrary point on the line 1-4.

Letting

$$x = x_1 \zeta_1 + x_2 (1 - \zeta_1)$$

$$y = y_1 \zeta_1 + y_2 (1 - \zeta_1)$$

$$s_{14}^2 = (1 - \zeta_1)^2 \{ (x_2 - x_1)^2 + (y_2 - y_1)^2 \}$$

But

$$\ell_{14}^2 = (x_2 - x_1)^2 + (y_2 - y_1)^2$$

$$\frac{s_{14}^2}{\ell_{14}^2} = (1 - \zeta_1)^2$$

or

$$\frac{s_{14}}{\ell_{14}} = 1 - \zeta_1 = \zeta_2$$

Therefore

$$x_1 \zeta_1 + x_2 (1 - \zeta_1) = x_1 \left(1 - \frac{s_{14}}{\ell_{14}}\right) + x_2 \left(\frac{s_{14}}{\ell_{14}}\right)$$

Substituting from

$$\frac{2s}{\ell} - 1 = \bar{s}$$

$$x_1 \zeta_1 + x_2 (1 - \zeta_1) = \frac{x_1}{2} (1 - \bar{s}_{14}) + \frac{x_2}{2} (1 + \bar{s}_{14})$$

and

$$y_1 \zeta_1 + y_2 (1 - \zeta_1) = \frac{y_1}{2} (1 - \bar{s}_{14}) + \frac{y_2}{2} (1 + \bar{s}_{14})$$

Similarly on the other two boundaries

$$x_2 \zeta_2 + x_3 \zeta_3 = \frac{x_2}{2} (1 - \bar{s}_{47}) + \frac{x_3}{2} (1 + \bar{s}_{47})$$

$$y_2 \zeta_2 + y_3 \zeta_3 = \frac{y_2}{2} (1 - \bar{s}_{47}) + \frac{y_3}{2} (1 + \bar{s}_{47})$$

and

$$x_1 \zeta_1 + x_3 \zeta_3 = \frac{x_1}{2} (1 + \bar{s}_{71}) + \frac{x_3}{2} (1 - \bar{s}_{71})$$

$$y_1 \zeta_1 + y_3 \zeta_3 = \frac{y_1}{2} (1 + \bar{s}_{71}) + \frac{y_3}{2} (1 - \bar{s}_{71})$$

Thus, for example

$$T_x^{14} = \left[\beta_1 + \frac{\beta_4}{2}\left(x_1(1-\bar{s}_{14}) + x_2(1+\bar{s}_{14})\right) + \frac{\beta_7}{2}\left(y_1(1-\bar{s}_{14}) + y_2(1+\bar{s}_{14})\right) + \frac{\beta_{10}}{4}\left(x_1(1-\bar{s}_{14}) + x_2(1+\bar{s}_{14})\right)\left(y_1(1-\bar{s}_{14}) + y_2(1+\bar{s}_{14})\right) + z\left\{\beta_{12} + \frac{\beta_{15}}{2}\left(x_1(1-\bar{s}_{14}) + x_2(1+\bar{s}_{14})\right) + \frac{\beta_{18}}{2}\left(y_1(1-\bar{s}_{14}) + y_2(1+\bar{s}_{14})\right) + \frac{\beta_{21}}{4}\left(x_1(1-\bar{s}_{14}) + x_2(1+\bar{s}_{14})\right)\left(y_1(1-\bar{s}_{14}) + y_2(1+\bar{s}_{14})\right)\right\}\right] n_x^{14} + \left[\beta_3 + \frac{\beta_6}{2}\left(x_1(1-\bar{s}_{14}) + x_2(1+\bar{s}_{14})\right) + \frac{\beta_9}{2}\left(y_1(1-\bar{s}_{14}) + y_2(1+\bar{s}_{14})\right) + z\left\{\beta_{14} + \beta_{17}\left(x_1(1-\bar{s}_{14}) + x_2(1+\bar{s}_{14})\right) + \frac{\beta_{20}}{2}\left(y_1(1-\bar{s}_{14}) + y_2(1+\bar{s}_{14})\right)\right\}\right] n_y^{14} \quad (23)$$

The expressions for all other boundary tractions are written in a similar manner. These give the elements of the matrix $\underset{\approx}{B}$ in Eq. (3).

2.8. External Load Calculations

Three types of loading are considered for the numerical work. They are:

(i) concentrated load at the center of plate

(ii) uniformly distributed load

(iii) loads varying sinusoidally in both directions.

Since the boundaries on which these transverse loads are prescribed are the triangular boundaries, it is necessary to consider only the boundary displacement distribution matrix

$\underset{\sim}{L}_j$ pertaining to these boundaries (Eq. (6c)). However, the nodal displacement vector is still common for both the types of boundaries since all the nodal degrees of freedom are involved when writing any boundary displacement matrix.

While solving the multilayer plate problem, the components of the prescribed tractions are given by:

$$\underset{\sim}{T}_i = \begin{Bmatrix} 0 \\ 0 \\ p(x,y) \\ 0 \\ 0 \\ 0 \end{Bmatrix}$$

where

p(x,y) is the distributed load on the top of the uppermost layer of the element.

It may be mentioned here that for the case of uniformly distributed load, p will be a constant value and the load calculations on elements with same geometry remain the same. In fact, in such a case, it is siffucient to evaluate the stiffness matrices for only typical elements and later perform the assembly procedure. On the other hand, for sinusoidal loading, the load intensity varies from point to point. With a fixed cartesian coordinate system, it is necessary to evaluate the loading vector for each and every element of the structure and complete the assembly.

CHAPTER III

ELASTICITY ANALYSIS OF MULTILAYER LAMINATES

Due to the recent developments in high-modulus fibers and to the necessity for light-weight, high-strength structures, composite material constructions are becoming increasingly popular. These constructions consist of several layers stacked one above the other at various orientations to each other unidirectionally reinforced composites are considered here. In particular, tire structure consists of layers of reinforcing cords embedded in rubber matrix.

It is well-known that for an orthotropic material (with three planes of elastic symmetry), the three-dimensional stress-strain relations are given by:

$$\epsilon_1 = \frac{1}{E_1}\left[\sigma_{11} - (\mu_{12}\sigma_{22} + \mu_{13}\sigma_{33})\right]$$

$$\epsilon_2 = \frac{1}{E_2}\left[\sigma_{22} - (\mu_{21}\sigma_{11} + \mu_{23}\sigma_{33})\right]$$

$$\epsilon_3 = \frac{1}{E_3}\left[\sigma_{33} - (\mu_{31}\sigma_{11} + \mu_{32}\sigma_{22})\right]$$

$$\gamma_{12} = \sigma_{12} / G_{12}$$

$$\gamma_{23} = \sigma_{23} / G_{23}$$

$$\gamma_{31} = \sigma_{31} / G_{31}$$

where

$$\frac{\mu_{13}}{E_1} = \frac{\mu_{31}}{E_3} \quad ; \quad \frac{\mu_{12}}{E_1} = \frac{\mu_{21}}{E_2} \quad ; \quad \frac{\mu_{23}}{E_2} = \frac{\mu_{32}}{E_3}$$

Unidirectionally reinforced composite is a special case of orthotropic composite in that the elastic properties in the two directions other than the direction of reinforcement will be same. If, for example, the properties in x_2- and x_3- directions are same, the above stress-strain relations reduce to equations in which:

$$E_2 = E_3 \quad , \quad \mu_{12} = \mu_{13} \; , \quad \mu_{21} = \mu_{31} \; , \quad \mu_{23} = \mu_{32}$$

$$G_{12} = G_{31}$$

Then

$$\epsilon_1 = \frac{1}{E_1} \left[\sigma_{11} - \mu_{12} (\sigma_{22} + \sigma_{23}) \right]$$

$$\epsilon_2 = \frac{1}{E_2} \left[\sigma_{22} - (\mu_{21} \sigma_{11} + \mu_{23} \sigma_{33}) \right]$$

$$\epsilon_3 = \frac{1}{E_2} \left[\sigma_{33} - (\mu_{21} \sigma_{11} + \mu_{23} \sigma_{22}) \right]$$

$$\gamma_{12} = \sigma_{12} / G_{12}$$

$$\gamma_{23} = \sigma_{23} / G_{23}$$

$$\gamma_{31} = \sigma_{31} / G_{12}$$

It can be seen that for such a case only six independent elastic constants (E_1, E_2, μ_{12}, G_{12}, μ_{23}, G_{23}) describe the stress-strain relations.

Thus, the compliance matrix used for each lamina or layer of the composite element is written in the matrix form as:

$$\begin{Bmatrix} \epsilon_1 \\ \epsilon_2 \\ \epsilon_3 \\ \gamma_{12} \\ \gamma_{23} \\ \gamma_{31} \end{Bmatrix} = \begin{bmatrix} 1/E_1 & -\mu_{12}/E_1 & -\mu_{12}/E_1 & 0 & 0 & 0 \\ -\mu_{21}/E_2 & 1/E_2 & -\mu_{23}/E_2 & 0 & 0 & 0 \\ -\mu_{21}/E_2 & -\mu_{23}/E_2 & 1/E_2 & 0 & 0 & 0 \\ 0 & 0 & 0 & 1/G_{12} & 0 & 0 \\ 0 & 0 & 0 & 0 & 1/G_{23} & 0 \\ 0 & 0 & 0 & 0 & 0 & 1/G_{12} \end{bmatrix} \begin{Bmatrix} \sigma_{11} \\ \sigma_{22} \\ \sigma_{33} \\ \sigma_{12} \\ \sigma_{23} \\ \sigma_{31} \end{Bmatrix} \quad (24)$$

The above relations hold for the principal axes of elastic symmetry in 1,2,3 directions.

For an arbitrary orientation of the lamina, as shown in Fig. 6, where the principal axes (1,2,3) do not coincide with the cartesian reference axes (x,y,z) of the laminate, the following transformation law is used:

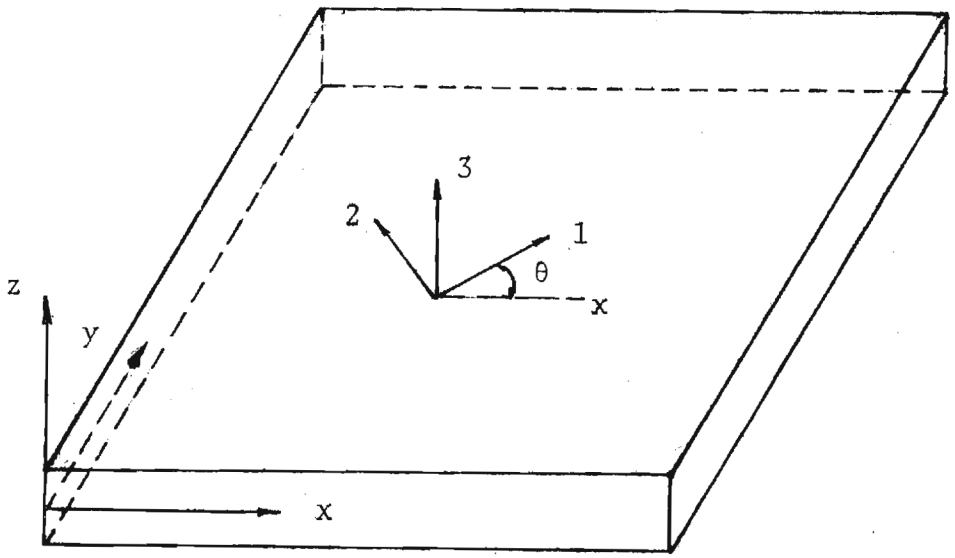

Fig. 6. Fiber Orientation Within Lamina Element

$$\begin{Bmatrix} \sigma_{xx} \\ \sigma_{yy} \\ \sigma_{zz} \\ \sigma_{xy} \\ \sigma_{yz} \\ \sigma_{zx} \end{Bmatrix} = \begin{bmatrix} m^2 & n^2 & 0 & -2mn & 0 & 0 \\ n^2 & m^2 & 0 & 2mn & 0 & 0 \\ 0 & 0 & 1 & 0 & 0 & 0 \\ mn & -mn & 0 & m^2-n^2 & 0 & 0 \\ 0 & 0 & 0 & 0 & m & n \\ 0 & 0 & 0 & 0 & -n & m \end{bmatrix} \begin{Bmatrix} \sigma_1 \\ \sigma_2 \\ \sigma_3 \\ \sigma_{12} \\ \sigma_{23} \\ \sigma_{31} \end{Bmatrix} \tag{25}$$

where $m = \cos\theta$ and $n = \sin\theta$, θ being the angle between the two sets of axes.

The above relation can be written in the abbreviated form as:

$$\underset{\sim}{\sigma}_x = \underset{\approx}{T}\, \underset{\sim}{\sigma}_1$$

and similarly

$$\underset{\sim}{\epsilon}_x = \underset{\approx}{T}\, \underset{\sim}{\epsilon}_1 \tag{26}$$

Inverting

$$\underset{\sim}{\sigma}_1 = \underset{\approx}{T}^{-1}\, \underset{\sim}{\sigma}_x \tag{27}$$

Writing Eq. (24) in a similar way, we have

$$\underset{\sim}{\epsilon}_1 = \underset{\approx}{S}\, \sigma_1 \qquad (28)$$

Substituting Eq. (28) and Eq. (27) in Eq. (23), we get

$$\underset{\sim}{\epsilon}_x = \underset{\approx}{T}\, \underset{\approx}{S}\, \underset{\approx}{T}^{-1}\, \underset{\sim}{\sigma}_x \qquad (29a)$$

or

$$\underset{\sim}{\epsilon}_x = \underset{\approx}{S}_x\, \underset{\sim}{\sigma}_x \qquad (29b)$$

Thus, the compliance matrix $\underset{\approx}{S}$ is transformed in order to refer to the cartesian coordinate system.

CHAPTER IV

NUMERICAL CALCULATIONS

4.1. Numerical Integration

When writing down the stiffness matrix, integrations over areas and volumes are encountered at several stages such as in Eq. (6). Since these terms involve matrices individually, the final outcome in each case is a matrix of some order. The matrix operations are discussed in Section 4.2. It may be too difficult or impractical to integrate these expressions in closed form. Also, the element of volume or surface over which the integration has to be carried out needs to be expressed in terms of the local coordinates (area coordinates, in our case) with appropriate limits of integration. Thus to get satisfactory results, numerical integration techniques are used.

The volume integral in terms of the cartesian coordinates is transformed, in general, to an integral of area coordinates by the following relation:

$$\iiint F(x,y,z)\,dx\,dy\,dz = \int_{-1}^{1}\int_{-1}^{1}\int_{-1}^{1} F(\xi,\eta,\zeta)\,\det[J]\,d\xi\,d\eta\,d\zeta$$

where the Jacobian matrix of transformation is given by an expression like Eq. (13). It should be noted here that this

transformation is valid for any general local coordinate system. In the present case, since area coordinates are being used to transform the cartesian (x,y) coordinates, ξ and η could be thought of as ζ_1 and ζ_2 (ζ_3 is not independent, Eq. (12)) and ζ could be z. Thus the above transformation can now be written as:

$$\int_0^1 \int_0^{1-\zeta_1} \int_{-1}^{1} \bar{F}(\zeta_1, \zeta_2, \bar{z}) \det[J] \, d\zeta_1 \, d\zeta_2 \, d\bar{z}$$

where det[J] now refers particularly to Eq. (13) and the above integral is for a case where z is simply transformed to $\bar{z}$ by Eq. (18a).

The numerical integration constants for evaluating the above integral have been devised by Radau based on Gauss expressions for numerical integration. Hence these constants are known as Gauss-Radau integrating constants involving area coordinates[14].

The integration in the z direction in the above expression is taken care of by simple Gauss quadrature formulae in one dimension. Thus in evaluating the volume integral in our case, two sets of integration constants are used. Gauss quadrature constants (Table 8.1 of Ref. 14) and Gauss-Radau constants (Table 8.2 of Ref. 14). For accuracy, five constants (n=5) are chosen in each case.

There are two categories of area integrals involved in

our numerical work. The first one, as indicated in the expression of Eq. (6a) pertains to the interlayer boundary and involves only coordinates ζ_1, ζ_2 and ζ_3 (z will have either +h or -h value) and hence the following transformation is effected:

$$\int\int F(x,y)\, dx\, dy = \int_0^1 \int_0^{1-\zeta_1} \bar{F}(\zeta_1 \zeta_2 \zeta_3)\, \det[J]\, d\zeta_2\, d\zeta_1$$

and the numerical integration is carried out using Gauss-Radau constants.

The second area integral is over rectangular boundaries (interelement boundary) as in Eq. (6b) and which involves two independent non-dimensionalized coordinates $\bar{s}$ and $\bar{z}$ each of which has integration limits -1 and +1. In this case, one-dimensional Gauss quadrature constants for each coordinate are applied. Thus, the same constants are chosen twice in this case.

The area integral giving the load vector (Eq. (6c)) is in terms of ζ_1, ζ_2 and ζ_3 only and Gauss-Radau constants are used for numerical integration.

4.2. Matrix Operations and Computer Program

The various matrices encountered in the calculations are given below. The notations are the same as those used in the derivation of the functional in Section 2.1.

Stress field:

$$\underset{(6\times1)}{\underset{\sim}{\sigma}} = \underset{(6\times31)}{\underset{\approx}{A}}\ \underset{(31\times1)}{\underset{\sim}{\beta}}$$

Boundary tractions:

interlayer boundary:

$$\underset{(6\times1)}{\underset{\sim}{T}_j} = \underset{(6\times31)}{\underset{\approx}{B}_j}\ \underset{(31\times1)}{\underset{\sim}{\beta}}$$

interelement boundary:

$$\underset{(9\times1)}{\underset{\sim}{T}_m} = \underset{(9\times31)}{\underset{\approx}{B}_m}\ \underset{(31\times1)}{\underset{\sim}{\beta}}$$

Displacement fields:

interlayer boundary:

$$\underset{(6\times1)}{\underset{\sim}{u}^j_{if}} = \underset{(6\times21)}{\underset{\approx}{L}_j}\ \underset{(21\times1)}{\underset{\sim}{q}}$$

interelement boundary:

$$\underset{(9\times1)}{\underset{\sim}{u}^m_{if}} = \underset{(9\times21)}{\underset{\approx}{L}_m}\ \underset{(21\times1)}{\underset{\sim}{q}}$$

Volume Integral:

$$\underset{(31\times31)}{\underset{\approx}{H}} = \int_{\Omega} \underset{(31\times6)}{\underset{\approx}{A}^T}\ \underset{(6\times6)}{\underset{\approx}{S}}\ \underset{(6\times31)}{\underset{\approx}{A}}\ d\Omega$$

Area Integrals:

interlayer boundary:

$$\underset{(31\times 21)}{\underset{\approx}{G}_j} = \int_{S_j} \underset{(31\times 6)}{\underset{\approx}{B}_j^T} \underset{(6\times 21)}{\underset{\approx}{L}_j}\, ds$$

interelement boundary:

$$\underset{(31\times 21)}{\underset{\approx}{G}_m} = \int_{\partial\Omega_m} \underset{(31\times 9)}{\underset{\approx}{B}_m^T} \underset{(9\times 21)}{\underset{\approx}{L}_m}\, ds$$

Order of stiffness matrix for each layer of element: 21 x 21

Order of stiffness matrix for the entire element: 33 x 33

The computer program is written for the multilayered plates according to the following steps:

(i) Read the number of elements, degrees of freedom for nodes, global nodal numbers for the corner and mid-side nodes.

(ii) Store all integration constants for use in one-dimensional Gauss quadrature formula and Gauss-Radau formula.

(iii) Read overall dimensions of plate, thickness of layers, material properties of layer and lamina orientations.

(iv) Calculate elements of matrices $\underset{\approx}{G}_j$ and $\underset{\approx}{G}_m$.

(v) Calculate the elements of the compliance matrix for each layer by using the transformation matrix (Eq. (25)).

(vi) Obtain the elements of the matrix involving volume integral for each layer. Perform the necessary operations as given in Eq. (7) thus getting the stiffness matrix for each layer.

(vii) By assembling the matrix elements for all layers, obtain the stiffness matrix for the element (layer assembly).

(viii) Obtain the load vector for any given transverse load.

(ix) Perform the assembly of elements of stiffness matrix for all elements geometrically similar to the one chosen above. (Element assembly.)

(x) Repeat steps (iv) to (ix) to cover all other typical elements to obtain the global stiffness matrix for the structure.

(xi) Apply appropriate boundary conditions.

(x) Solve a set of simultaneous equations to get the displacements.

It is to be noted that two distinct assembly procedures are adopted here. The interlayer assembly procedure consists in writing down the stiffness matrix for the element consisting of several layers. For a particular manner of numbering the element nodes, the process remains the same for all elements. The (21 x 21) matrix for each layer is merged into a (33 x 33) matrix for the element. The numbering of the nodes for one element follows the description given in Section 2.5

and shown in Fig. 2.

The interelement assembly is carried out as in any other finite element assembly. To save the computer storage space , the assembled global matrix is written directly in the banded form. Typical mesh patterns and the nodal numbering adopted to obtain an economical storage capacity are shown in Fig. 7. These numbers refer to the nodes which has all the layers incorporated in it and thus the stiffness matrix for any element here would have already incorporated the stiffness matrices of all the layers.

Two commonly used subroutines, one for matrix multiplication and the other for transposing the matrix are written. A library program was used to invert any square symmetric matrix.

The final set of equations (in the banded form) are solved by Gaussian elimination technique as suggested by Zienkiewicz[14].

Once the displacements are known, they are substituted in Eq. (10) and the stresses are derived.

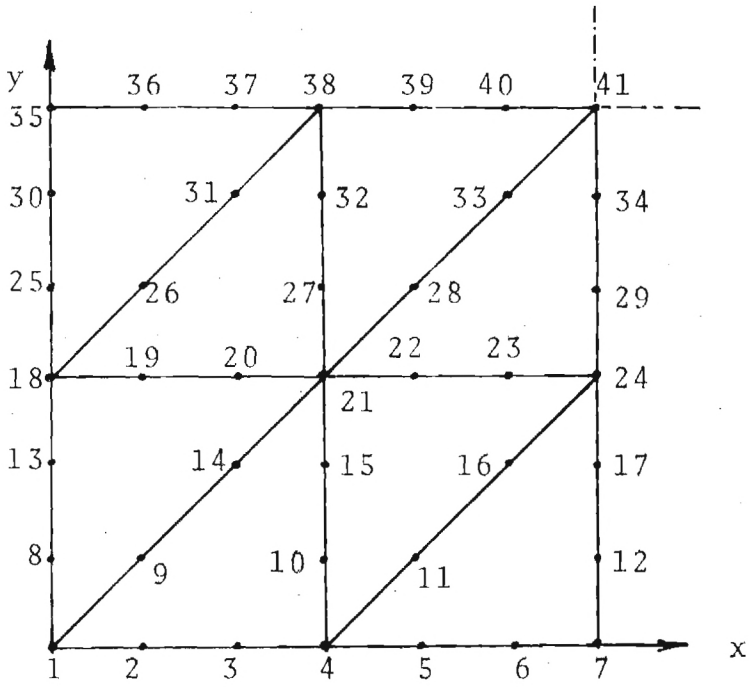

2x2 mesh (N=2)

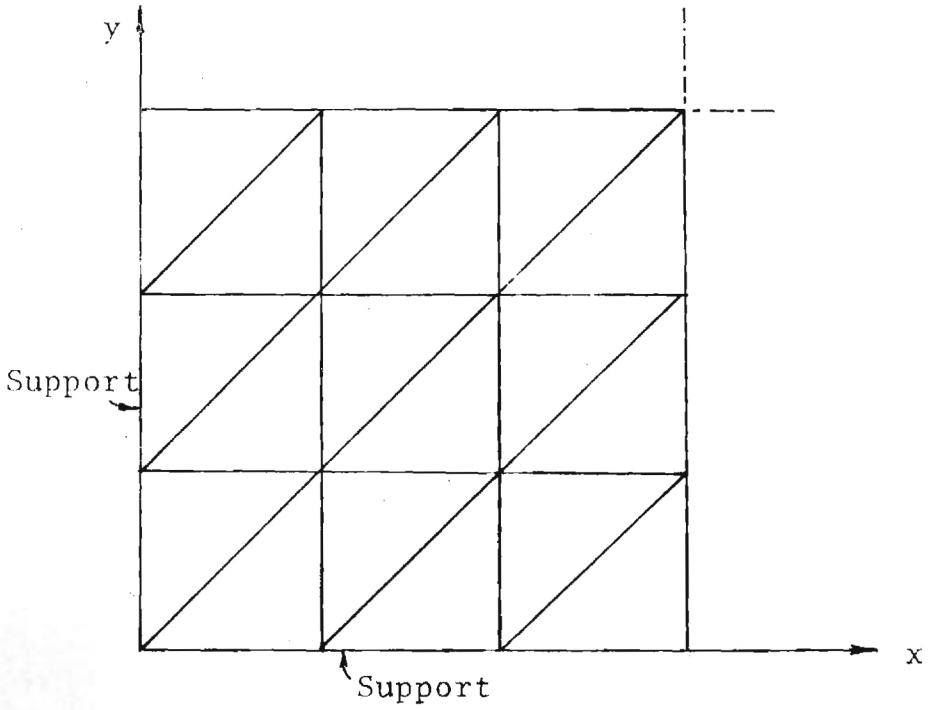

3x3 mesh (N=3)

Fig. 7. Typical Mesh Patterns for a Quarter Plate

CHAPTER V

RESULTS AND DISCUSSION

In order to check the suitability of the hybrid model developed in this study, several numerical problems are solved. These results are compared with the available results.

5.1. Convergence Study

To observe the convergence of the results obtained from the present hybrid stress finite element model, a simple numerical problem of a single layer square plate subjected to a concentrated load at the center is solved. The plate is assumed to be simply supported all over and is considered isotropic. The geometric and physical properties of the plate are:

length of side, a = 10 in

thickness of plate = 1 in

Poisson's ratio = 0.3

Modulus of Elasticity E = 30×10^6 psi.

The vertical deflections at the center of the plate are obtained for various mesh patterns with increasing number of meshes as shown in Fig. 7. The results are shown in Fig. 8 where the ratio of present value of central deflection to the exact value is plotted against the number of mesh

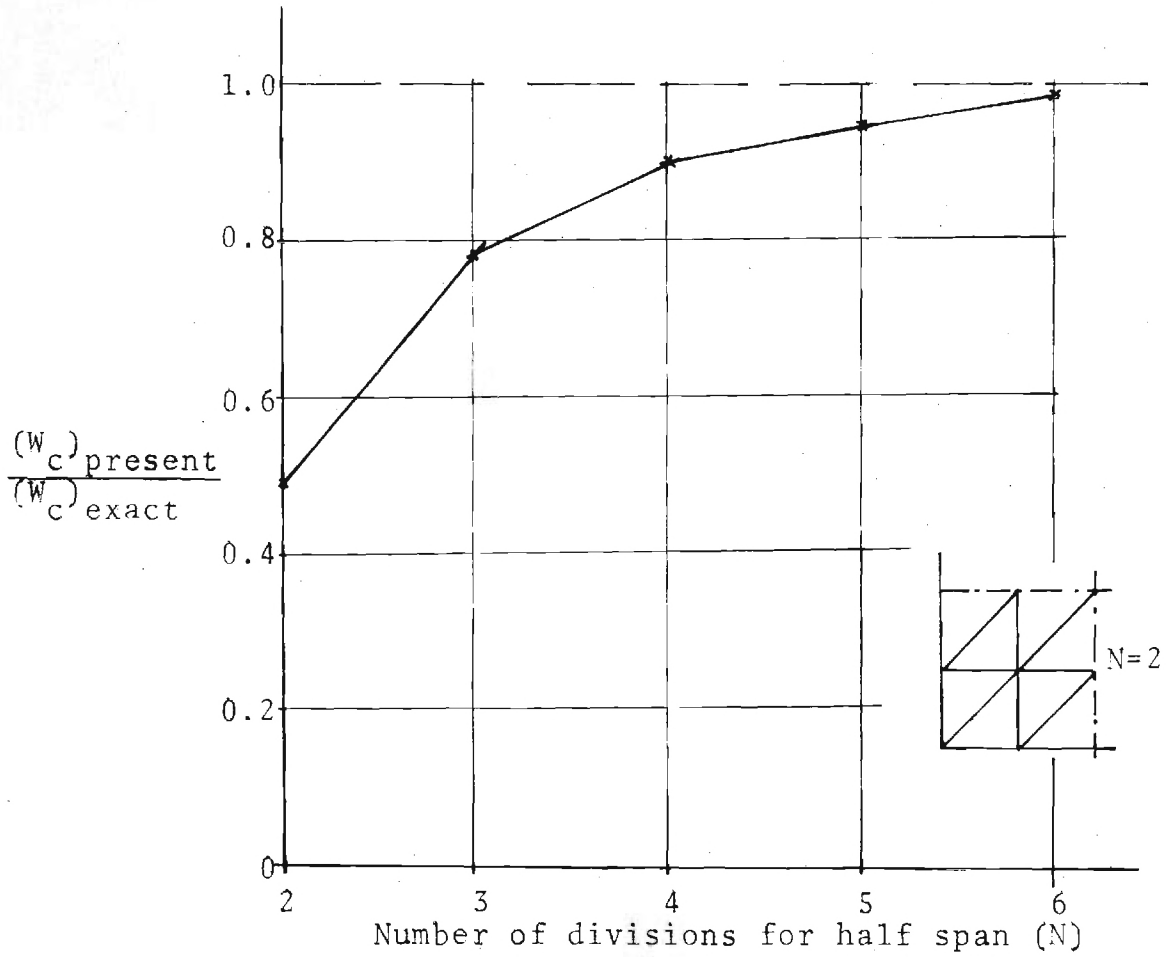

Fig. 8. Convergence Study for the Present Model (simply supported square plate with concentrated load at center)

divisions for half span. Since the plate is symmetric in its geometry, loading and boundary condition only one-quarter plate is taken for analysis. The plot shows a progressive convergence and with N = 6, the result is only about 3% smaller than the exact value. It should be noted here that in this case of a single layered plate, the number of degrees of freedom per element reduces to 21.

5.2. Comparative Results

To study the applicability of the present method to numerical problems of layered plates, two typical examples of 3-layered plates are chosen for detailed analysis. The geometry of the plate and other details are shown in Fig. 9. The notations L and T refer to the two principal axes of symmetry in the plane of the plate. In the following problems longitudinal axis of the top and bottom layers coincide with the x-axis (i.e. $\theta = 0$) and that of the middle layer is perpendicular to these (i.e. $\theta = 90$). Thus we have 0°/90°/0° orientation of the laminates and the elements of matrix $\underset{\approx}{T}$ in Eq. (22) are known. Only a sinusoidal load with a unit central intensity and varying as

$$p(x,y) = \sin\frac{\pi x}{a} \sin\frac{\pi y}{a}$$

is considered to be acting transversely on the plate.

The properties of the lamina with respect to their

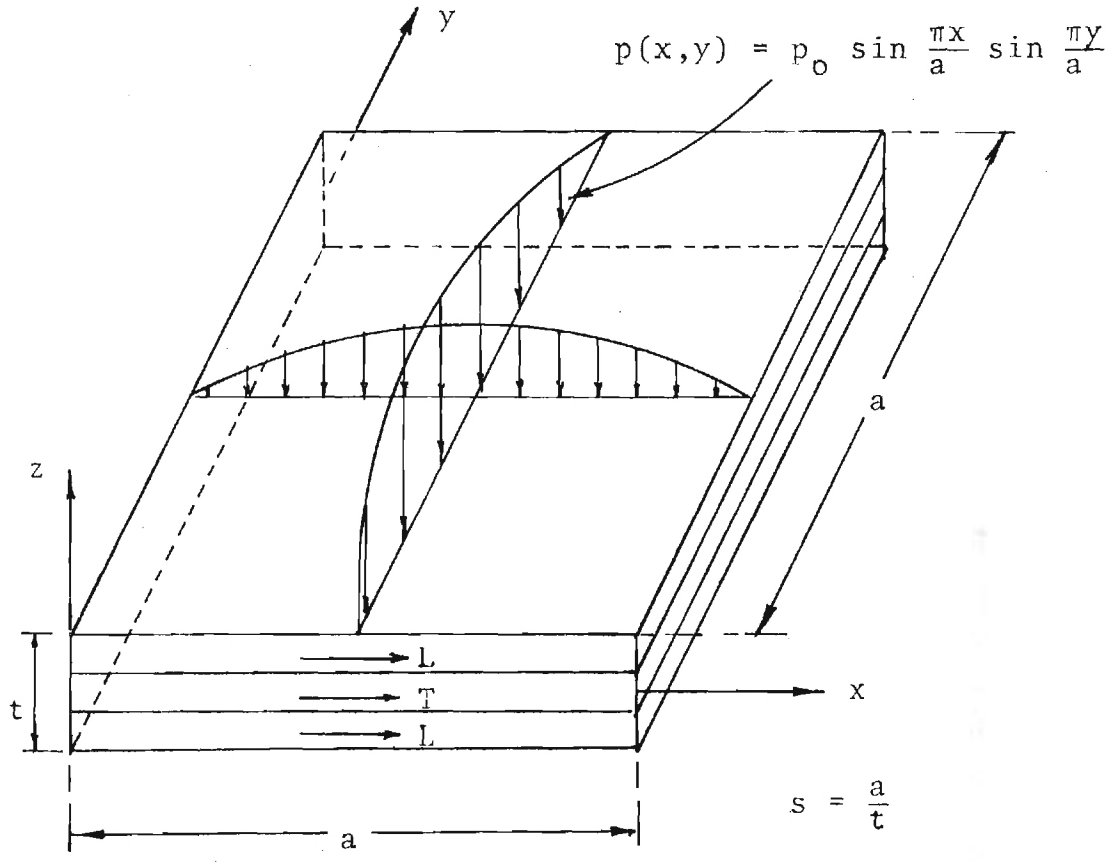

Fig. 9. Details for Three-Layer Square Plate Under Sinusoidal Load

principal axes of symmetry (Fig. 6) are:

$$E_1 = 25 \times 10^6 \text{ psi}$$

$$E_2 = 1 \times 10^6 \text{ psi}$$

$$G_{12} = 0.5 \times 10^6 \text{ psi}$$

$$G_{23} = 0.2 \times 10^6 \text{ psi}$$

$$\mu_{12} = \mu_{23} = 0.25$$

Thus we have the six independent elastic constants that describe the stress-strain relations for each layer (Eq. (24)).

The span to depth ratio ($S = \frac{a}{t}$) is varied in the following examples and the stresses and displacements are normalized for plotting purposes as follows:

$$\bar{\sigma}_x = \frac{1}{S^2} \sigma_x$$

$$\bar{\sigma}_{xy} = \frac{1}{S^2} \sigma_{xy}$$

$$\bar{\sigma}_{xz} = \frac{1}{S} \sigma_{xz}$$

$$\bar{u} = \frac{E_2}{t S^3} u$$

and

$$\bar{z} = \frac{z}{t}$$

The simply supported boundary conditions are (Fig. 9)

at $x = 0$ or a, $v = w = 0$

at $y = 0$ or a, $u = w = 0$

In the graphs that follow the examples, results are plotted as obtained by three methods. Firstly, results from the classical laminated plate theory (due to Reissner) are shown. These results do not take into account transverse shear deformation. The next two sets of results, one obtained by Barker-Lin-Dana (Ref. 11) and the other by the present study, both account for transverse shear deformation in their analyses.

The results given by Barker-Lin-Dana utilize a 2 x 2 mesh in the quarter plate. Since their method is mainly a three dimensional finite element analysis, each of the three layers is assumed to have three elements in the thickness direction. Each quadrilateral element has two triside nodes and each node has three degrees of freedom. Thus each element has 72 degrees of freedom.

Case 1: This example has a span to depth ratio equal to four (i.e. S = 4). A 2 x 2 mesh is used in quarter plate and it has 990 degrees of freedom. Fig. 10 shows the plotting of the variation of the in-plane displacement u at (a,a/2) through the thickness. It can be seen that the results obtained by the three dimensional analysis and the present study agree fairly well. The result of the classical plate theory does not agree well with the above results due to the fact that transverse shear deformation has not been considered here. Fig. 11 shows the variation of the normal stress σ_x at the center of the plate and Fig. 12 shows the

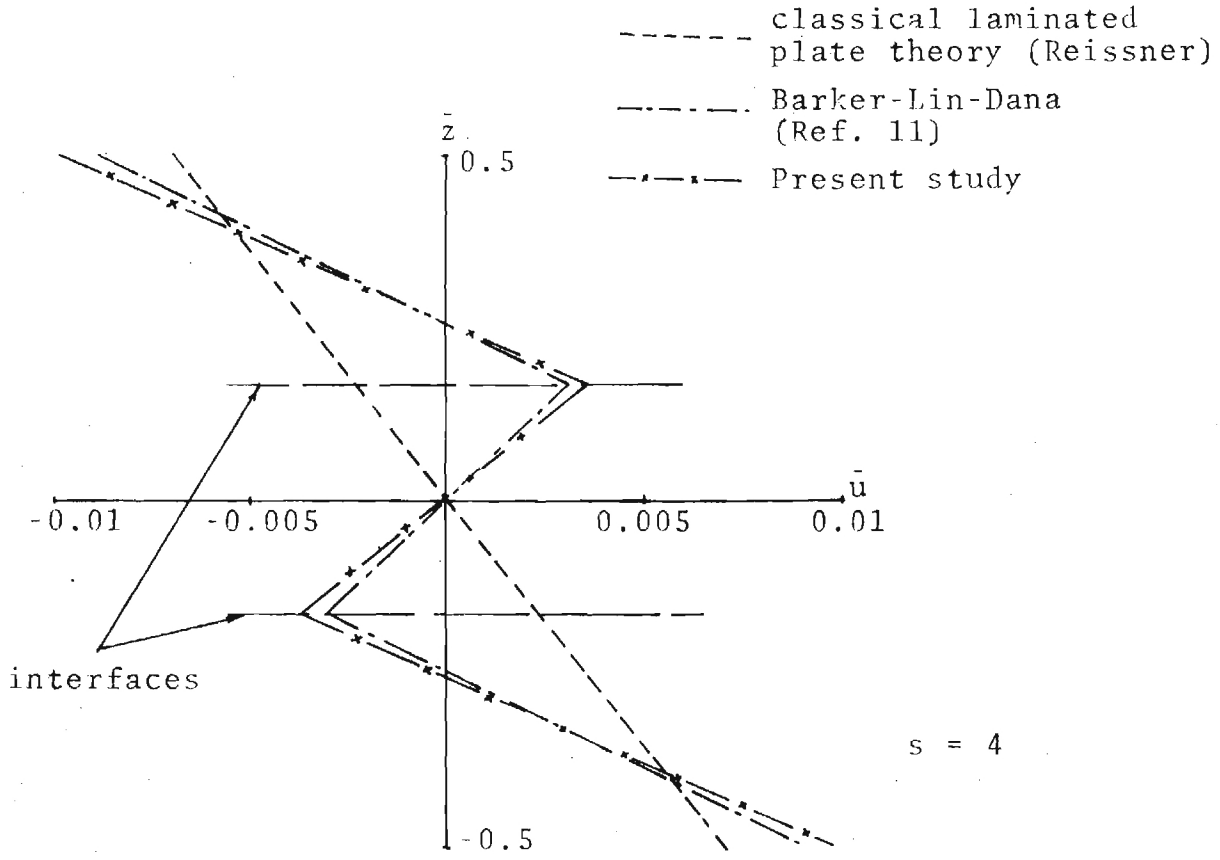

Simply supported 3-layer square plate
with sinusoidal loading

Fig. 10. Variation of In-Plane Displacement $\bar{u}$ (a, $\frac{a}{2}$, z)

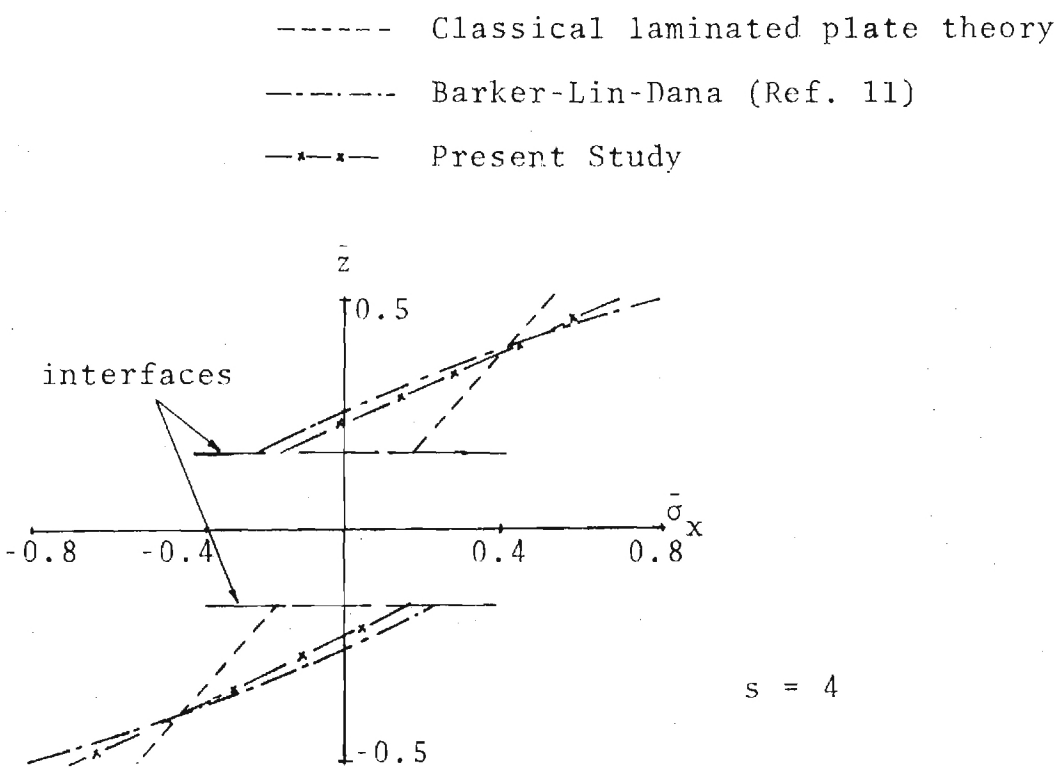

Simply supported 3-layer square plate
with sinusoidal loading

Fig. 11. Variation of Normal Stress $\bar{\sigma}_x$ $(\frac{a}{2}, \frac{a}{2}, z)$

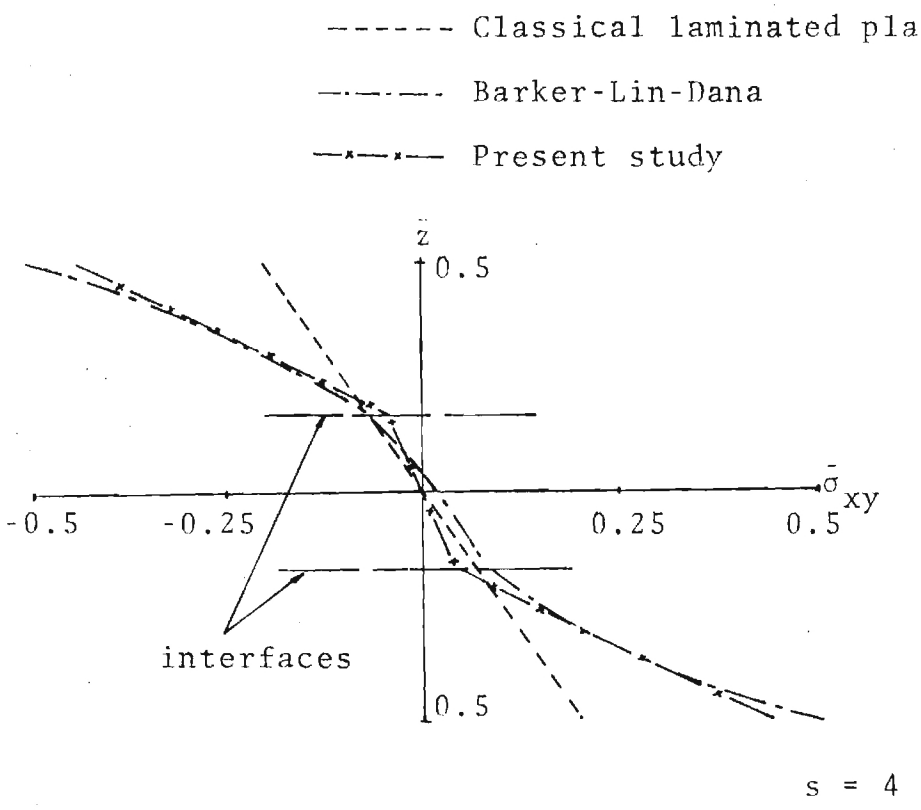

Simply supported 3-layer square plate
with sinusoidal loading

Fig. 12. Variation of In-Plane Shear Stress $\bar{\sigma}_{xy}$ (a,a,z)

variation of in-plane shear stress σ_{xy} at the corner of the plate. Fig. 13 is a plot of the variation of transverse shear stress σ_{xz} through the thickness.

In all these cases, good agreement can be inferred between the results obtained in the present study and the three-dimensional finite element analysis. However, the results of the classical plate theory can not be relied on in all these cases.

Case 2: The next four figures pertain to the case where the span to depth ratio is increased to 10 (i.e. S = 10). In this case Barker-Lin-Dana have used a 3 x 3 mesh for a quarter plate with only two elements through the thickness of each layer. Thus the number of degrees of freedom for the quarter plate is 1344. However, the same material properties as in the previous example are retained here. Fig. 14 shows the variation of the in-plane displacement u at the side of the plate. Figs. 15 and 16 show the variation of the normal and in-plane shear stresses at the center and the corner of the plate, respectively. Fig. 17 shows variation of the transverse shear stress at the side of the plate.

It can be seen from these plots that there is a very good agreement between the results obtained by the present study and by the three dimensional finite element analysis. Also the results due to classical plate theory tend to agree with the finite element results more in this case than in

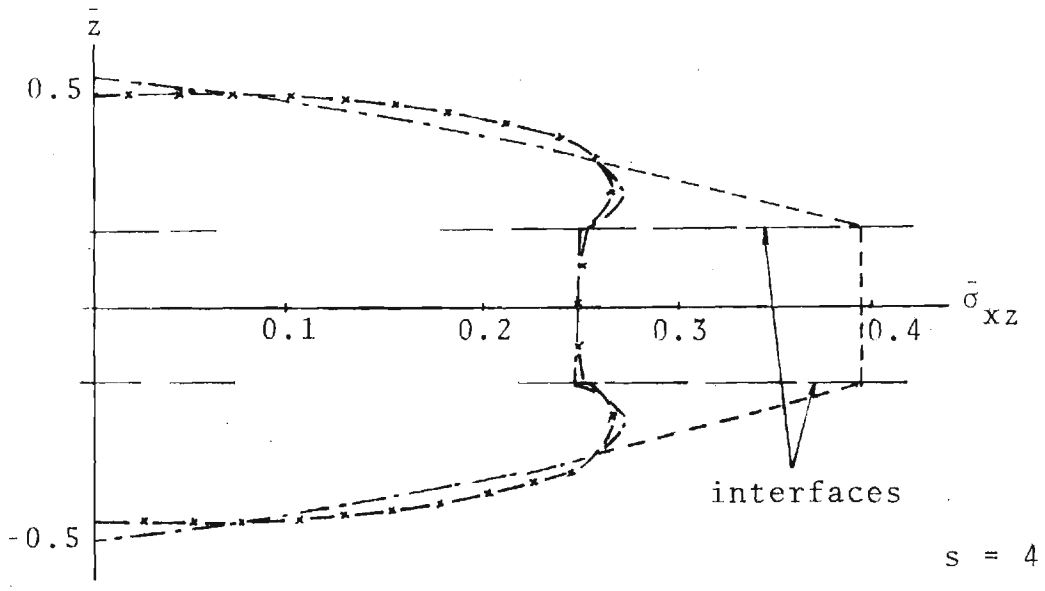

Simply supported 3-layer square plate
with sinusoidal loading

Fig. 13. Variation of Transverse Shear Stress $\bar{\sigma}_{xz}$ (a, $\frac{a}{2}$, z)

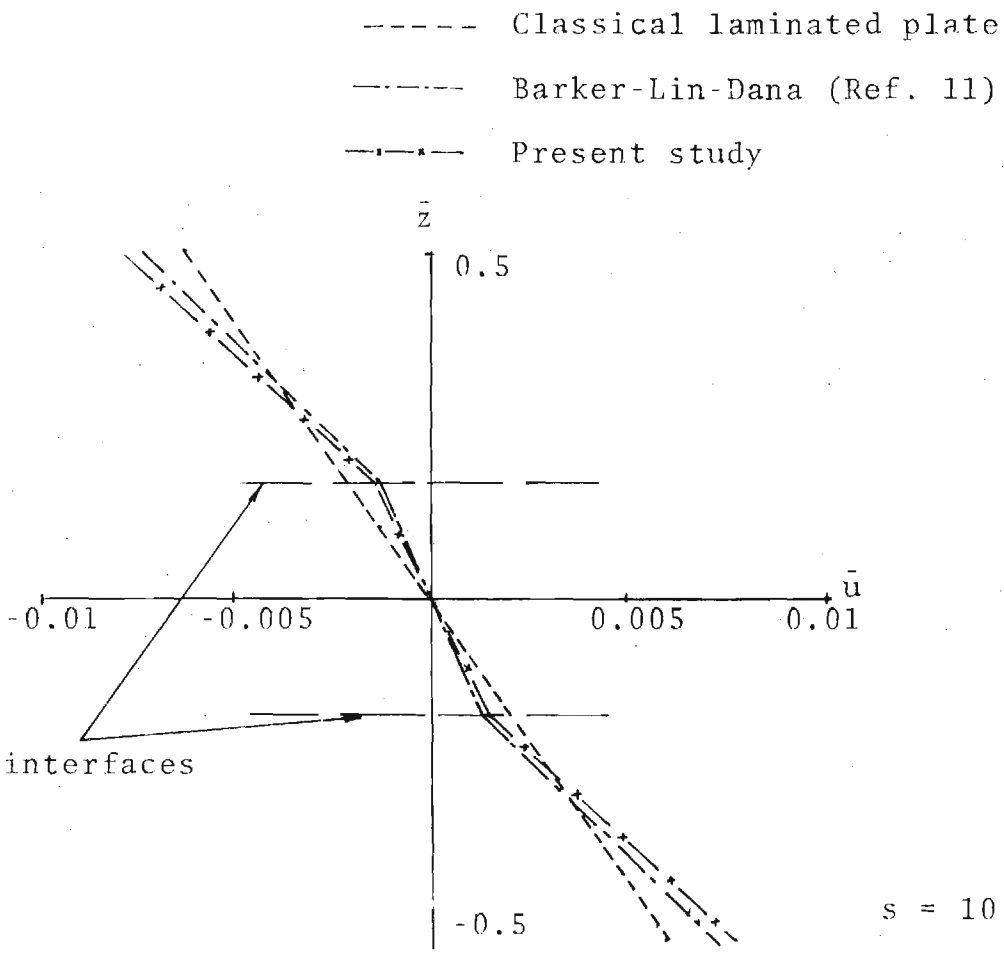

Simply supported 3-layer plate under sinusoidal loading

Fig. 14. Variation of In-Plane Displacement $\bar{u}$ (a, $\frac{a}{z}$, z)

------ Classical laminated plate theory

—·—·— Barker-Dana-Lin

—•— x —— Present study

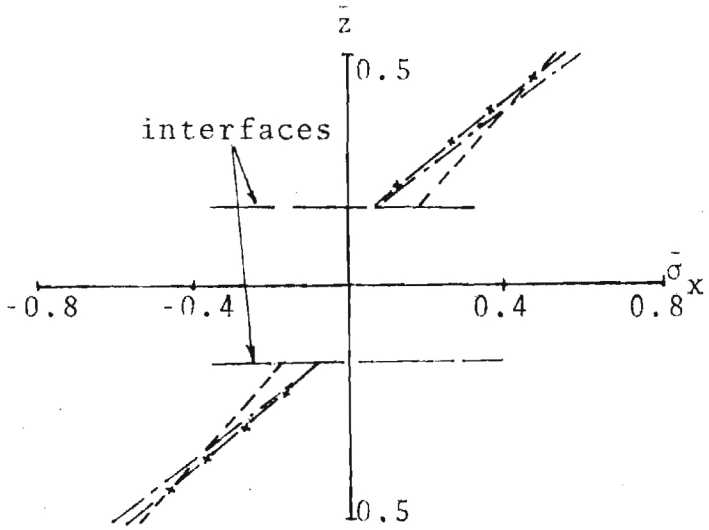

s = 10

Simply supported 3-layer plate under sinusoidal loading

Fig. 15. Variation of Normal Stress $\bar{\sigma}_x$ $(\frac{a}{2}, \frac{a}{2}, z)$

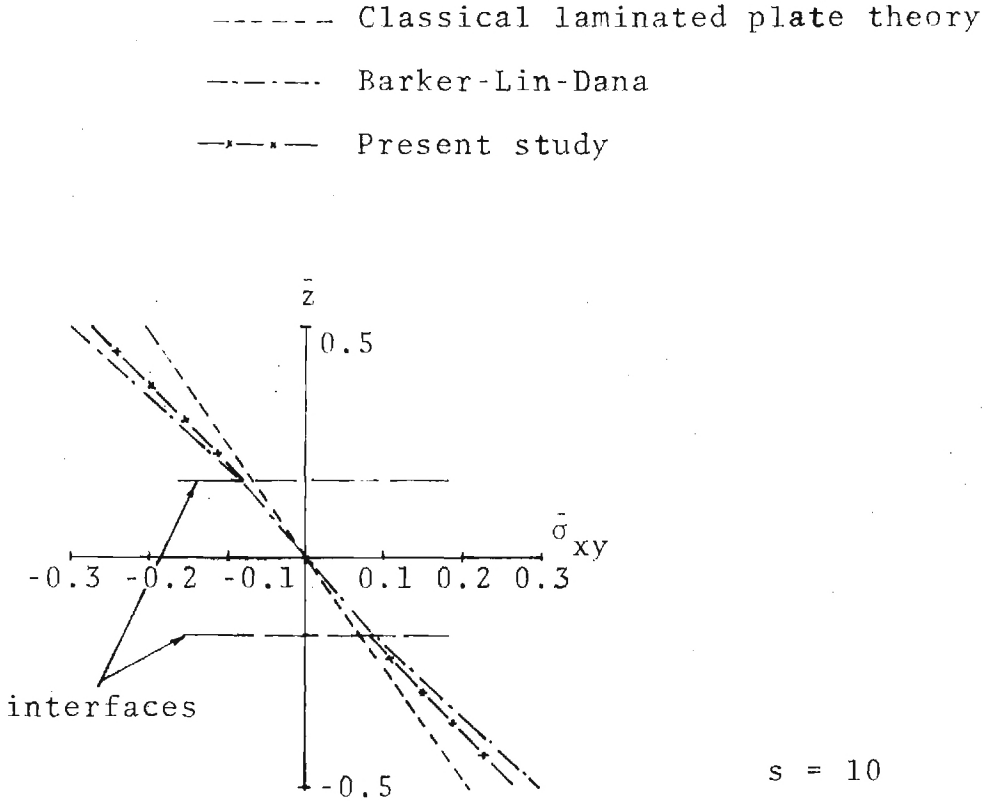

Simply supported 3-layer plate under sinusoidal loading

Fig. 16. Variation of In-Plane Shear Stress $\bar{\sigma}_{xy}$ (a,a,z)

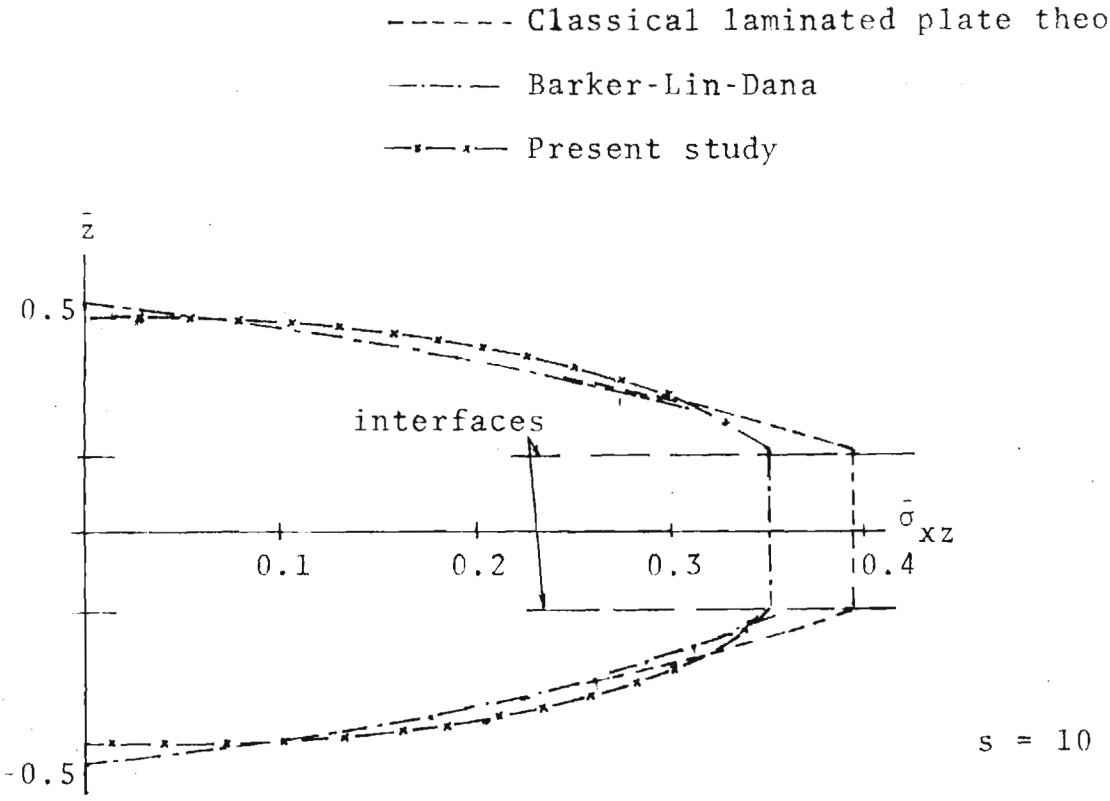

Simply supported 3-layer plate under
sinusoidal loading

Fig. 17. Variation of Transverse Shear Stress $\bar{\sigma}_{xz}$ (a, $\frac{a}{2}$, z)

the previous case. This explains the well known fact that the effect of transverse shear deformation becomes smaller as the plate becomes thinner.

Viewing all these results in an overall fashion, it is evident that the transverse shear deformations are effectively taken care of by the present finite element model particularly in case of laminated composites such as automobile tires where the distortion of the section of the plate can be expected.

Also as can be seen from u-displacement in Fig. 10 (case of a thick plate) the original normal is seen to be distorted considerably where as the u-displacement in the latter case (case of thin plate, Fig. 14) shows a distortion which is far less than the first case.

The good comparisons indicate that the present model could be extended to the analysis of shells for the case of automobile tires. The present finite element formulation can also be modified to take into account large deformations to make the analysis of the tire problem more accurate.

APPENDIX

COMPUTER PROGRAM

```
      PROGRAM MAIN(INPUT,OUTPUT,TAPE5=INPUT,TAPE6=OUTPUT)
      DIMENSION A(6,31),AL(5),BL(5),CL(5),DL(5), BE(9,31),BT(31,9), ZA(
     15),ZH(5), U(9,21),X(5 ,3),Y(5 ,3),TO1(31,31),  B(6,6),BA(6,31),H(3
     21,31),HS(31,31),AI(31, 6),JC(31),     TT(31,31),HT(21,21),
     3  BC(31,3),BD(31,3),BE(31,3),UA(3,21),UB(3,21),UC(3,21),TV(31,21),
     4 TO2(31,21),DS(31,6), T1(31,21),T2(21,21),T3(31,21),UI(31,31),
     5    AV(46,46),   Q(46), NBCC(24),NBIXC(24),NBCM(24),NO(15),IREF(7),
     6HV(33,33),IGLCOR(50,3),IGLMID(50,6),NCO(40),NUM(206),NUMB(50,3),
     7 QL(33),QE(33,1),QQ(6,1), JC1(6), XX(3),YY(3),T(6,33),TR(33,6),
     8 THE(6),TRN(6,6),TTR(6,6),TRNN(6,6),T11(31,21,2),TO22(31,21,2),
     9HII(31,31,2),AA(6,31),BQ(6,1)
      REAL NX12,NY12,NX23,NY23,NX13,NY13,L12,L23,L13
      DATA IREF/1,2,3,4,5,6,7/
C     READING DATA- NO. OF ELEMENTS,TOTAL NO. OF CORNER NODES,TOTAL NO.
C     OF MIDSIDE NODES, DOF FOR CORNER NODE,DOF FOR MIDSIDE NODE
      READ(5,10) NELTS,NTNCOR,NTNMID,NDFCOR,NDFMID
   10 FORMAT(5I5)
      READ(5,*) KQ,NBAND
C     READING GLOBAL NOS. OF CORNER NODES FOR THE STRUCTURE
      READ(5,*)(NCO(I),I=1,NTNCOR)
C     READING SEQUENTIAL GLOBAL NODAL NOS. OF CORNER AND MIDSIDE NODES
C     FOR EACH ELEMENT
      READ(5,*)  ((IGLCOR(I,J),J=1,3),I=1,NELTS)
      READ(5,*)  ((IGLMID(I,J),J=1,6),I=1,NELTS)
      NU=-1
      DO 4 I=1,NTNCOR
      LL=NCO(I)
      NU=NU+1
      NUM(LL)=NU
    4 CONTINUE
      DO 3  II=1,NELTS
      DO 3   I=1,3
      L9=IGLCOR(II,I)
    3 NUMB(II,I)=NUM(L9)
C     STORAGE OF ALL INTEGRATION CONSTANTS FOR USE IN GAUSS QUADRATURE
C     AND GAUSS-RADAU FORMULAE
      BL(1)=0.0469100770
      BL(2)=0.2307653449
      BL(3)=0.5
      BL(4)=0.7692346551
      BL(5)=0.9530899230
      AL(1)=0.0398098571
      AL(2)=0.1980134179
      AL(3)=0.4379748102
      AL(4)=0.6954642734
      AL(5)=0.9014649142
      CL(1)=0.1007941926
      CL(2)=0.2084506672
      CL(3)=0.2646623916
      CL(4)=0.2426935942
      CL(5)=0.1598203766
      DL(1)=0.1184634425
      DL(2)=0.2393143353
      DL(3)=0.2844444444
      DL(4)=0.2393143353
      DL(5)=0.1184634425
      ZA(1)=0.9061798459387
      ZA(2)=0.5384693101057
      ZA(3)=0.0
      ZA(4)=-0.5384693101057
      ZA(5)=-0.9061798459387
      ZH(1)=0.2369268850562
      ZH(2)=0.4786286704994
```

```
      ZH(3)=0.568888888889
      ZH(4)=0.478628704094
      ZH(5)=0.236926885056
C     READING THICKNESS,POISSONS RATIO AND ELASTIC MODULII
      READ(5,*) THICK,PROP,EXL,EXT,GLT,GTT
C     READING OVERALL DIMENSIONS OF THE PLATE
      READ(5,*) ALE,BLE
C     READING ORIENTATION OF THE PRINCIPAL AXES
      READ(5,*) (THE(I),I=1,3)
      B(1,1)=1.0/EXL
      B(1,2)=-PROP/EXL
      B(1,3)=B(1,2)
      B(2,1)=B(1,2)
      B(2,2)=1.0/EXT
      B(2,3)=-PROP/EXT
      B(3,1)=B(1,3)
      B(3,2)=B(2,3)
      B(3,3)=1.0/EXT
      B(4,4)=1.0/GLT
      B(5,5)=1.0/GTT
      B(6,6)=1.0/GLT
      NTOT=(NTNCOR*NDECOR)+(NTNMID*NDEMID)
      DO 2 I=1,NTOT
      Q(I)=0.0
      DO 2 J=1,NBAND
    2 AV(I,J)=0.0
      DO 134 I=1,6
      DO 134 J=1,31
  134 AA(I,J)=0.0
      NU=0
      DO 98 IJ=1,2
      NU=NU+1
C     READING THE COORDINATES FOR A TYPICAL ELEMENT
      READ(5,8)(X(IJ,J),J=1,3)
    8 FORMAT(3F15.6)
      READ(5,8)(Y(IJ,J),J=1,3)
      L12=SQRT(((X(IJ,1)-X(IJ,2))**2.0)+((Y(IJ,1)-Y(IJ,2))**2.0))
      L23=SQRT(((X(IJ,2)-X(IJ,3))**2.0)+((Y(IJ,2)-Y(IJ,3))**2.0))
      L13=SQRT(((X(IJ,1)-X(IJ,3))**2.0)+((Y(IJ,1)-Y(IJ,3))**2.0))
      NX12=(Y(IJ,2)-Y(IJ,1))/L12
      NY12=(X(IJ,1)-X(IJ,2))/L12
      NX23=(Y(IJ,3)-Y(IJ,2))/L23
      NY23=(X(IJ,2)-X(IJ,3))/L23
      NX13=(Y(IJ,1)-Y(IJ,3))/L13
      NY13=(X(IJ,3)-X(IJ,1))/L13
C     EVALUATION OF THE JACOBIAN OF TRANSFORMATION
      DETJ=((X(IJ,1)-X(IJ,3))*(Y(IJ,2)-Y(IJ,3)))-((Y(IJ,1)-Y(IJ,3))*(X(I
     1J,2)-X(IJ,3)))
      DO 30 I=1,31
      DO 30 J=1,21
      T1(I,J)=0.0
      T2(I,J)=0.0
      T3(I,J)=0.0
   30 TQ2(I,J)=0.0
      DO 14 I=1,33
      DO 14 J=1,33
   14 HV(I,J)=0.0
      DO 24 M=1,9
      DO 24 N=1,31
   24 DE(M,N)=0.0
      DO 23 M=1,9
      DO 23 N=1,21
   23 U(M,N)=0.0
```

```
C       EVALUATION OF AREA INTEGRALS
        DO 31 K1=1,5
        DO 32 K2=1,5
        BF(1,1)=NX12
        BF(1,3)=NY12
        ESPL=(1.0+ZA(K1))/2.0
        ESMN=(1.0-ZA(K1))/2.0
        EX12=(X(IJ,1)*ESMN)+(X(IJ,2)*ESPL)
        EY12=(Y(IJ,1)*ESMN)+(Y(IJ,2)*ESPL)
        BF(1,4)=EX12*NX12
        BF(1,6)=EX12*NY12
        BF(1,7)=EY12*NX12
        BF(1,9)=EY12*NY12
        BF(1,10)=EX12*EY12*NX12
        BF(1,12)=ZA(K2)*THICK*NX12
        BF(1,14)=ZA(K2)*THICK*NY12
        XZH12=ZA(K2)*THICK*EX12
        YZH12=ZA(K2)*THICK*EY12
        BF(1,15)=XZH12*NX12
        BF(1,17)=XZH12*NY12
        BF(1,18)=YZH12*NX12
        BF(1,20)=YZH12*NY12
        BF(1,21)=YZH12*EX12*NX12
        BF(2,2)=NY12
        BF(2,3)=NX12
        BF(2,5)=BF(1,6)
        BF(2,6)=BF(1,4)
        BF(2,8)=BF(1,9)
        BF(2,9)=BF(1,7)
        BF(2,11)=EX12*EY12*NY12
        BF(2,13)=BF(1,14)
        BF(2,14)=BF(1,12)
        BF(2,16)=BF(1,17)
        BF(2,17)=BF(1,15)
        BF(2,19)=BF(1,20)
        BF(2,20)=BF(1,18)
        BF(2,22)=YZH12*EX12*NY12
        THZ=THICK*ZA(K2)
        STHZ=(THZ**2.0)/2.0
        THZ=-THZ
        BF(3,4)=THZ*NX12
        BF(3,6)=THZ*NY12
        BF(3,8)=BF(3,6)
        BF(3,9)=BF(3,4)
        BF(3,10)=-BF(1,18)
        BF(3,11)=-BF(1,17)
        BF(3,15)=-STHZ*NX12
        BF(3,17)=-STHZ*NY12
        BF(3,19)=BF(3,17)
        BF(3,20)=BF(3,15)
        BF(3,21)=BF(3,20)*EY12
        BF(3,22)=BF(3,17)*EX12
        BF(3,23)=NY12
        BF(3,24)=NX12
        BF(3,25)=BF(1,6)
        BF(3,26)=BF(1,4)-BF(1,9)
        BF(3,27)=BF(1,7)
        BF(3,28)=BF(2,11)-(BF(2,6)*EX12/2.0)
        BF(3,29)=BF(1,10)-(BF(1,9)*EY12/2.0)
        BF(3,30)=(EX12**2.0)*NY12
        BF(3,31)=(EY12**2.0)*NX12
        EX23=(X(IJ,2)*ESMN)+(X(IJ,3)*ESPL)
        EY23=(Y(IJ,2)*ESMN)+(Y(IJ,3)*ESPL)
```

```
BF(4,1)=NX23
BF(4,3)=NY23
BF(4,4)=FX23*NX23
BF(4,6)=FX23*NY23
BF(4,7)=FY23*NX23
BF(4,9)=FY23*NY23
BF(4,10)=BF(4,4)*FY23
XZH23=ZA(K2)*THICK*FX23
YZH23=ZA(K2)*THICK*FY23
BF(4,12)=ZA(K2)*THICK*NX23
BF(4,14)=ZA(K2)*THICK*NY23
BF(4,15)=XZH23*NX23
BF(4,17)=XZH23*NY23
BF(4,18)=YZH23*NX23
BF(4,20)=YZH23*NY23
BF(4,21)=YZH23*FX23*NX23
BF(5,2)=NY23
BF(5,3)=NX23
BF(5,5)=BF(4,6)
BF(5,6)=BF(4,4)
BF(5,8)=BF(4,9)
BF(5,9)=BF(4,7)
BF(5,11)=FX23*FY23*NY23
BF(5,13)=BF(4,14)
BF(5,14)=BF(4,12)
BF(5,16)=BF(4,17)
BF(5,17)=BF(4,15)
BF(5,19)=BF(4,20)
BF(5,20)=BF(4,18)
BF(5,22)=YZH23*FX23*NY23
BF(6,4)=THZ*NX23
BF(6,6)=THZ*NY23
BF(6,8)=BF(6,6)
BF(6,9)=BF(6,4)
BF(6,10)=-BF(5,20)
BF(6,11)=-BF(5,16)
BF(6,15)=-STHZ*NX23
BF(6,17)=-STHZ*NY23
BF(6,19)=BF(6,17)
BF(6,20)=BF(6,15)
BF(6,21)=BF(6,20)*FY23
BF(6,22)=BF(6,17)*FX23
BF(6,23)=NY23
BF(6,24)=NX23
BF(6,25)=BF(4,6)
BF(6,26)=BF(4,4)-BF(4,9)
BF(6,27)=BF(4,7)
BF(6,28)=BF(5,11)-(BF(5,6)*FX23/2.0)
BF(6,29)=BF(4,10)-(BF(4,9)*FY23/2.0)
BF(6,30)=(FX23**2.0)*NY23
BF(6,31)=(FY23**2.0)*NX23
FX13=(X(IJ,1)*FSPL)+(X(IJ,3)*FSMN)
FY13=(Y(IJ,1)*FSPL)+(Y(IJ,3)*FSMN)
BF(7,1)=NX13
BF(7,3)=NY13
BF(7,4)=FX13*NX13
BF(7,6)=FX13*NY13
BF(7,7)=FY13*NX13
BF(7,9)=FY13*NY13
BF(7,10)=BF(7,4)*FY13
BF(7,12)=ZA(K2)*THICK*NX13
BF(7,14)=ZA(K2)*THICK*NY13
XZH13=ZA(K2)*THICK*FX13
```

```
YZH13=ZA(K2)*THICK*EY13
BF(7,15)=XZH13*NX13
BF(7,17)=XZH13*NY13
BF(7,18)=YZH13*NX13
BF(7,20)=YZH13*NY13
BF(7,21)=YZH13*EX13*NX13
BF(8,2)=NY13
BF(8,3)=NX13
BF(8,5)=BF(7,6)
BF(8,6)=BF(7,4)
BF(8,8)=BF(7,9)
BF(8,9)=BF(7,7)
BF(8,11)=EX13*EY13*NY13
BF(8,13)=BF(7,14)
BF(8,14)=BF(7,12)
BF(8,16)=BF(7,17)
BF(8,17)=BF(7,15)
BF(8,19)=BF(7,20)
BF(8,20)=BF(7,18)
BF(8,22)=YZH13*EX13*NY13
BF(9,4)=THZ*NX13
BF(9,6)=THZ*NY13
BF(9,8)=BF(9,6)
BF(9,9)=BF(9,4)
BF(9,10)=-BF(8,20)
BF(9,11)=-BF(8,16)
BF(9,15)=-STHZ*NX13
BF(9,17)=-STHZ*NY13
BF(9,19)=BF(9,17)
BF(9,20)=BF(9,15)
BF(9,21)=BF(9,20)*EY13
BF(9,22)=BF(9,17)*EX13
BF(9,23)=NY13
BF(9,24)=NX13
BF(9,25)=BF(7,6)
BF(9,26)=BF(7,4)-BF(7,9)
BF(9,27)=BF(7,7)
BF(9,28)=BF(8,11)-(BF(8,6)*EX13/2.0)
BF(9,29)=BF(7,10)-(BF(7,9)*EY13/2.0)
BF(9,30)=(EX13**2.0)*NY13
BF(9,31)=(EY13**2.0)*NX13
SMN=1.0-ZA(K1)
SPL=1.0+ZA(K1)
ZMN=(1.0-ZA(K2))/4.0
ZPL=(1.0+ZA(K2))/4.0
U(1,1)=SMN*ZPL
U(1,4)=SMN*ZMN
U(1,8)=SPL*ZPL
U(1,11)=SPL*ZMN
U(2,2)=U(1,1)
U(2,5)=U(1,4)
U(2,9 )=U(1,8)
U(2,12)=U(1,11)
STMN=1.0-(3.0*ZA(K1))
STPL=1.0+(3.0*ZA(K1))
U(3,3)=-(SMN*STMN*STPL)/16.0
U(3,10)=-(SPL*STMN*STPL)/16.0
U(3, 6)=(9.0*SPL*SMN*STMN)/16.0
U(3, 7)=(9.0*SPL*SMN*STPL)/16.0
U(4,8)=U(1,1)
U(4,11)=U(1,4)
U(4,15)=U(1,8)
U(4,18)=U(1,11)
```

```
      U(5,9)=U(1,1)
      U(5,12)=U(1,4)
      U(5,16)=U(1,8)
      U(5,19)=U(1,11)
      U(6,10)=U(2,3)
      U(6,13)=U(2,6)
      U(6,14)=U(2,7)
      U(6,17)=U(2,10)
      U(7,1)=U(1,8)
      U(7,4)=U(1,11)
      U(7,15)=U(1,1)
      U(7,18)=U(1,4)
      U(8,2)=U(7,1)
      U(8,5)=U(7,4)
      U(8,16)=U(7,15)
      U(8,19)=U(7,18)
      U(9,3)=U(3,10)
      U(9,17)=U(3,3)
      U(9,20)=U(3, 6)
      U(9,21)=U(3, 7)
      CALL MXTRN(BE,BT,9,31,9,31)
      DO 11 M=1,31
      DO 11 N=1,3
      BC(M,N)=BT(M,N)
      N1=N+3
      BD(M,N)=BT(M,N1)
      N2=N1+3
   11 BE(M,N)=BT(M,N2)
      DO 12 M=1,3
      DO 12 N=1,21
      UA(M,N)=U(M,N)
      M1=M+3
      UB(M,N)=U(M1,N)
      M2=M1+3
   12 UC(M,N)=U(M2,N)
      CALL MXMLT(BC,UA,TM,31,3,21,31,3)
      DO 15 MM=1,31
      DO 15 NN=1,21
   15 T1(MM,NN)=(T1(MM,NN)+TM(MM,NN)*ZH(K1)*ZH(K2))
      CALL MXMLT(BD,UB,TM,31,3,21,31,3)
      DO 16 MM=1,31
      DO 16 NN=1,21
   16 T2(MM,NN)=(T2(MM,NN)+TM(MM,NN)*ZH(K1)*ZH(K2))
      CALL MXMLT(BE,UC,TM,31,3,21,31,3)
      DO 17 MM=1,31
      DO 17 NN=1,21
   17 T3(MM,NN)=(T3(MM,NN)+TM(MM,NN)*ZH(K1)*ZH(K2))
   32 CONTINUE
   31 CONTINUE
      DO 44 M=1,31
      DO 44 N=1,21
      T1(M,N)=T1(M,N)*L12*THICK/2.0
      T2(M,N)=T2(M,N)*L23*THICK/2.0
      T3(M,N)=T3(M,N)*L13*THICK/2.0
      T1(M,N)=T1(M,N)+T2(M,N)+T3(M,N)
   44 T11(M,N,NU)=T1(M,N)
C     MATRIX T1 CONTAINS THE ELEMENTS OF MATRIX DUE TO AREA INTEGRAL
C     OVER INTERELEMENT BOUNDARY
      DO 56 I=1,9
      DO 56 J=1,21
   56 U(I,J)=0.0
      DO 25 I=1,9
      DO 25 J=1,31
```

```
25  BF(I,J)=0.0
    DO 33 I=1,5
    DO 34 J=1,5
    EL1=AL(I)
    EL4=1.0-EL1
    EL2=(BL(J)-(BL(J)*EL1))
    EL3=EL4-EL2
    WT=EL4*CL(I)
    WT=WT*DL(J)
    TEL11=((3.0*EL1)-1.0)
    TEL12=((3.0*EL1)-2.0)
    TEL21=((3.0*EL2)-1.0)
    TEL22=((3.0*EL2)-2.0)
    TEL31=((3.0*EL3)-1.0)
    TEL32=((3.0*EL3)-2.0)
    X123=(X(IJ,1)*EL1)+(X(IJ,2)*EL2)+(X(IJ,3)*EL3)
    Y123=(Y(IJ,1)*EL1)+(Y(IJ,2)*EL2)+(Y(IJ,3)*EL3)
    STH=(THICK**2.0)/2.0
    BF(1, 4)=-THICK
    BF(1, 9)=BF(1, 4)
    BF(1, 10)=-THICK*Y123
    BF(1, 15)=-STH
    BF(1, 20)=-STH
    BF(1, 21)=-STH*Y123
    BF(1, 24)=1.0
    BF(1, 26)=X123
    BF(1, 27)=Y123
    BF(1, 28)=-(X123**2.0)/2.0
    BF(1, 29)=X123*Y123
    BF(1, 31)=Y123**2.0
    BF(2, 6)=BF(1, 4)
    BF(2,8)=BF(2,6)
    BF(2, 11)=-THICK*X123
    BF(2, 17)=-STH
    BF(2, 19)=-STH
    BF(2, 22)=-STH*X123
    BF(2, 23)=1.0
    BF(2, 25)=X123
    BF(2, 26)=-Y123
    BF(2, 28)=BF(1, 29)
    BF(2, 29)=-BF(1, 31)/2.0
    BF(2, 30)=X123**2.0
    BF(4, 4)=BF(1, 4)
    BF(4, 9)=BF(1, 9)
    BF(4, 10)=BF(1 ,10)
    BF(4, 15)=-BF(1, 15)
    BF(4, 20)=-BF(1, 20)
    BF(4, 21)=-BF(1, 21)
    BF(4, 24)=-1.0
    BF(4, 26)=-BF(1, 26)
    BF(4, 27)=-BF(1, 27)
    BF(4, 28)=-BF(1, 28)
    BF(4, 29)=-BF(1, 29)
    BF(4, 31)=-BF(1, 31)
    BF(5, 6)=BF(2, 6)
    BF(5, 8)=BF(2, 8)
    BF(5, 11)=BF(2, 11)
    BF(5, 17)=-BF(2, 17)
    BF(5, 19)=-BF(2, 19)
    BF(5, 22)=-BF(2, 22)
    BF(5, 23)=-1.0
    BF(5, 25)=-BF(2, 25)
    BF(5, 26)=Y123
```

```
      BE(5, 28)=-BE(2, 28)
      BE(5, 29)=-BE(2, 29)
      BE(5, 30)=-BE(2, 30)
      U(1, 1)=EL1
      U(1, 8)=EL2
      U(1, 15)=EL3
      U(2, 2)=EL1
      U(2, 9)=EL2
      U(2, 16)=EL3
      U(3, 3)=(EL1*TEL11*TEL12)/2.0
      U(3, 10)=(EL2*TEL21*TEL22)/2.0
      U(3, 17)=(EL3*TEL31*TEL32)/2.0
      U(3, 6)=(9.0*EL1*EL2*TEL11)/2.0
      U(3, 7)=(9.0*EL1*EL2*TEL21)/2.0
      U(3, 13)=(9.0*EL2*EL2*TEL21)/2.0
      U(3, 14)=(9.0*EL3*EL2*TEL31)/2.0
      U(3, 20)=(9.0*EL3*EL1*TEL31)/2.0
      U(3, 21)=(9.0*EL3*EL1*TEL11)/2.0
      U(4, 4)=EL1
      U(4, 11)=EL2
      U(4, 18)=EL3
      U(5,5)=EL1
      U(5,12)=EL2
      U(5,19)=EL3
      U(6,3)=U(3,3)
      U(6,6)=U(3,6)
      U(6,13)=U(3,13)
      U(6,14)=U(3,14)
      U(6, 17)=U(3, 17)
      U(6, 10)=U(3, 10)
      U(6, 7)=U(3, 7)
      U(6, 20)=U(3, 20)
      U(6, 21)=U(3, 21)
      CALL MXTRN(BE,BS,6,31,9,31)
      CALL MXMLT(BS,U ,TQ1,31,6,21,31,9)
      DO 18 MM=1,31
      DO 18 NN=1,21
      TQ1(MM,NN)=TQ1(MM,NN)*WT
   18 TQ2(MM,NN)=TQ2(MM,NN)+TQ1(MM,NN)
   34 CONTINUE
   33 CONTINUE
      DO 22 M=1,31
      DO 22 N=1,21
      TQ2(M,N)=TQ2(M,N)*DETJ
   22 TQ22(M,N,NU)=TQ2(M,N)
C     MATRIX TQ2 CONTAINS ELEMENTS OF MATRIX DUE TO AREA INTEGRAL OVER
C     INTERLAYER BOUNDARY
      CALL MXTRN(T1,TT,31,21,31,31)
      CALL MXTRN(TQ2,TQ1,31,21,31,31)
      MA=-2
      MAA=43
      DO 112 KJ=1,3
      DO 13 I=1,21
      DO 13 J=1,21
   13 HT(I,J)=0.0
      DO 83 I=1,31
      DO 83 J=1,31
   83 H(I,J)=0.0
C     EVALUATION OF ELEMENTS OF COMPLIANCE MATRIX FOR EACH LAYER
      THRD=THE(KJ)*3.14159265/180.0
      COST=COS(THRD)
      SINT=SIN(THRD)
      TRN(1,2)=SINT**2.0
```

```
      TRN(1,1)=COST**2.0
      TRN(1,4)=-2.0*COST*SINT
      TRN(2,2)=TRN(1,1)
      TRN(2,1)=TRN(1,2)
      TRN(2,4)=-TRN(1,4)
      TRN(3,3)=1.0
      TRN(4,1)=COST*SINT
      TRN(4,2)=-COST*SINT
      TRN(4,4)=COST**2.0-SINT**2.0
      TRN(5,5)=COST
      TRN(5,6)=SINT
      TRN(6,5)=-SINT
      TRN(6,6)=COST
      DO 52 MM=1,6
      DO 52 NN=1,6
   52 TRNN(MM,NN)=TRN(MM,NN)
      CALL INVERS(TRNN,6,6,JC1,TTR,D2)
      CALL MXMLT(P,TTR,TRNN,6,6,6,6,6)
      CALL MXMLT(TRN,TRNN,TTR,6,6,6,6,6)
C     MATRIX TTR CONTAINS ELEMENTS OF COMPLIANCE MATRIX
C     EVALUATION OF VOLUME  INTEGRAL
      DO 51 I=1,5
      DO 51 J=1,5
      EL1=AL(I)
      EL2=(BL(J)-(BL(J)*EL1))
      EL4=1.0-EL1
      EL3=EL4-EL2
      WT=EL4*CL(I)
      WT=WT*DL(J)
      DO 51 K=1,5
      A(1,1)=EL1+EL2+EL3
      A(1,4)=(X(IJ,1)*EL1)+(X(IJ,2)*EL2)+(X(IJ,3)*EL3)
      A(1,7)=(Y(IJ,1)*EL1)+(Y(IJ,2)*EL2)+(Y(IJ,3)*EL3)
      A(1,10)=A(1,4)*A(1,7)
      A(1,12)=ZA(K)*THICK
      A(1,15)=A(1,12)*A(1,4)
      A(1,18)=A(1,12)*A(1,7)
      A(1,21)=A(1,12)*A(1,4)*A(1,7)
      A(2,2)=A(1,1)
      A(2,5)=A(1,4)
      A(2,8)=A(1,7)
      A(2,11)=A(1,10)
      A(2,13)=A(1,12)
      A(2,16)=A(1,15)
      A(2,19)=A(1,18)
      A(2,22)=A(1,21)
      A(4,3)=A(1,1)
      A(4,6)=A(1,4)
      A(4,9)=A(1,7)
      A(4,14)=A(1,12)
      A(4,17)=A(1,15)
      A(4,20)=A(1,18)
      A(5,6)=-A(1,12)
      A(5,8)=-A(1,12)
      A(5,11)=-A(1,15)
      A(5,17)=((THICK**2.0)*(ZA(K)**2.0))/2.0
      A(5,17)=-A(5,17)
      A(5,19)=A(5,17)
      A(5,22)=A(5,17)*A(1,4)
      A(5,23)=A(1,1)
      A(5,25)=A(1,4)
      A(5,26)=-A(1,7)
      A(5,28)=A(1,10)
```

```
      A(5,29)=-(A(1,7)*A(2,8))/2.0
      A(5,30)=A(1,4)*A(2,5)
      A(6,4)=A(5,6)
      A(6,9)=A(5,8)
      A(6,10)=-A(1,12)*A(1,7)
      A(6,15)=A(5,10)
      A(6,20)=A(6,15)
      A(6,21)=A(5,17)*A(1,7)
      A(6,24)=A(5,23)
      A(6,26)=A(1,4)
      A(6,27)=A(1,7)
      A(6,28)=-A(5,30)/2.0
      A(6,29)=A(1,10)
      A(6,31)=-A(5,29)*2.0
      DO 133 I=1,6
      DO 133 J=1,31
  133 AA(6,31)=AA(6,31)+A(6,31)
      CALL MXMLT(TTR,A,BA,6,6,31,6,6)
      CALL MXTRN(A,AT,6,31, 6,31)
      CALL MXMLT(AT,BA,HS,31,6,31,31,6)
      DO 45 M=1,31
      DO 45 N=1,31
   45 H(M,N)=H(M,N)+HS(M,N)*ZH(K)*WT
   51 CONTINUE
      DO 55 M=1,31
      DO 55 N=1,31
   55 H(M,N)=H(M,N)*THICK*DETJ
C     MATRIX H CONTAINS ELEMENTS OF MATRIX DUE TO VOLUME INTEGRAL OVER
C     EACH LAYER OF ELEMENT
      CALL INVERS (H,31,21,JC,HI,D1)
      DO 159 M=1,31
      DO 159 N=1,31
  159 HII(M,N,NU)=HI(M,N)
      CALL MXMLT (HI,TQ2,T2,31,31,21,31,31)
      CALL MXMLT (TQ1,T2,H,21,31,21,31,31)
      DO 155 I=1,21
      DO 155 J=1,21
  155 HT(I,J)=HT(I,J)+  H(I,J)
      CALL MXMLT (HI,T1,T3,31,31,21,31,31)
      CALL MXMLT (TT,T3,TM,21,31,21,31,31)
      DO 156 I=1,21
      DO 156 J=1,21
  156 HT(I,J)=HT(I,J)+TM (I,J)
      CALL MXMLT (TQ1,T3,TM,21,31,21,31,31)
      DO 157 I=1,21
      DO 157 J=1,21
  157 HT(I,J)=HT(I,J)+TM (I,J)
      CALL MXMLT (TT,T2,TM ,21,31,21,31,31)
      DO 158 I=1,21
      DO 158 J=1,21
  158 HT(I,J)=HT(I,J)+TM (I,J)
C     PERFORMING ASSEMBLY OF MATRIX ELEMENTS FOR ALL LAYERS
      MAA=MAA-1
      MB=MA+KJ
      MBB=MB+(2**(KJ-1))
      IF(MB.EQ.1) MB=-1
      MC=-7+MBB
      MD=-7
      DO 120 ME=1,3
      MD=MD+7
      MAA=MAA-1
      IF(MAA) 128,129,120
  128 MC=MC+6
```

```
      IF(IABS(MAA).GE.39) MC=MC+1
      GO TO 130
  129 MC=MC+7
  130 DO 120 MF=1,5
      MC=MC+1
      IF(MF.EQ.3) GO TO 122
      MEE=ME+MD
      GO TO 123
  122 MC=MC+MB
      GO TO 120
  123 MG=-7+MBB
      MH=-7
      DO 124 MI=1,3
      MH=MH+7
      MAA=MAA-1
      IF(MAA) 131,132,132
  131 MG=MG+6
      IF(IABS(MAA).GE.3) MG=MG+1
      GO TO 133
  132 MG=MG+7
  133 DO 119 MJ=1,5
      MG=MG+1
      IF(MJ.EQ.3) GO TO 125
      MJJ=MJ+MH
      GO TO 126
  125 MG=MG+MB
      GO TO 119
  126 HV(MC,MG)=HV(MC,MG)+HT(MEE,MJJ)
  119 CONTINUE
      IF(MAA) 118,124,124
  118 IF(IABS(MAA).GT.2.AND.IABS(MAA).LT.40) MG=MG-1
  124 CONTINUE
      NA=-1
      DO 121 NB=3,17,7
      NA=NA+1
      NAA=NB+3
      NBB=NAA+1
      NC=ND+2+(4*NA)
      ND=NAA+(4*(NA+1))
      NE=NBB+(4*(NA+1))
      HV(MC,NC)=HV(MC,NC)+HT(MEE,NB)
      HV(MC,ND)=HV(MC,ND)+HT(MEE,NAA)
      HV(MC,NE)=HV(MC,NE)+HT(MEE,NBB)
      HV(NC,MC)=HV(NC,MC)+HT(NB ,MEE)
      HV(ND,MC)=HV(ND,MC)+HT(NAA,MEE)
  121 HV(NE,MC)=HV(NE,MC)+HT(NBB,MEE)
  120 CONTINUE
      NE=-1
      DO 127 NG=3,17,7
      NE=NE+1
      NEE=NG+3
      NGG=NEE+1
      NH=NG+2+(4*NE)
      NI=NEE+(4*(NE+1))
      NJ=NGG+(4*(NE+1))
      NK=-1
      DO 127 NL=3,17,7
      NK=NK+1
      NKK=NL+3
      NLL=NKK+1
      NHH=NL+2+(4*NK)
      NII=NKK+(4*(NK+1))
      NJJ=NLL+(4*(NK+1))
```

```
      HV(NH,NHH)=HV(NH,NHH)+HT(NG,NL)
      HV(NH,NII)=HV(NH,NII)+HT(NG,NKK)
      HV(NH,NJJ)=HV(NH,NJJ)+HT(NG,NLL)
      HV(NI,NII)=HV(NI,NII)+HT(NEE,NKK)
      HV(NI,NHH)=HV(NI,NHH)+HT(NEE,NL)
      HV(NI,NJJ)=HV(NI,NJJ)+HT(NEE,NLL)
      HV(NJ,NJJ)=HV(NJ,NJJ)+HT(NGG,NLL)
      HV(NJ,NII)=HV(NJ,NII)+HT(NGG,NKK)
  127 HV(NJ,NHH)=HV(NJ,NHH)+HT(NGG,NL)
  112 CONTINUE
      L7=(3*K9)/4
      IJJ=0
      MM=0
      M=0
  200 II=IJ+IJJ
      IF(II.GT.NELTS) GO TO 98
      DO 145 NN=1,33
  145 CL(NN)=0.0
      MM=MM+1
      M=MM-1
      XL=X(IJ,2)*M
      YL=Y(IJ,3)*M
      K10=K9/4
      IF(MM.LE.K10) GO TO 6
      MM=1
      M=M+1
      XL=X(IJ,2)*(MM-1)
      YL=Y(IJ,3)*M
    6 DO 7 NN=1,3
      XX(NN)=X(IJ,NN)+XL
    7 YY(NN)=Y(IJ,NN)+YL
      DETJ=((XX(1)-XX(3))*(YY(2)-YY(3)))-((YY(1)-YY(3))*(XX(2)-XX(3)))
C     EVALUATION OF ELEMENTS OF LOADING VECTOR
      GQ(3,1)=-1.0
      DO 135 I=1,5
      DO 135 J=1,5
      EL1=AL(I)
      EL4=1.0-EL1
      EL2=(BL(J)-(BL(J)*EL1))
      EL3=EL4-EL2
      WT=EL4*CL(I)
      WT=WT*DL(J)
      TEL11=((3.0*EL1)-1.0)
      TEL12=((3.0*EL1)-2.0)
      TEL21=((3.0*EL2)-1.0)
      TEL22=((3.0*EL2)-2.0)
      TEL31=((3.0*EL3)-1.0)
      TEL32=((3.0*EL3)-2.0)
      T(1,1)=EL1
      T(1,12)=EL2
      T(1,23)=EL3
      T(2,2 )=EL1
      T(2,13)=EL2
      T(2,24)=EL3
      T(3,5 )=EL1*TEL11*TEL12/2.0
      T(3,16)=EL2*TEL21*TEL22/2.0
      T(3,27)=EL3*TEL31*TEL32/2.0
      T(3,10)=9.0*EL1*EL2*TEL11/2.0
      T(3,11)=9.0*EL1*EL2*TEL21/2.0
      T(3,21)=9.0*EL3*EL2*TEL21/2.0
      T(3,22)=9.0*EL3*EL2*TEL31/2.0
      T(3,32)=9.0*EL3*EL1*TEL31/2.0
      T(3,33)=9.0*EL3*EL1*TEL11/2.0
```

```
      T(4,3 )=EL1
      T(4,14)=EL2
      T(4,25)=EL3
      T(5,4 )=EL1
      T(5,15)=EL2
      T(5,26)=EL3
      T(6,5 )=T(3,5)
      T(6,10)=T(3,10)
      T(6,21)=T(3,21)
      T(6,22)=T(3,22)
      T(6,27)=T(3,27)
      T(6,16)=T(3,16)
      T(6,11)=T(3,11)
      T(6,32)=T(3,32)
      T(6,33)=T(3,33)
      CALL MXTRN(T,TR,6,33,6,33)
      CALL MXMLT (TR,QQ,QE,33,6,1,33,6)
      DO 21 NN=1,33
   21 QL(NN)=QL(NN)+QE(NN,1)*WT
  135 CONTINUE
      DO 146 NN=1,33
  146 QL(NN)=QL(NN)*DETJ
C     PERFORMING ASSEMBLY OF MATRIX ELEMENTS FOR ALL ELEMENTS
      K3=-2
      DO 57 IK=1,3
      K3=K3+2
      IKK=IGLCOR(II,IK)-IGLCOR(1,1)
      DO 57 JK=1,9
      JKK=JK-2
      K3=K3+1
      K4=IGLCOR(II,IK)+(8*NUMP(II,IK))+1+JKK
      Q(K4)=Q(K4)+QL(K3)
      K5=-2
      DO 71 LK=1,3
      K5=K5+2
      LKK=IGLCOR(II,LK)-IGLCOR(1,1)
      LKKK=IGLCOR(II,LK)
      DO 71 MK=1,9
      K5=K5+1
      IF(K5.LT.K3) GO TO 71
      MKK=MK-K4-1
      K6=IGLCOR(II,IK)+(8*NUM(LKKK))+1+MKK
      IF(K6.LE.0) GO TO 79
      AV(K4,K6)=AV(K4,K6)+HV(K3,K5)
      GO TO 71
   79 K6=K6-MKK
      MKK=MK-2
      K6=K6+MKK
      K7=K4-K6+1
      AV(K6,K7)=AV(K6,K7)+HV(K5,K3)
   71 CONTINUE
      M3=0
      M4=0
   94 M5=M3
      IF(M5.GT.4) GO TO 57
      M4=M4+9
      DO 74 LK=1,2
      LKK=M5+LK
      DO 75 I=1,NTNCOR
      IF(IGLMID(II,LKK).LT.NCO(I)) GO TO 93
   75 CONTINUE
   93 LKKK=NCO(I)
      K8=IGLMID(II,LKK)+NUM(LKKK)*8
```

```
      M3=LKK
      M4=M4+1
      IF (K8.LT.K4) GO TO 77
      K7=K8-K4+1
      AV(K4,K7)=AV(K4,K7)+HV(K3,M4)
      GO TO 74
   77 K7=K4-K8+1
      AV(K8,K7)=AV(K8,K7)+HV(M4,K3)
   74 CONTINUE
      GO TO 94
   57 CONTINUE
      M3=0
      M4=0
   48 M5=M3
      IF(M5.GT.4) GO TO 29
      M4=M4+9
      DO 49 LK=1,2
      LKK=M5+LK
      DO 50 I=1,NTNCOR
      IF(IGLMID(II,LKK).LT.NCO(I)) GO TO 87
   50 CONTINUE
   87 LKKK=NCO(I)
      K4=IGLMID(II,LKK)+NUM(LKKK)*8
      M3=LKK
      M4=M4+1
      Q(K4)=Q(K4)+QL(M4)
      M6=0
      M7=0
   97 M8=M6
      IF(M8.GT.4) GO TO 49
      M7=M7+9
      DO 26 MK=1,2
      MKK=M8+MK
      M6=MKK
      M7=M7+1
      IF (M7.LT.M4) GO TO 26
      DO 27 I=1,NTNCOR
      IF(IGLMID(II,MKK).LT.NCO(I)) GO TO 28
   27 CONTINUE
   28 MKKK=NCO(I)
      K8=IGLMID(II,MKK)+NUM(MKKK)*8
      IF(K8.LT.K4) GO TO 78
      K7=K8-K4+1
      AV(K4,K7)=AV(K4,K7)+HV(M4,M7)
      GO TO 26
   78 K7=K4-K8+1
      AV(K8,K7)=AV(K8,K7)+HV(M7,M4)
   26 CONTINUE
      GO TO 97
   49 CONTINUE
      GO TO 48
   29 CONTINUE
      IJJ=IJJ+2
      GO TO 200
   98 CONTINUE
C     MATRIX AV CONTAINS ELEMENTS OF STIFFNESS MATRIX
C     APPLICATION OF BOUNDARY CONDITIONS
C     NO. OF CORNER NODES WHERE BOUNDARY CONDITIONS ARE SPECIFIED
      READ(5,*) NOBCC
C     NO. OF MIDSIDE NODES WHERE BOUNDARY CONDITIONS ARE SPECIFIED
      READ(5,*) NOBCM
      READ(5,*) (NBCC(L),L=1,NOBCC)
      READ(5,*) (NFIXC(L),L=1,NOBCC)
```

```
      READ(5,*) (NBCM(L),L=1,NOBCM)
      DO 69 L=1,NOBCC
      DO 19 I=1,9
   19 NO(I)=0
      L1=NFIXC(L)
      L2=IREF(L1)
      L5=NBCC(L)
      L3=(NBCC(L)-1)+(8*NUM(L5))
      IF(L2.EQ.1) GO TO 60
      IF(L2.EQ.2) GO TO 61
      IF(L2.EQ.3) GO TO 62
      IF(L2.EQ.4) GO TO 63
      IF(L2.EQ.5) GO TO 64
      IF(L2.EQ.6) GO TO 65
      IF(L2.EQ.7) GO TO 66
   60 NO(1)=L3+1
      NO(2)=L3+3
      NO(3)=L3+6
      NO(4)=L3+8
      GO TO 67
   61 NO(1)=L3+2
      NO(2)=L3+4
      NO(3)=L3+7
      NO(4)=L3+9
      GO TO 67
   62 NO(1)=L3+5
      GO TO 67
   63 NO(1)=L3+1
      NO(2)=L3+2
      NO(3)=L3+3
      NO(4)=L3+4
      NO(5)=L3+6
      NO(6)=L3+7
      NO(7)=L3+8
      NO(8)=L3+9
      GO TO 67
   64 NO(1)=L3+2
      NO(2)=L3+4
      NO(3)=L3+5
      NO(4)=L3+7
      NO(5)=L3+9
      GO TO 67
   65 NO(1)=L3+1
      NO(2)=L3+3
      NO(3)=L3+5
      NO(4)=L3+6
      NO(5)=L3+8
      GO TO 67
   66 NO(1)=L3+1
      NO(2)=L3+2
      NO(3)=L3+3
      NO(4)=L3+4
      NO(5)=L3+5
      NO(6)=L3+6
      NO(7)=L3+7
      NO(8)=L3+8
      NO(9)=L3+9
   67 CONTINUE
      DO 82 L4=1,9
      IF(NO(L4).EQ.0) GO TO 82
      DO 95 M=1,NBAND
      IF(M.GT.NO(L4)) GO TO 95
      MM=M-1
```

```
      MM=NO(L4)-MM
      AV(MM,M)=0.0
   95   AV(NO(L4),M)=0.0
   82 CONTINUE
      IF (L2.EQ.3) Q(NO(1))=0.0
      IF (L2.EQ.5) Q(NO(3))=0.0
      IF (L2.EQ.6) Q(NO(3))=0.0
      IF (L2.EQ.7) Q(NO(5))=0.0
   69 CONTINUE
      DO 90 L=1,NOBCM
      DO 85 I=1,NTNCOR
      IF(NBCM(L).LT.NCO(I)) GO TO 86
   85 CONTINUE
   86 LL=NCO(I)
      L3=NBCM(L)+NUM(LL)*8
      Q(L3)=0.0
      DO 91 L4=1,NBAND
      IF(L4.GT.L3) GO TO 91
      MM=L4-1
      MM=L3-MM
      AV(MM,L4)=0.0
   91 AV(L3,L4)=0.0
   90 CONTINUE
      DO 89 I=1,NTOT
   89 IF (AV(I,1).EQ.0.0) AV(I,1)=1.0
C     SOLUTION OF EQUATIONS USING GAUSSIAN ELIMINATION TECHNIQUE
      DO 35 N=1,NTOT
      I=N
      DO 36 L=2,NBAND
      I=I+1
      IF(AV(N,L)) 37,36,37
   37 C=AV(N,L)/AV(N,1)
      J=0
      DO 38 K=L,NBAND
      J=J+1
      IF(AV(N,K)) 39,38,39
   39 AV(I,J)=AV(I,J)-C*AV(N,K)
   38 CONTINUE
   40 AV(N,L)=C
      Q(I)=Q(I)-C*Q(N)
   36 CONTINUE
   35 Q(N)=Q(N)/AV(N,1)
      N=NTOT
   41 N=N-1
      IF(N) 43,43,42
   42 L=N
      DO 46 K=2,NBAND
      L=L+1
      IF(AV(N,K)) 47,46,47
   47 Q(N)=Q(N)-AV(N,K)*Q(L)
   46 CONTINUE
      GO TO 41
   43 CONTINUE
C     VECTOR Q CONTAINS DISPLACEMENT VALUES AT ALL NODES OF STRUCTURE
C     EVALUATION OF STRESS RESULTANTS
      NU=0
      DO 131 IJ=1,NELTS
      NU=NU+1
      DO 116 I=1,31
      DO 116 J=1,21
      T11(I,J,NU)=T11(I,J,NU)+T022(I,J,NU)
  116 T1(I,J)=T11(I,J,NU)
      DO 117 I=1,31
```

```
      DO 117 J=1,31
  117 HI(M,N)=HII(M,N,NH)
      DO 132 I=1,3
      CALL MXMLT(HI,T1,TQ2,31,31,21,31,31)
      CALL MXMLT(A,TQ2,BA,6,31,21,6,31)
      CALL MXMLT(BA,Q,BQ,6,21,1,6,46)
C     VECTOR BQ CONTAINS STRESS RESULTANTS FOR EACH LAYER OF ELEMENT
  117 CONTINUE
  131 CONTINUE
      STOP
      END
      SUBROUTINE MXMLT(R1,R2,R3,I5,J5,K5,I1,I2)
      DIMENSION R1(I1,J5),R2(I2,K5),R3(I1,K5)
      DO 111 M1=1,I5
      DO 111 N1=1,K5
      R3(M1,N1)=0.0
      DO 111 M2=1,J5
  111 R3(M1,N1)=R3(M1,N1)+R1(M1,M2)*R2(M2,N1)
      RETURN
      END
      SUBROUTINE MXTRN(R1,R2,I5,J5,I1,I2)
      DIMENSION R1(I1,J5),R2(I2,I5)
      DO 110 K=1,I5
      DO 110 L=1,J5
  110 R2(L,K)=R1(K,L)
      RETURN
      END
```

REFERENCES

1. Pian, T. H. H., "Derivation of Element Stiffness Matrices by Assumed Stress Distributions," AIAA Journal, Vol. 2, No. 7, pp. 1333-1336, (1964).

2. Pian, T. H. H. and Tong, P., "Basis of Finite Element Methods for Solid Continua," International Journal of Numerical Methods in Engineering, Vol. 1, pp. 3-28, (1969).

3. Pian, T. H. H., "Formulations of Finite Element Methods for Solid Continua," Recent Advances in Matrix Methods in Structural Analysis and Design, University of Alabama, pp. 49-83, (1971).

4. Pian, T. H. H. and Tong, P., "Finite Element Methods in Continuum Mechanics," Advances in Applied Mechanics, Vol. 12, pp. 2-58, (1972).

5. Atluri, S. N., Class Notes on Finite Element Methods, School of Engineering Science and Mechanics, Georgia Institute of Technology, (1974-75).

6. Atluri, S. N., "A New Assumed Stress Hybrid Finite Element Model for Solid Continua," AIAA Journal, Vol. 9, No. 8, pp. 1647-1649, (1971).

7. Fraeijs de Veubeke, B., "Displacement and Equilibrium Models in the Finite Element Method," Stress Analysis, John Wiley, New York, pp. 145-197, (1965).

8. Fraeijs de Veubeke, B. and Sander, G., "An Equilibrium Model for Plate Bending," International Journal of Solids and Structures, Vol. 4, No. 4, pp. 447-468, (1968).

9. Mau, S. T., Tong, P., and Pian, T. H. H., "Finite Element Solutions for Laminated Thick Plates," Journal of Composite Materials, Vol. 6, pp. 304-311, (1972).

10. Pian, T. H. H., and Mau, S. T., "Some Recent Studies in Assumed Stress Hybrid Model," Proceedings of the Second U. S.-Japan Seminar on Matrix Methods in Structural Analysis and Design, California, (1972).

11. Barker, R. M., Liu, Fu-Tien, Dana, J. R., "Three Dimensional Finite Element Analysis of Laminated Composites," Computers and Structures, Vol. 2, pp. 1013-1029, (1972).

12. Ahmad, S. and Irons, B. M., "An Assumed Stress Approach to Refined Isoparametric Finite Elements in Three Dimensions," Symposium on Finite Element Methods in Engineering, University of New South Wales, pp. 85-100, (1974).

13. Silvester, P., "Higher Order Polynomial Triangular Finite Elements for Potential Problems," International Journal of Engineering Science, Vol. 7, No. 8, pp. 849-861.

14. Zienkiewicz, O. C., The Finite Element Method in Engineering Sciences, McGraw-Hill, New York, (1971).

15. Purdy, J. F., "Mathematics Underlying the Design of Pneumatic Tires," Edwards Brothers, Michigan, (1963).

16. Hofferberth, W., "Zur Festigkeit des Luftreifens," Kautschuk und Gummi, Vol. 9, WT 225-WT231, (1956).

17. Biderman, V. L., "Calculation of the Profile and Stresses in Elements of Pneumatic Tires Under Inflation Pressure," (Russian), Transactions Tire Research Institute, Moscow, Vol. 3, pp. 16-51, (1957).

18. Brewer, H. K., "Tire Stresses and Deformation from Composite Theory," American Society for Testing Materials, pp. 47-76, (1970).

19. Dunn, S. E. and Zorowski, C. F., U. S. National Bureau of Standards, Office of Vehicle Systems Research, Contract No. CST-376, (1970).

20. Deak, A. L. and Atluri, S. N., Interim Report, Air Force Contract F 33615-72-C-1004, (1972).

APPENDIX I

Summary: In this appendix, the way to extend the developments discussed in the text to the incremental analysis of the nonlinear problem of finite deformations of the tire are presented. The present incremental analysis is a consistently formulated hybrid stress method wherein the influence of large deformations in the equilibrium equations is accounted for. This is done by choosing the incremental stresses, which satisfy the incremental equilibrium equations in the updated Lagrangean form, in such a way that they include the effects of initial stresses and incremental displacements.

Each material particle in the original reference configuration C_1 is identified, in general, by curvilinear coordinates $\xi^\alpha (\alpha = 1, 2, 3)$. The numerical values of ξ^α which define a particle in C_1 define the same particle in every subsequent configuration (also referred to as convected coordinates). To describe the motion of the body relative to C_1, a fixed rectangular cartesian coordinate system $x_\alpha (\alpha = 1, 2, 3)$ in three-dimensional space is also established. Thus, a continuous one-to-one motion of the particle, as the continuum deforms, is defined by relations,

$$x_\alpha = x_\alpha (\xi^\beta, t) \tag{1}$$

such that

$$\det \left| \frac{\partial x_\alpha}{\partial \xi^\beta} \right| > 0 \tag{1a}$$

In general, we define C_N to be the configuration of the body before the addition of the n^{th} increment of load; whereas, C_{N+1} is the body after the addition of the n^{th} load-increment. In configuration C_N, the states of

stress, strain, and deformation are presumed to be known. During the process of the n^{th} load-increment, the configuration C_N is treated to be in a state of "initial stress". Incremental displacements due to the addition of the n^{th} load-increment are measured from C_N. In the following we treat, as a generic case, the movement of the continuum from the reference state C_N to further deformed state C_{N+1} through small but finite increments in stresses, displacements, and external loads.

The position vector of a particle in C_N is denoted by $\underset{\sim}{r}$ and that of the same particle in C_{N+1} is denoted by $\underset{\sim}{R}$. If x_i are the cartesian coordinates of the point in C_N and $\underset{\sim}{e}_i$ are cartesian bases, it follows

$$\underset{\sim}{r} = x_i \underset{\sim}{e}_i \tag{2}$$

The covariant base vectors tangent to ξ^i lines in configuration C_N are given by,

$$\underset{\sim}{g}_\alpha = \frac{\partial r}{\partial \xi^\alpha} = \frac{\partial x_i}{\partial \xi^\alpha} \underset{\sim}{e}_i \tag{3}$$

the covariant and contravariant metric tensors, and contravariant base vectors in C_N are given by,

$$g_{\alpha\beta} = \underset{\sim}{g}_\alpha \cdot g_\beta \; ; \; [g^{\alpha\beta}] = [g_{\alpha\beta}]^{-1} \; ; \; \underset{\sim}{g}^\alpha = g^{\alpha\beta} \underset{\sim}{g}_\beta \tag{4}$$

The vector field of incremental displacement from C_N to C_{N+1}, is measured in the basis system of C_N as

$$\underset{\sim}{\Delta u} = \Delta u_\alpha \underset{\sim}{g}^\alpha = \Delta u^\alpha \underset{\sim}{g}_\alpha \tag{5}$$

which gives the usual representation of Green's strain tensor, in C_N as

$$\Delta\epsilon_{\lambda\mu} = \frac{1}{2}[\Delta u_{\lambda,\mu} + \Delta u_{\mu,\lambda} + \Delta u^\nu{}_{,\lambda} \, \Delta u_{\nu,\mu}] \tag{6}$$

where a comma denotes a covariant differentiation with respect to coordinates ξ^i in C_N, using the metric tensors g_{ij}, g^{ij} of C_N. For later use we note that the geometry of C_{N+1} is characterized by the basis vactors and metric tensors,

$$\underset{\sim}{G}_\alpha = \frac{\partial \underset{\sim}{R}}{\partial \xi^\alpha} = \frac{\partial (\underset{\sim}{Y} + \underset{\sim}{u})}{\partial \xi^\alpha} = (\delta^\beta{}_\alpha + u^\beta{}_\alpha)\underset{\sim}{g}_\beta \; ; \; G_{\alpha\beta} = g_{\alpha\beta} + 2\Delta\epsilon_{\alpha\beta} \tag{7}$$

In the reference state C_N, which is presumed to be known, let the initial Piola-Kirchoff stresses be represented by the symmetric tensor $\sigma^{o\lambda\mu}$, measured per unit area in C_N. Let the initial body forces and surface tractions measured per unit volume and unit area respectively, in the current reference state, be given, respectively, by

$$\overline{F}^o = \overline{F}^{o\lambda}\, g_\lambda \; ; \; \overline{T}^o = \overline{T}^{o\lambda}\, g_\lambda \tag{8}$$

where a bar (—) denotes a prescribed quantity. One can then prescribe additional body forces $\Delta\overline{F}^\lambda$, additional surface tractions $\Delta\overline{T}^\lambda$ on a portion S_1 of the surface of the body, and additional displacements $\Delta\overline{u}^\lambda$ on a portion S_2 of the surface of the body; where the displacements Δu^λ are measured from C_N, in the basis vector system $\overline{g}_\lambda$ of C_N. Let the corresponding increment in the Piola-Kirchoff stresses measured per unit area in C_N be represented by the symmetric tensor $\Delta\sigma^{\lambda\mu}$. The principle of virtual work then states,

$$\int_V [(\sigma^{o\lambda\mu} + \Delta\sigma^{\lambda\mu})\, \delta\Delta\, e_{\lambda\mu} - (\overline{F}^{o\lambda} + \Delta\overline{F}^\lambda)\, \delta\Delta\, u_\lambda]\, dV$$

$$- \int_{S_1} (\overline{T}^{o\lambda} + \Delta\overline{T}^\lambda)\, \delta\Delta\, u_\lambda\, dS = 0 \tag{9}$$

where $\Delta e_{\lambda\mu}$ is given by Eq. (6). In Eq. (9) the volume V, and the surfaces S_1 and S_2 refer to the known current reference state C_N, and a "δ" denotes variations. We note that $\delta\Delta u_\lambda$ vanishes on S_2. Eq. (9) can be written as,

$$\int_V [\Delta\sigma^{\lambda\mu}\,\delta\Delta\, e_{\lambda\mu} + \frac{\sigma^{o\lambda\mu}}{2}\,\delta\,(\Delta u_{\nu,\lambda}\,\Delta u^{\nu}_{,\mu}) - \Delta F^{\lambda}\,\delta\Delta\, u_\lambda]\, dV$$

$$- \int_{S_1} \Delta\bar{T}^{\lambda}\,\delta\Delta u_\lambda\, dS \qquad (10)$$

$$= \int_V [-\frac{\sigma o^{\lambda\mu}}{2}\,(\delta\Delta u_{\lambda,\mu} + \delta\Delta u_{\mu,\lambda}) + F^{o\lambda}\,\delta\Delta u_\lambda]\, dV$$

$$+ \int_{S_1} T^{o\lambda}\,\delta\Delta u_\lambda\, dS\ .$$

If it is now assumed that the known initial stress state ($\sigma^{o\lambda\mu}$; $\bar{F}^{o\lambda}$; $\bar{T}^{o\lambda}$) in C_N is in equilibrium prior to the addition of the incremental loads for step N, then the right hand side of Eq. (10) can be shown to be identically equal to zero. However, due to the numerical incremental solution technique for solving a large strain problem, the initial stress state in C_N <u>may</u> not be in equilibrium. It is shown later that it is possible to derive an equilibrium error check if the right hand side terms in Eq. (10) are retained.

Assuming that the elastic stress-strain relations are of the type

$$\Delta\sigma^{\lambda\mu} = \Delta\sigma^{\lambda\mu}\ (\sigma^{o\alpha\beta},\ \Delta e_{\alpha\beta}) \qquad (11)$$

or

$$\Delta e_{\lambda\mu} = \Delta e_{\lambda\mu} \ (\sigma^{o\alpha\beta}, \Delta\sigma^{\alpha\beta}) \tag{11a}$$

one can define an elastic strain energy function

$$dA = \Delta\sigma^{\lambda\mu} \ d\Delta e_{\lambda\mu} \tag{12}$$

Using Eq. (12), Eq. (10) may be written as,

$$\delta\{\int_V [A(\sigma^{0\alpha\beta}, \Delta u^{\alpha}) + \frac{1}{2}\sigma^{0\lambda\mu}\Delta u_{\nu,\mu}\Delta u^{\nu}_{,\mu} - \Delta\bar{F}^{\lambda}\Delta u_{\lambda}]\,dV - \int_{S_1}\Delta\bar{T}^{\lambda}\Delta u_{\lambda}\,dS\} \tag{13}$$

$$= \int_V (-\sigma^{0\lambda\mu}\delta\Delta u_{\lambda,\mu} + F^{0\lambda}\delta\Delta u_{\lambda})\,dV + \int_{S_1}\bar{T}^{0\lambda}\delta\Delta u_{\lambda}\,dS$$

It must be stressed again that the right hand side in Eq. (13) is a correction term to "check" that the initial stresses in C_N satisfy the equilibrium equations and boundary conditions. Thus, theoretically, if the reference state C_N is one of equilibrium, in which case the right hand side of Eq. (13) vanishes, the equation (13) can be shown to yield the equilibrium equations, for the Piola-Kirchoff incremental stresses (due to n^{th} loading increment) referred to the current known reference state C_N, as follows:

$$\Delta\sigma^{\lambda\mu}_{,\mu} + [(\sigma^{0\nu\mu} + \Delta\sigma^{\nu\mu})\,\Delta u^{\lambda}_{,\mu}]_{,\nu} + \Delta\bar{F}^{\lambda} = 0 \tag{14}$$

and

$$\Delta\bar{T}^{\lambda} = \Delta\sigma^{\lambda\mu} n_{\mu} + (\sigma^{0\nu\mu} + \Delta\sigma^{\nu\mu}) \Delta u^{\lambda}_{,\mu} n_{\nu} \quad \text{on} \quad S_1 \tag{15}$$

The principle of virtual work as given by Eq. (13) can now be generalized through the usual methods, into a couterpart of Hu-Washizu variational principle in linear elasticity. That is, we add to the functional in Eq. (13) the constraint conditions

$$\Delta e_{\lambda\mu} = \frac{1}{2}(\Delta u_{\lambda,\mu} + \Delta u_{\mu,\lambda} + \Delta u^{\nu}_{,\mu} \Delta u_{\nu,\mu}) \tag{16}$$

and

$$\Delta u_{\lambda} = \Delta\bar{u}_{\lambda} \text{ on } S_2$$

Then considering the Lagrangian multipliers corresponding to constraint condition (16) and (16a) as $\Delta\sigma^{\lambda\mu}$ and ΔT^{λ}, respectively, we can formulate the generalized functional,

$$\pi_g = \pi_g(\Delta e_{\lambda\mu}; \Delta u_{\lambda}; \Delta\sigma^{\lambda\mu}; \Delta T^{\lambda}) \tag{17}$$

where

$$\pi_g = \int_V \{A(\Delta e_{\lambda\mu}, \sigma^{0\lambda\mu}) + \frac{1}{2}\sigma^{0\lambda\mu} \Delta u^{\nu}_{,\lambda} \Delta u_{\nu,\mu} - \Delta\bar{F}^{\lambda} \Delta u_{\lambda}$$

$$- \Delta\sigma^{\lambda\mu}[\Delta e_{\lambda\mu} - \frac{1}{2}(\Delta u_{\lambda,\mu} + \Delta u_{\mu,\lambda} + \Delta u^{\nu}_{,\mu} \Delta u_{\nu,\mu})]\}dV$$

$$- \int_{S_1} \Delta\bar{T}^{\lambda} \Delta u_{\lambda} \, dS - \int_{S_2} \Delta T^{\lambda}(\Delta u_{\lambda} - \Delta\bar{u}_{\lambda}) \, dS - \varepsilon^{*}$$

where

$$\epsilon^* = \int_V (- \sigma^{0\lambda\mu} \Delta u_{\lambda,\mu} + F^0{}_\lambda \Delta u_\lambda) \, dV + \int_{S_1} \bar{T}^{0\lambda} \Delta u_\lambda \, dS \qquad (19)$$

ϵ^* is the correction term to "check" the equilibrium of initial stress state in the reference state C_N. Noting that the variation of ϵ^* with respect to Δu_λ is zero if the reference state equilibrium is theoretically satisfied, one can show that the Euler equations corresponding to $\delta\pi_g = 0$ are, (a) the equilibrium equations, Eq. (14); (b) the strain-displacement relations, Eq. (6); (c) the stress-strain relations, Eq. (12); (d) the displacement boundary conditions $\Delta u_\lambda = \Delta\bar{u}_\lambda$ on S_2; and (e) the stress boundary conditions, Eq. (15).

Suppose now that in Eq. (18) one assumes that the incremental equilibrium equations, Eq. (14), the traction conditions, Eq. (15), and the stress-strain relations (12) are satisfied a <u>priori</u>. Noting that assuming Eq. (12) <u>a priori</u> is equivalent to assuming the existence of a potential B such that

$$B = \Delta\sigma^{\lambda\mu} \Delta e_{\lambda\mu} - A \qquad (20)$$

and using Eq. (14), (15), and (20), one can reduce π_g to π_c, where

$$\pi_c = - \int_V B(\Delta\sigma^{\lambda\mu}; \sigma^{o\lambda\mu}) \, dV + \int \frac{1}{2} \sigma^{o\lambda\mu} \Delta u^\nu{}_{,\lambda} \Delta u_{\nu,\mu} dv + \int_{S_2} \Delta T^\lambda \qquad (21)$$

$$\Delta\bar{u}_\lambda \, dS - \epsilon^*$$

obviously, when π_c is varied with respect to $\Delta\sigma^{\lambda\mu}$ satisfy the <u>a priori</u> conditions

$$\delta\Delta\sigma^{\lambda\mu}{}_{,\mu} + \delta[(\sigma^{0\nu\mu} + \Delta\sigma^{\nu\mu}) \Delta u^\lambda{}_{,\mu}]_{,\nu} = 0 \qquad (22)$$

and

$$\delta\Delta\sigma^{\lambda\mu}\, n_\mu + \delta\left[\sigma^{o\nu\mu} + \Delta\sigma^{\nu\mu}\right] \Delta u^{\lambda}_{,\mu}\, n_\nu = 0 \tag{23}$$

it can be shown that the Euler equations corresponding to the variation of π_c with respect to $\Delta\sigma^{\lambda\mu}$, are

$$\Delta e_{\lambda\mu} = \frac{1}{2}(\Delta u_{\lambda\mu} + \Delta u_{\mu,\lambda} + \Delta u^{\nu}_{,\lambda}\, \Delta u_{\nu,\mu}) \tag{24}$$

and

$$\Delta u_\lambda = \Delta\bar{u}_\lambda \text{ on } S_2$$

Even though the functional ϵ^* in Eq. (21) is a constant with respect to variations in $\Delta\sigma^{\lambda\mu}$ and hence doesn't contribute any terms in the variational equation $\delta\pi_c = 0$ when the variations are with respect to $\Delta\sigma^{\lambda\mu}$, it is shown later that within the framework of the hybrid stress finite element model, an equilibrium check on the initial stresses can be performed by retaining ϵ^* in Eq. (21). If the condition $\Delta T^\lambda = \Delta\bar{T}^\lambda$ on S_1, is not satisfied <u>a priori</u>, then we can introduce it as a subsidiary condition and consider

$$\pi_c^* = -\int_V B(\Delta\sigma^{\lambda\mu};\, \sigma^{o\lambda\mu})\, dV + \int_V \frac{1}{2}\sigma^{o\lambda\mu}\, \Delta u^{\nu}{}_{,\lambda} \Delta u_{\nu,\mu}\, dV + \int_{S_2} \Delta T^\lambda \Delta u_\lambda\, dS +$$

$$\int_{S_1} (\Delta\bar{T}^\lambda - \Delta T^\lambda)\, \Delta u_\lambda\, dS - \epsilon^* \tag{26}$$

Next, certain simplifications can be made, in order to facilitate the above developments for numerical calculations. One can assume that each increment is such that the incremental displacements Δu_λ are of order $0(\epsilon)$; whereas the initial stresses are of order $0(1)$. Thus,

$$\Delta u_\lambda \sim 0\ (\epsilon) \tag{27}$$

$$\sigma^{o\lambda\mu} \sim 0(1) \tag{28}$$

Then, the incremental strain-displacement relations are

$$\Delta e_{\lambda\mu} = \frac{1}{2}(\Delta u_{\lambda,\mu} + \Delta u_{\mu,\lambda}) + 0(\epsilon^2) \tag{29}$$

Likewise, for elastic materials

$$\Delta\sigma^{\lambda\mu} \sim 0(\epsilon) \tag{30}$$

Using Eqs. (27) and (30), the equilibrium equation (14) can be simplified as,

$$\Delta\sigma^{\lambda\mu}{}_{,\mu} + [\sigma o^{\nu\mu}\, \Delta u^{\lambda}{}_{,\mu}]_{,\nu} + \Delta\bar{F}^{\lambda} = 0 \tag{31}$$

and the traction vector ΔT^{λ} can be simplified as,

$$\Delta T^{\lambda} = \Delta\sigma^{\lambda\mu}\, n_{\mu} + \sigma^{o\nu\mu}\, \Delta u^{\lambda}{}_{,\mu}\, n_{\nu} \tag{32}$$

From Eqs. (29), (31), and (32), it is clear that if in the functional

$$\pi_c^* = -\int_V B(\Delta\sigma^{\lambda\mu},\, \sigma^{o\lambda\mu})\, dV + \int_V \frac{1}{2}\sigma^{o\lambda\mu}\, \Delta u_{\nu,\lambda}\Delta u^{\nu},_{,\mu}\, dV + \int_{S_2} \Delta T^{\lambda}\Delta\bar{u}_{\lambda}\, dS$$

$$+ \int_{S_1} (\Delta\bar{T}^{\lambda} - \Delta T^{\lambda})\, \Delta u_{\lambda}\, dS - \epsilon * \tag{33}$$

we assume <u>a priori</u>, the linearized equilibrium equation in terms of incremental and initial Piola-Kirchoff stresses, taken per unit area in C_N, as

$$\Delta\sigma^{\lambda\mu}{}_{,\mu} + [\sigma^{o\nu\mu}\, \Delta u^{\lambda}{}_{,\mu}]_{,\nu} + \Delta\bar{F}^{\lambda} = 0 \tag{34}$$

where a comma in Eq. (34) refers to covariant differentiation with respect to ξ^i lines in C_N (using the metric tensors $g_{\alpha\beta}$ and $g\alpha\beta$ in C_N), then the variational equation

$$\delta_{\Delta\sigma^{\lambda\mu}} \pi_c^* = 0 \tag{35}$$

leads to the Euler equations

$$\Delta e_{\lambda\mu} = \frac{1}{2}(\Delta u_{\lambda,\mu} + \Delta u_{\mu,\lambda}) \tag{36}$$

and

$$\Delta u^\lambda = \Delta \bar{u}^\lambda \quad \text{on} \quad S_2 \tag{37}$$

Thus, any incremental stress field that satisfies the incremental equilibrium equation (34) exactly also leads to compatible displacement fields if the variational Eq. (35) is satisfied. Thus the above variational principle is consistent.

Following Pian and Tong [1], one can modify the functional in Eq. (33) for the hybrid stress formulation of the finite element model as

$$\pi_c^* = \sum_{n=1}^{M} \{ -\int_{V_n} B(\Delta\sigma^{\lambda\mu}, \sigma^{\circ\lambda\mu})\, dV + \int_V \frac{1}{2} \sigma^{\circ\lambda\mu}\, \Delta u^\nu{}_{,\lambda} \Delta u_{\nu,\mu} + \int_{\partial V_n} \Delta T^\lambda \Delta u_{\lambda L}$$

$$dS - e^*\} \tag{38}$$

where M is the number of elements, V_n the volume of the n^{th} element, ∂V_n the interelement boundary of the n^{th} element. In the above, $\Delta u_{\lambda L}$, which are physically the interelement boundary displacements, take on the meaning of Lagrangian Multipliers that can be used to satisfy the interelement traction continuity requirements on the average. These interelement boundary

displacements $u_{\lambda L}$ are prescribed such that they inferently satisfy the interelement displacement compatibility condition.

Thus, in the construction of the finite element model, one assumes (a) an equilibrating stress field within each element, and (b) a set of element boundary displacements in terms of a finite number of nodal values such that interelement displacement compatibility is inherently satisfied. The incremental stress field within each element satisfies the equation

$$\Delta\sigma^{\lambda\mu}{}_{,\mu} + [\sigma^{o\nu\mu}\,\Delta u^{\lambda}{}_{,\mu}]_{,\nu} + \Delta\bar{F}^{\lambda} = 0 \tag{39}$$

or

$$\Delta\sigma^{\lambda\mu}{}_{,\mu} = -\,\Delta\bar{F}^{\lambda} - (\sigma^{o\nu\mu}\,\Delta u^{\lambda}{}_{,\mu})_{,\nu} \tag{40}$$

Thus, we can assume, in each element

$$\{\Delta\sigma\} = [H]\{B\} + \{\Delta\sigma_p\} + [A]\{\Delta q\} \tag{41}$$

where $[H]$ is the matrix of homogeneous solution, and $\Delta\sigma_p$ is any particular solution corresponding to an increment in external loads. The meaning of the last term is explained below.

The coefficient matrix A results from the last forcing term in Eq. (40), where the initial stress $\sigma^{o\lambda\mu}$ is known. Also, in the hybrid stress method we assume compatible interelement boundary displacements as

$$\{\Delta u_{\lambda L}\} = [L_B]\{\Delta q\} \tag{42}$$

where Δ_q is the vector of generalized nodal displacements, and L_B is a matrix of interpolation polynomials in terms of the boundary coordinates.

From these boundary data one can interpolate for the interior displacements* as

$$\{\Delta u\} = [L]\{\Delta q\} \tag{43}$$

Using Eq. (43) the necessary interior displacement gradients may easily be obtained. From these one can construct the matrix A such that,

$$[A]\{\Delta q\} \equiv [(\sigma^{0\nu\mu}\, \Delta u^{\lambda}_{,\mu})_{,\nu}] \tag{44}$$

Similarly, from (32) one obtains for the element boundary tractions

$$\{\Delta T\} = [R][\beta] + [\Delta T_p] + [M][\Delta q] \tag{45}$$

Finally, from a stress-strain law of the type shown by Eq. (11a) one may construct the following strain-stress relation†

$$\Delta e_{\alpha\beta} = [E^0_{\alpha\beta\varepsilon\rho} + 2E^1_{\alpha\beta\gamma\delta\varepsilon\rho}\, \sigma^{0\gamma\delta}]\, \Delta\sigma^{\varepsilon\rho} + \text{H.O.T.} \tag{46}$$

or

$$\Delta e_{\alpha\beta} = E_{\alpha\beta\gamma\delta}(\sigma^{0\nu\mu})\, \Delta\sigma^{\gamma\delta} \tag{47}$$

We note that the compliance depends on the initial stress state when material nonlinearities are included.

Now one is in the position to facilitate Eq. (38) for numerical computation. Using Eq. (47), (here onwards, the distinction between square or row, or column natrices is omitted, but implied), one obtains,

$$\int_{V_n} B(\Delta\sigma^{\lambda\mu}, \sigma^{0\lambda\mu})\, dV = \frac{1}{2}\int_{V_n} \Delta\sigma^T E \Delta\sigma\, dV = \frac{1}{2}\int_{v} \{\beta^T (H^T E H)\, \beta$$

$$+ \Delta q^T (A^T E A)\, \Delta q + 2\beta^T (H^T E A)\, \Delta q + 2\beta^T (H^T E)\, \Delta\sigma_p \tag{48}$$

$$+ 2\Delta q^T (A^T E)\, \Delta\sigma_p + \text{constant}\} \, dV$$

where

β = unknown stress coefficients

Δq = unknown generalized displacement increments

A^T = transpose of A, etc.

Carrying out the integration in (48) one obtains

$$\int_{V_n} B(\Delta\sigma^{\lambda\mu}, \sigma^{0\lambda\mu})\, dV \equiv \frac{1}{2}\beta^T B\beta + \frac{1}{2}\Delta q^T C\Delta q + \beta^T D\Delta q + \beta^T \Delta Q_1 + \Delta q^T \Delta Q_2 \tag{49}$$

with obvious definitions for the matrices B, C, D, ΔQ, and ΔQ_2.

Likewise,

$$\int_{\partial V_n} \Delta T^{\lambda}\, \Delta u_{\lambda L}\, dS = \int_{\partial V_n} \Delta T^T\, \Delta u_L\, dS = \int_{\partial V_n} [\beta^T (R^T L_B)\, \Delta q + (\Delta T^T{}_P\, L_B)\, \Delta q + \Delta q^T M^T L_B\, \Delta q)\, dS \tag{50}$$

where L_B is the matrix for the boundary displacements given in Eq. (42).

Carrying out the integration in (50) one obtains

$$\int_{\partial V_n} \Delta T^{\lambda}\, \Delta u_{\lambda}\, dS = \beta^T S\Delta q + T^T \Delta q + \Delta q^T P\Delta q \tag{51}$$

with obvious definition for the matrices S, T, and P. Likewise, in the integral

$$\varepsilon^* = \int_V (- \sigma^{o\lambda\mu} \Delta u_{\lambda,\mu} + F^{o\lambda} \Delta u_\lambda) \, dV + \int_{S_1} \bar{T}^{o\lambda} \Delta u_\lambda \, dS \tag{52}$$

Since $\sigma^{o\lambda\mu}$, $F^{o\lambda}$, $\bar{T}^{o\lambda}$ are known, the integral in Eq. (52), can in general be written

$$\varepsilon^* = [Q_c]\{\Delta q\} \tag{53}$$

Thus, substituting Eqs. (49), (51), and (53) into (38),

$$\pi_c^* = \sum_{n=1}^{N} \{ - \frac{1}{2} \beta^T B \beta + \beta^T (S - D) \Delta q - \beta^T \Delta Q_1 - \frac{1}{2} \Delta q^T (C - 2P) \Delta q - \Delta q^T (\Delta Q_2 - T) \}_n - [Q_c]\{\Delta q\} \tag{54}$$

We note that in Eq. (52) only the unknown stress coefficients β's are independent for each finite element. Thus, taking the variation with respect to β in each element, one obtains

$$- B\beta - \Delta Q_1 + (S - D) \Delta q = 0 \tag{55}$$

from which

$$\beta = - B^{-1} \Delta Q_1 + B^{-1} (S - D) \Delta q \tag{56}$$

The substitution of Eq. (56) into Eq. ( ) yields

$$\pi_c^* = \sum_{n=1}^{N} \{ \frac{1}{2} \Delta q^T [(S - D)^T B^{-1} (S - D) - C + 2P] \Delta q - 2\Delta q^T (S - D)^T B^{-1} \Delta Q_1 - \Delta q^T (\Delta Q_2 - T) - [Q_c]\{\Delta q\} \}_n \tag{57}$$

Taking the variation with respect to Δq,

$$\sum_{n=1}^{N} \{k\Delta q - Q\}_n = 0 \tag{58}$$

with

$$k = (S - D)^T B^{-1} (S - D) - C + (P + P^T) \tag{59}$$

$$\Delta Q = 2(S - D)^T B^{-1} \Delta Q_1 - \Delta Q_2 + T - Q_c \tag{60}$$

where k is the element stiffness matrix and ΔQ is the load matrix. We note that the vector Q_c of element generalized nodal forces (the last term on the right hand side of Eq. (60) which results from ϵ^* in Eq. (53) can be referred to as "residuals", since that they can be used to measure the residual error in nodal point equilibrium at the beginning of any load step.

If in Eqs. (60), we set C = 0; $\Delta Q_2 = 0$ and P = 0, then we recover the usual linear theory. Accordingly, we may rewrite Eqs. (60) as

$$k = k_1 + k_2$$

$$k_1 = S^T B^{-1} S$$

$$k_2 = D^T B^{-1} D - (D^T B^{-1} S + S^T B^{-1} D) - C + P + P^T \tag{62}$$

$$\Delta Q_1^* = 2S^T B^{-1} \Delta Q_1 + T$$

$$\Delta Q_2^* = -2D^T B^{-1} \Delta Q_1 - \Delta Q_2$$

where

k_1 = conventional linear hybrid stiffness matrix

k_2 = incremental stiffness matrix

ΔQ_1 = conventional load matrix

ΔQ_2 = incremental load matrix

Q_c = residuals to check equilibrium in reference state.

It can be easily verified that the incremental sriffness matrix is symmetric and positive semi-definite just as the conventional linear hybrid stress stiffness matrix. Also, in general, the sum of the number of β's (stress coefficients) for each element and the number of rigid body degrees of freedom for each element should be in excess of the number of q's (generalized nodal displacements) of the same element.

Once an element shape is selected and appropriate choices for the field variables in each element as outlined earlier are made, the integrals in Eq. (62) can be evaluated numerically to find the element stiffness matrix and nodal load matrix. Employing the usual techniques of finite element assemblage, one can now derive a system of linear incremental equations, governing the behavior during the n^{th} load step, for the entire structure,

$$([K_1] + [K_2])_N \{\Delta R\}_N = \{\Delta F_1\}_N + \{\Delta F_2\}_N + \{F_c\}_N \qquad (63)$$

where matrices $[K_1]$, $[K_2]$, $\{\Delta R\}$, $\{\Delta F_1\}$, $\{\Delta F_2\}$, and $\{F_c\}$ are obtained by assembling the respective individual element matrices k_1, k_2, Δq, ΔQ_1^*, ΔQ_2^* and Q_c.

The procedure for the solution od Eq. (63), with the equilibrium check and corrective cycling procedure, has already been discussed in detail by Hofmeister, Greenbaum, and Evensen [16], and is not repeated here. It should also be pointed out that at some stage in the process of incrementation, for example in state C_M, the matrix $[K_1 + K_2]_M$ might become singular and $\{\Delta R\}_M$ can no longer be unique. This, in structural stability problems, the values of $\overline{F}_M^{o\lambda}$ and $\overline{T}_M^{o\lambda}$ corresponding to the case when $[K_1 + K_2]_M$ is singular, are the critical loads.

At this point it is worth noting that the total stresses $\sigma^{o\lambda\mu} + \Delta\sigma^{\lambda\mu}$ from load step N became initial stresses for step N + 1. For step N, the stresses $\sigma^{o\lambda\mu} + \Delta\sigma^{\lambda\mu}$ were treated as the Piola-Kirchoff stresses referred to the state C_N before the addition of the n^{th} load step. Thus, for treating the incremental problem corresponding to the (N + 1) the load increment, these total stresses $(\sigma^{o\lambda\mu} + \Delta\sigma^{\lambda\mu})$ at the end of step N must be converted to Piola-Kirchoff stresses $S^{o\lambda\mu}$ referred to the state C_{N+1} before the addition of the $(N + 1)^{th}$ load increment (or equivalently the state at the end of n^{th} step). Thus,

$$S^{o\lambda\mu} = (I_3)^{-1/2}(\sigma^{o\lambda\mu} + \Delta\sigma^{\lambda\mu}) \tag{64}$$

where

$$I_3 = \det[\delta^{\lambda}_{\ \mu} + 2\Delta e^{\lambda}_{\ \mu}] \ ; \ \Delta e^{\lambda}_{\ \mu} = g^{\lambda\nu}\Delta e_{\mu\nu} \tag{65}$$

In Eq. (65), $\Delta e_{\mu\nu}$ is the incremental Green's strain tensor in the n^{th} load step as defined in Eq. (6).

Also, it is worth noting that when the volume and surface integrals for each discrete element considered in Eqs. (49), (51), and (52) are evaluated for the element in the configuration C_N, the infinitesimal volume in state C_N is given by

$$dV = \sqrt{g}\, d\xi^1 d\xi^2 d\xi^3 \quad \text{in} \quad C_N \tag{66}$$

where $g = \det |g_{\alpha\beta}|$ and $g_{\alpha\beta}$ is the metric in C_N. Due to incremental deformation in the n^{th} load step, the discrete element shape and volume in C_{N+1} would be different from those in C_N. In C_{N+1}, the infinitesimal volume is given by

$$dV_1 = \sqrt{G}\, d\xi^1\, d\xi^2\, d\xi^3 \quad \text{in} \quad C_{N+1} \tag{68}$$

where

$$G = \det | G_{\alpha\beta} |$$

$$= \det | g_{\alpha\beta} | \cdot \det[\delta^{\lambda}_{\mu} + 2g^{\lambda\nu}\, \Delta e_{\mu\nu}] \tag{68}$$

where $G_{\alpha\beta}$ is the metric in C_{N+1} and $\Delta e_{\mu\nu}$ is given by Eq. (6). Thus, in evaluating the volume integrals for the deformed element in C_{N+1}, Eq. (67) is used for infinitesimal volume instead of (66), and the limits of integration on ξ^i are the same as those in C_N. Similar results can be derived for surface integrals.

APPENDIX II

Summary: In this appendix, some comments on the solution of the problem of contact of a toroidal shell are given. Once the incremental solution for finite deformations of an inflated tire is obtained, the solution for the contact problem can be achieved in an incremental form, as indicated below.

A Formulation for the Solution of Contact Problem: First, the inflation problem is solved, and then one proceeds with the contact problem.

The contact problem must be considered in a step-by-step fashion. Since the contact forces and the corresponding contact area are not known in advance, one must make certain a priori assumptions to facilitate a direct numerical solution.

Thus, we assume that certain nodes are in contact with the ground. This fact is expressed by a kinematic restraint on the corresponding nodal displacements. Next, one calculates the nodal contact forces necessary to bring the above nodes in contact. Since the contact is unbounded, all contact forces must be compressive. Obviously, certain nodal contact forces may turn out to be tensile. The implication is that one made an erroneous assumption on the contact area which may easily be remedied by removing the corresponding node from contact.

Contact Problem: The element stiffness and load matrices are defined by Equations of the general form (See text)

$$k = B^{T} H^{-1} B \qquad (1)$$

$$p = (B^T H^{-1} H_p - B_p^T)\, a \tag{2}$$

Then, the merge of the above equations yields

$$K_{ij}\, q_j = Q_i \tag{3}$$

$$i, j = 1, 2, \ldots N$$

where K_{ij} is the structure stiffness matrix, q_i is the generalized displacement vector, and Q_i is the vector of the unknown nodal contact forces. From Equation (3), the generalized displacements may be expressed in terms of the contact forces by

$$q_i = K_{ij}^{-1}\, Q_j \tag{4}$$

which may be written in the following partitioned form

$$\begin{array}{c} q_\alpha \\ \hline q_\Omega \end{array} = \begin{array}{cc} K_{\alpha\beta}^{-1} & K_{\alpha R}^{-} \\ \hline K_{\Omega\beta}^{-1} & K_{\Omega R}^{-1} \end{array} \begin{array}{c} 0 \\ \hline Q_R \end{array} \tag{5}$$

where

$$\alpha = 1, 2, \ldots N_\alpha$$

$$\Omega = 1, 2, \ldots 3N_c$$

$$R = 1, 2, \ldots N_c$$

$$N_\alpha = N - N_c$$

N_c = number of nodes in contact

For each node in contact, one may assign one algebraic equation based on geometrical considerations. It will be assumed that the contact surface is parallel to the X_2X_3 - plane and the wheel load is in the X_1-direction.

At each node, the rectilinear displacement vector may be written as

$$\bar{u} = \sum_{i=1}^{3} q_i \bar{A}_i \tag{6}$$

where the $\bar{A}_i$'s are unit base vectors of the reference configuration, Figure

Let P be a reference node in contact with a rigid, frictionless contact surface, and let "N" denote a generic node to be brought in contact with the contact plane.

Then, the rectilinear displacements of the reference node and the generic node are related by

$$\bar{r}_P \cdot \bar{e}_1 = \bar{r}_N \cdot \bar{e}_1 \tag{7}$$

where

$$\begin{aligned} \bar{r}_p &= \bar{R}_P + \bar{u}_P \\ \bar{r}_N &= \bar{R}_N + \bar{u}_N \end{aligned} \tag{8}$$

where $\bar{R}_P$ and $\bar{R}_N$ refer to the pre-contact node positions, Figure A.1. The displacement vectors in Equation (8) are

$$\bar{u}_p = \sum_{i=1}^{3} q_{p+i} \bar{A}_{p,i}$$

$$\bar{u}_N = \sum_{i=1}^{3} q_{n+i} \bar{A}_{N,i} \tag{9}$$

where

$$p = (P - 1) \times 5$$

$$n = (N - 1) \times 5 \tag{10}$$

The substitution of Equations (8) and (9) into Equation (7) yields

$$R_i^P + \sum_{i=1}^{3} q_{p+i} A_{i1}^P = R_1^N + \sum_{i=1}^{3} q_{n+i} A_{i1}^N \tag{11}$$

where

$$\bar{R}_p = \sum_{i=1}^{3} R_i^P \bar{e}_i$$

$$\bar{R}_N = \sum_{i=1}^{3} R_i^N \bar{e}_i$$

$$\bar{A}_{p,i} = \sum_{k=1}^{3} A_{ik}^P \bar{e}_k$$

$$\bar{A}_{N,i} = \sum_{k=1}^{3} A_{ik}^N \bar{e}_k \tag{12}$$

and where the $\bar{e}_i$'s are Cartesian base vectors, Figure 1.

Equation (11) may be rewritten as

$$\sum_{i=1}^{3}\left(q_{n+i}A_{il}^{N} - q_{p+i}A_{il}^{P}\right) = d_N \tag{13}$$

where

$$d_N = R_1^P - R_1^N \tag{14}$$

In matrix form, Equation (13) reads

$$C_{R\Omega}q_{\Omega} = d_R \tag{15}$$

$$R = 1,2, \ldots, N_c$$

$$\Omega = 1,2, \ldots, 3N_c$$

for the preassigned contact points. From Equation (3), the contact displacements

$$q_{\Omega} = K_{\Omega R}^{-1} Q_R \tag{16}$$

are substituted into Equation (15),

$$C_{R\Omega}K_{\Omega S}^{-1}Q_S = d_R \tag{17}$$

which is solved for the nodal contact forces, Thus,

$$Q_S = D_{SR}d_R \tag{18}$$

where

$$D_{SR} = \left(C_{S\Omega}K_{\Omega R}\right)^{-1} \tag{19}$$

Since the contact is unbounded, the following relation must hold

$$Q_S < 0 \tag{20}$$

$$S = 1, 2, \ldots, N_c$$

Suppose one finds n_c nodes for which

$$Q_S > 0 \tag{21}$$

$$S = 1, 2, \ldots, n_c$$

Then, these n_c-nodes must be removed from contact. Thus, the number of pre-assigned contact nodes becomes

$$N_c^* = N_c - n_c \tag{22}$$

and one must repeat the procedure from Equations (5) through (20). Note the inverse stiffness matrix (flexibility) may be saved from the previous calculation. Therefore, Equation (5) is merely re-partitioned according to the contact nodes N_c^* defined by Equation (22).

If Equation (20) holds, then one brings additional nodes in contact. The procedure terminates when

$$\sum_{s=1}^{N_c} Q_S = w \tag{23}$$

where w is the wheel load.